8-2017

Investigation of Uranium and Thorium Uptake in Pinus taeda (Loblolly Pine) and Dichanthelium commutatum (Variable Panicgrass) from a Naturally Occurring Source

Sam Santoso
Clemson University, ssantos@g.clemson.edu

INVESTIGATION OF URANIUM AND THORIUM UPTAKE IN PINUS TAEDA (LOBLOLLY PINE) AND DICHANTHELIUM COMMUTATUM (VARIABLE PANICGRASS) FROM A NATURALLY OCCURRING SOURCE

A Thesis
Presented to
the Graduate School of
Clemson University

In Partial Fulfillment
of the Requirements for the Degree
Master of Science
Hydrogeology

---

by
Sam Santoso
August, 2017

Accepted by:
Dr. Brian A. Powell, Committee Chair
Dr. Nicole Martinez
Dr. Nishanth Tharayil

ABSTRACT

Mobilization of radioactivity from natural sources could lead to concentrations of naturally occuring radioactive material (NORM) in groundwaters past the EPA maximum concentration limit (MCL) for drinking water (Hughes et al., 2005; Powell et al., 2007). The Piedmont and Blue Ridge aquifers are a continuous source of water for much of the Eastern U.S., however there are sources of natural contamination due to the area's geologic history. In the Tamassee and Salem Quadrangles (N 34° 56.152' W 83° 00.284) area of Upstate South Carolina off Highway 130 near Burgess Creek, an abandoned logging road dug through a sandy loam unit.This site has been previously referenced as the O'Leary prospect.This sandy loam unit contains a monazite placer sand deposit with elevated levels of naturally occuring uranium (U) and thorium (Th). The current work examines uptake of uranium and thorium in *Pinus taeda* (Loblolly Pine) and *Dichanthelium commutatum* (Variable Panicgrass) plants growing at the site and draws correlations between the extent of uptake and various soil characteristics including iron content, pH, organic matter content, and particle size. This study found Th and U concentrations are not correlated to particle size, pH, or organic matter. There is a correlation between iron, U, and Th in the plant shoots. Furthermore, higher concentrations of Th and U can be found in soils surrounding grass versus pine plants, and also in grass plants over pine plants.

DEDICATION

This page of space is dedicated to positive progress in the sciences. Hopefully with progress comes a better and brighter future.

ACKNOWLEDGMENTS

I would like to acknowledge the love and support of my wonderful family at home. Home cooked food relatively close is a blessing. My Advisor, Dr. Brian Powell, for deciding to take me on at a high flux time, and doing a great side project where I never harmed botanical life, and can enjoy the Geology. Dr. Martinez and Dr. Tharayil for their great feedback, positivity, and interest in this work. My friends, fellow students, and Post Doc's in Dr. Powell's research group who helped me with instrumentation and advice whether it's 8 A.M. or 12 Midnight. The Hydrogeology department classes that helped me see the depth I thought I needed and more. The home away from home, Clemson, is nothing without knowing the EEES, and Hydrogeology Department students are with me for questions. Naming people in memory of their aid: Mom, Dad, Sari, Simon, Brian Powell, Nicole Martinez, Nishanth Tharyil, Andreas, Melody, Coffee, Brennan, Bryan, Ashley, Noelia, Thomas, Nate, Rob B, Maddie, Kyle, Rob M, Kathryn, Sarah, and others. Carpe diem. Coffee diem.

TABLE OF CONTENTS

Page

LIST OF TABLES

LIST OF FIGURES

CHAPTER ONE

Introduction

In 2001 well water in Simpsonville, a rural community in South Carolina, tested above the maximum concentration limit (MCL) for uranium (Hughes et al., 2005; Powell et al., 2007). This finding is important because research has shown that long term exposure to the alpha particle decay of radioactive elements such as uranium can lead to cancer. This well was contaminated due to the exposed rocks in the fault line in the Piedmont. The Piedmont and Blue Ridge region, which refer to both the aquifier and geographical region that stretches from the southeast to the northeast of the continental United States as seen in Figure 1.1, exhibits a variety of topographical features and their corresponding issues (Back and LeGrand, 1988). The southeastern section, with its increasing population and four definite seasons, has seen extensive urbanization, resulting in increased demands on the water supply. This increased demand has led to increased reliance on the Piedmont and Blue Ridge aquifer, which receives an average of 115 cm rainfall per year. This resulting surface water, which eventually drains into streams and subsequently into the unconfined aquifer, can transport and mix with radioactive minerals.

Figure 1.1. Piedmont and Blue Ridge aquifer highlighted in red (Back and LeGrand, 1988).

The resulting level of radioactivity is calculated as the amount of radiation given off in units of decay per time as detected using a NaI spectrometer from Canberra (InSpector 1000). Based on previous research, this study examines the uptake relationships between thorium (Th), uranium (U), and iron (Fe) in the soil and the shoots and roots of the *Pinus taeda* (loblolly pine) and *Dichanthelium commutatum* (variable panicgrass) in this region to investigate how insoluble thorium and uranium enter the plant. Specifically, this research focuses on the uptake pathways of the two plants, the corresponding uptake by location of the plants in area, and the presence of iron.

General Geology

The geology of the Piedmont and Blue Ridge dates as far back as the Early to Mid- Paleozoic Era (540 mya – 300 mya (millions of years ago)) for their gneiss and schists, and the Early Mesozoic (252 mya) for the complex changes in the area. The most common feature in the region is the northeastern/southwestern tilting metamorphosed chain of sedimentary rocks that exhibits mafics, intrusives, clastic sediments, and altered volcanic rocks, with the metamorphic and igneous rocks being primarily seen in the lower Piedmont. During the Permian (300 mya) Period, the Alleghenian orogeny created this mountain chain, causing complex changes to its lithology that added to the natural contamination of radionuclides and arsenic in the crystalline rock aquifer. The erosion of such metamorphic rocks as granite, sillimanite schist, pegmatite granite, and carbontites can lead to alluvial deposits containing radionuclides (Overstreet, 1967; William, 2011). Unique to the Piedmont and Blue Ridge is the unconsolidated upper 2 to 20 m of sediment exhibiting loosely highly weathered saprolite, the red to brown bedrock which is composed primarily of sandy clay with fragments of solid rock, that plays an important role in the hydrogeologic features and high silica (Back and LeGrand, 1988).

General Hydrogeology of the Area

The complex folds and intricate geology of the area lead to topographically extensive hills and mountains, while the underground exhibits a banded mesh composed of several geological units. There are no simple flat-lying formations; instead the water travels within two very different media: fractured bedrock and/or saprolite (Back and LeGrand, 1988). Most of the local aquifers in the system, which are unconfined, are not artesian unless the well is tapped to a very deep hydrogeologic unit with very low

recharge. The water table is relatively close to the surface and mimics the topography except on a steep ridge where the groundwater can be seen percolating downwards.

This study focuses on the Savannah watershed, its hydrology shown in Figure 1.2. The water within the area outlined in green drains and remains in that area because it is the highest point. The specific area in the Savannah watershed studied here has a number of hillsides with exposed soil where water has percolated through.

Figure 1.2. Savannah Watershed with the green outlining the study site (USGS, 2016).

Radiometry of area

Figure 1.3 shows the contiguous United States, much of Canada, and almost all of Alaska. Using remote sensing data allows for the creation of aeroradiometric grids based on the number of gamma rays exposed from the earth's surface with a sensitivity of 1° x

2° quadrangles (~ 80 mi^2). These maps give an estimate of the thorium and uranium in surficial bedrock units (Kucks, 2005). While the white cells in the image represent those containing no data, the maximum U reported is 6 ppm eU, and Thorium reports a maximum of 24.0 ppm eTh, both with 0.1 resolution (e representing equivalent).

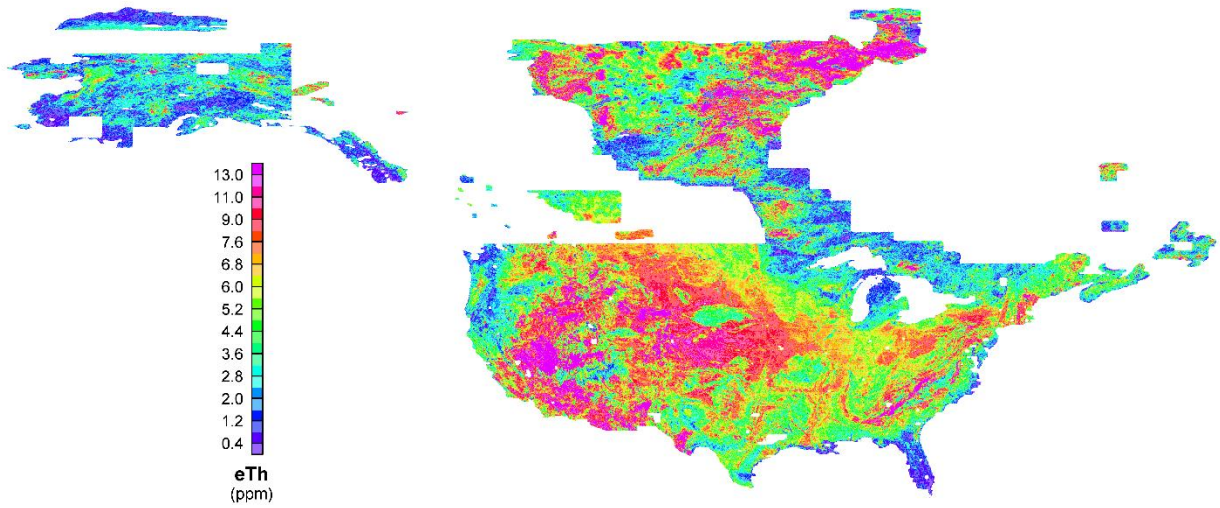

Figure 1.3. Aeroradiometric map of the United States, Alaska, and parts of Canada showing eTh in ppm (Kucks, 2005).

Combining the radiometry and general geology of the Southeast in USGS Circular 1336 Map, Van Gosen et al. (2009) indicate that the purest thorium minerals are found in Monazite (Ce,La,Y,Th) PO_4, Thorite (Th,U)SiO_4, Brockite (Ca,Th,Ce)(PO4)•H_2O, Xenotime (Y,Th)PO_4, and Euxenite (Y,Ca,Ce,U,Th)$(Nb,Ta,Ti)_2O_6$. Most known deposits containing thorium are in veins, alkaline intrusions, carbonatite stocks, or black sand placer deposits, with the Piedmont region exhibiting black sand placer deposits, alluvial stream and beach deposits from erosion of alkaline igneous terranes (Paleozoic-Mesozoic). These deposits, known as the North and South Carolina placers, are pocketed throughout the area and have been mined for ThO_2. Monazite is a phosphate mineral which can contain up to twenty percent

thorium and is resistant to chemical weathering with a high specific gravity similar to ilmenite, rutile, and magnetite.

Plant Characteristics and Physiology

Several scenarios below explain the potential processes that facilitate plants to take-up essential and non-essential nutrients, including the exudation of complexing agents, various nitrogen-filled environments, and various rhizosphere conditions, specifically focusing on loblolly pine and variable panicgrass. Based on expertise, knowledge of the area, and USDA websites, the identification of the pine tree as a loblolly is based on its geographic location, the pre-existing pines in area, its fragrant smell, and its pale green needles (Arbor Day Foundation, 2016). Variable panicgrass is identified based on the fact that it grows in bunches, with ligules (membrane-like tissues of delicate hairs) that are prevalent on the shoot. While it is sometimes confused with deer-tongue grass, they differ in their seed heads as the latter does not exhibit the ligules found in the panicgrass (Missouri, 2015; USDA, 2016).

Uptake Strategies or Metabolic Differences of Plant Uptake

Research over the past 30 years has found that there are two distinct root mechanism responses to iron deficiencies (Marschner and Romheld, 1994). Strategy 1 plants like the loblolly pine are non-graminaceous monocots, which primarily use an increased production of reductase and chelators for getting Fe^{3+} to Fe^{2+} into the root for nutritional use (Barker and Pilbeam, 2016). Strategy 2 plants, the graminaceous species like variable panicgrass, primarily rely on enhanced synthesis and secretion of

phytosiderophores in the rhizosphere area which chelating nutrients and potentially other metals as well. These strategies are shown in Figure 1.4 below.

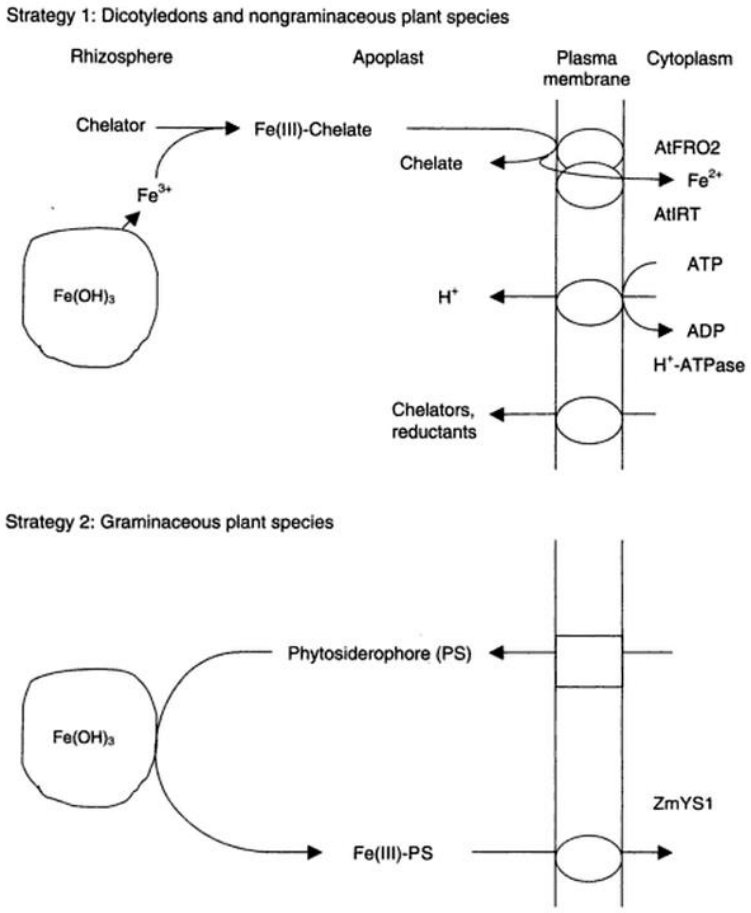

Figure 1.4. Diagram of iron uptake in strategy 1 and 2 plants (Barker and Pilbeam, 2016).

Depending on the plant, the plasma membrane of Strategy 1 species use inducible reductase (Buckhout et al., 1989; Holden et al., 1991) to create a need for transfer cells, chelators, and reductants. However, Strategy 2 plants use the biosynthetic pathways of phytosiderophore synthesis and its genetic regulation, meaning that depending on the condition of the soil and the rhizosphere, these plants are more effective at taking up Fe

than chelators. This is seen in the modified Figure 1.5 below from Zhang et al. (1991) and reproduced by Marschner (1994).

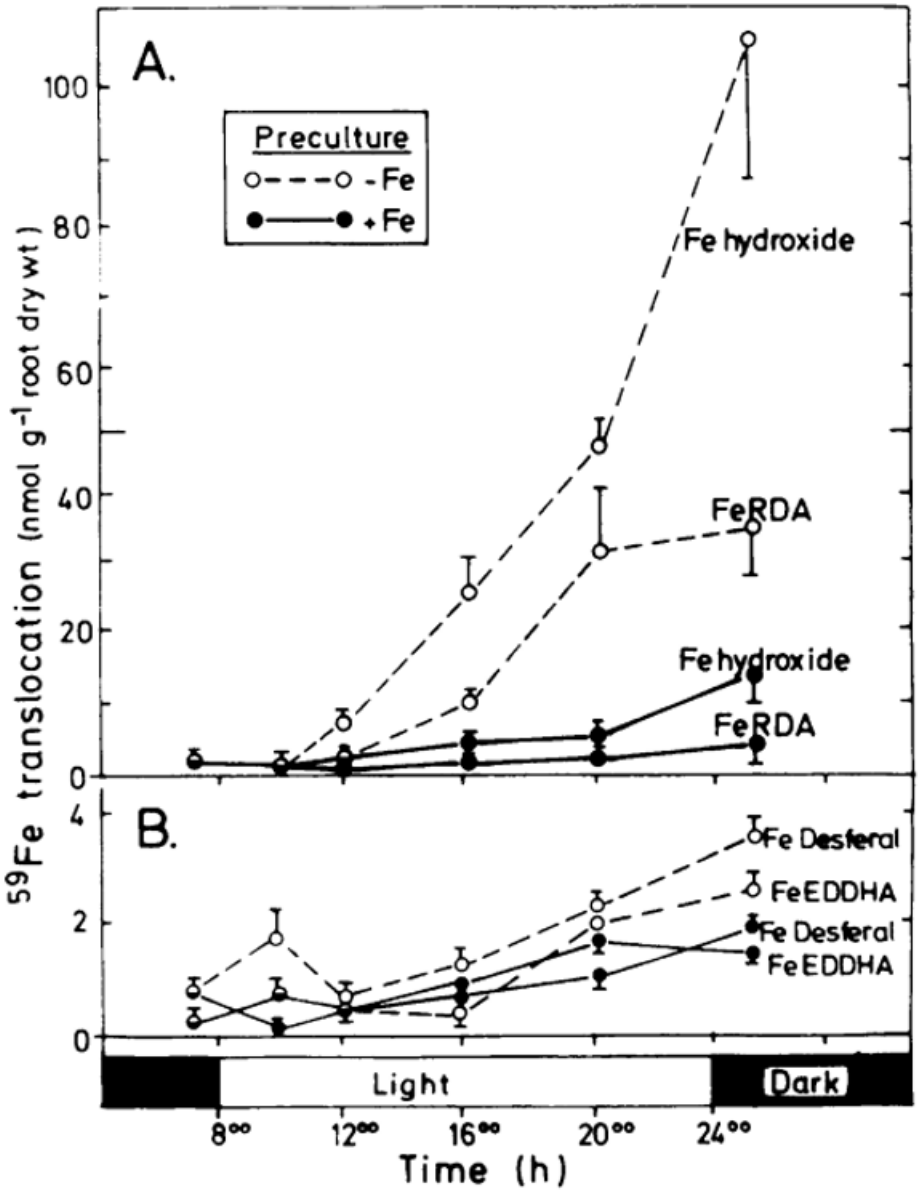

Figure 1.5. Modified image from Zhang et al. 1991 which shows the translocation of Fe from pre-loaded apoplasmic (extracellular) roots under multiple conditions to the shoots for wheat plants. Dotted line represents Fe deficient plant.

Understanding this is crucial for understanding that under certain conditions roots with iron deficient soils can possibly translocate iron from the root at higher rates than chelators.

Nutritional Uptake

A wide variety of factors contribute to the successful growth and development of a plant, with Masclaux-Daubresse et al. (2010) concluding that one of the most important is nitrogen assimilation and remobilization, collectively referred to as nitrogen use efficiency, its importance being emphasized by the investment in nitrogen fertilizers. Nitrogen, like phosphates, is a key essential nutrient and, as such, is significant in the global economy and a driver for continued plant research.

Iron (Fe) is more complicated as too little causes deficiencies in growth but too much is toxic for most plants (Morrissey and Guerinot, 2009). According to Morrissey and Guerinot (2009), little is known concerning which chelates transport Fe onto the root epidermis. This process varies from plant to plant, involving such organs as root symplast, phloem, nicotianamine, yellow stripe genes (YS), or iron transport genes. Different YS genes respond differently to environmental stress, for instance loading iron into different parts of the plant (i.e. seeds.) Previous research has suggested that 90 percent of the ferritin is present in the plastid, food storage for plants.

Uptake of Non-Essential Elements

Also important to the uptake and the health of plants overall are the heavy metals found in soils and especially sewage, which contains a mix of non-essential elements and nutritional elements that plants can take-up. The study conducted by Camobreco et al.

(1996) investigated if heavy metals can be removed from soils by soluble organics through preferential flow paths and enhanced metal mobility in the soil by constructing 8 soil profile columns, four being undisturbed soils, and four homogenized of the same mineralogy. To add metals, they simulated rain with metal chlorides at concentrations low enough to be complexed by organics, finding preferential paths in the undisturbed columns through which organics can cause Cu and P to leach out at rates faster than normal, similar to Cd and Zn. These results indicate that the homogenized soil samples adsorbed the metals applied, suggesting that heavy metals can be taken out of soils by soluble organic chelators through preferential flow paths and enhanced metal mobility through the soil.

In more recent research, Zhao et al. (2008) focused on *Oryza sativa* (rice) in reducing environments. Aware that the nonessential nutrient arsenic (As) is taken up by phosphate transporters as arsenate in such environments, they found that its uptake is highly efficient with silicon as arsenite then changes to arsenate as it enters the root. This uptake pathway, however, is variable depending on the need for essential nutrients. For example, as Lakshmanan and Venkateswarlu (1988) found in their study, the uranium concentration factor decreased in vegetables with soil additions of uranium-rich water, remaining in water.

While heavy metals represent a group of non-essential elements, harmful because of their wide-spread use and their toxicity, other such nutrients include the actinides, which release energy through radioactive decay. These elements are of particular interest to the research reported, specifically, plutonium, uranium, and thorium.

Plutonium (Pu) Uptake

Plutonium has ionic potentials similar to Uranium (IV); however, it occurs less frequently in nature (Railsback, 2012). Lee et al. (2002) looked at Pu in shoots of Indian mustard (*Brassica juncea*) and sunflower (*Helianthus annuus*) in a translocation and uptake study using hydroponics with three variable nutrient solutions: Pu-nitrate, Pu-citrate, and Pu-DTPA. They found that plants that received Pu-DTPA Pu concentrations increased in shoots but decreased in roots, with the increasing concentrations of Pu-DTPA resulting in an increase of Pu of only up to 10 µg DTPA mL^{-1} in Indian mustard and 5 µg DTPA mL^{-1} for sunflower.

Concentration ratios (CR) are a measurable quantification of how much of an element is being taken-up into a plant based on the amount available in the soil, given below in equation 1.1. Both plants were similar to the Pu concentration in the roots and shoot, but increased in the transport indices (Pu content in shoot / Pu content in whole plant) with increased DTPA concentrations.

$$\text{Concentration Ratio}(CR) = \frac{Element\ Concentration_{dry\ plant\ fraction}}{Element\ Concentration_{soil\ or\ nutrient\ solution}} \qquad \text{Eq. 1.1}$$

Lee et al. (2002) conducted further research on the uptake of Pu in Indian mustard (*Brassica juncea*) and sunflower (*Helianthus annuus*) using soil amendments allowed it to grow in three different soil types for two weeks: acidic (Crowley pH = 4.80), calcareous (Weswood pH = 7.55), and a neutral soil (Crockett pH = 6.55) as seen in Table 1.1 below. They found that Indian mustard accumulates Pu more easily in aquatic environments than sunflower. They also found that using DTPA as a complexing agent lowered Pu concentration in the roots but increased Pu concentration in the shoots. More

importantly, further adding to the complexity of the biogeochemical system, is their finding that Pu uptake varied significantly in both plants with varying concentrations of Pu and of the complexing agent DTPA. One of their conclusions was that in acidic soils exchangeable Pu was higher than in neutral and calcareous soils. This study combined with their previous one indicates that Pu uptake varies based on soil additions, soil conditions, pH, particle size, carbonates and DTPA, being dependent on the plant species.

Table 1.1. Selected physical properties of soils from Lee et al. (2002).

Soil	**Particle Size Distribution (%)**			**pH**
	Sand	Silt	Clay	
Weswood	67.6	25.6	6.8	7.55
Crockett	39.6	23.6	36.8	6.55
Crowley	56.8	19.7	23.5	4.80

Uranium (U) Uptake

Uranium (U) has been a frequent area of research for Lee et al. (1993), especially in the work they conducted at the Oak Ridge National Laboratory (ORNL). Their goal was to investigate the solubility of uranium by conducting equilibrium studies predicting the components of U, Ca, Mg, and CO_3^{-2} using geochemical modeling to mimic the spillage of heavily laden U and to process the effluent and the soil. Through modeling, they found that uranyl-carbonate complexes are the most stable and dominant in a solution with carbonate species. The heavy use of carbonates for erosion control at road maintenance and construction sites can lead to uranium being solubilized in nearby soils. These highly mobile uranyl-carbonate species could become serious issue for human health.

Ebbs et al. (1998) studied methods for improving phytoextraction of U from contaminated soils using GEOCHEM-PC to model the U species with pH values at 5.0, 6.0, and 8.0. This modeling showed a high percent (80%) of free uranyl $(UO_2)^{2+}$ cation to be available at pH 5.0-5.5. Above a pH range of 5.5, U takes a hydroxide form, and at pH 8.0 is a carbonate complex. Subsequent plant uptake studies considering varying U species and nutrient solutions showed $(UO_2)^{2+}$ to be the form plants most frequently uptake. In addition, they investigated the phytoextraction for the plants under study, concluding that the red beet phytoextracted U from the soil and that the largest shoot U concentration was as a free uranyl cation at pH 5.0 in peas. There is a difference in growth in peas when exposed to U and P versus just U, meaning the plant could have different complexation strategies, a situation supported by evidence showing a reduction in lateral root length in peas exposed to U and P. Ebbs (1998) also screened several plants for their uranium accumulation, finding beet and crown vetch to be the highest, but from a per plant basis tepary bean was highest, perhaps because the seed stage of some had larger P reserves. Additional research by Ebbs et al. (1998) supports the addition of citric acid to increase the solubility of soils, a condition that could help phytoremediate soils up to 500 mg U / Kg soil. The accumulation of U can vary in different structures of the plant as Lakshmanan and Venkateswarlu (1988) found with rice, the lowest concentration being in the grain and the highest in the straw.

Th Uptake

The non-essential elements uptake focused on in this study includes Th, U, and Pu. Radioactive thorium occurs naturally in the earth's crust as Th-232 (Sheppard, 1980),

which itself occurs primarily as a tetravalent ion, meaning that there is typically a low Th/U ratio in natural waters. Th occurs largely as an accessory mineral in high metamorphic and igneous rocks, and is the daughter product of U-238. Sheppard also reports a thorium soil concentration range of 0.2 mg/kg to 9.5 mg/kg with higher concentrations of Th in alluvial soils than podzolic, although it is uniformly distributed throughout the soil profile. Early research conducted by Hansen and Stout (1968) found four types of soil-thorium adsorption reactions: "(1) $Th(OH)^4$ precipitation from calcareous soil buffering, (2) strong adsorption on clay soils from dilute solutions (< 1g Th/L, pH > 2), (3) strong adsorption on organic soils under neutral and acidic conditions, and (4) reduced adsorption in basic solutions caused by humic acid dissolution."

More recently, Sheppard and Evenden (1988) published a critical review of their current knowledge of the plant/soil CR for both uranium and thorium, an area which had not been widely discussed previously, finding they varied across the three levels of factors affecting the CR. On a large or macro-scale, plants may have a predicted growth rate pattern that indicates linear growth depending on the amount of nutrients available. On a medium or meso-scale plants or organisms attempt to regulate their uptake. On the small or micro-scale the plant root surfaces actively and passively modify soil constituents by producing exudates, enzymes, chelators, metabolic byproducts, or waste.

Various methods can be used for total elemental analysis. Statistically, dry plants and dry soils give CR results with less uncertainty, and if the samples are ashed, there is less variability from the water content. Increasing the sample size would also improve the statistics associated with CR analysis. By increasing the sample size the distribution of

CR would tend to be normally distributed based on the central limit theorem (Sheppard and Evenden, 1988; Davis, 2002). Variations in a distribution can be seen in Figure 1.6, which graphs the several-fold higher concentrations in silt versus the sand fraction of soils.

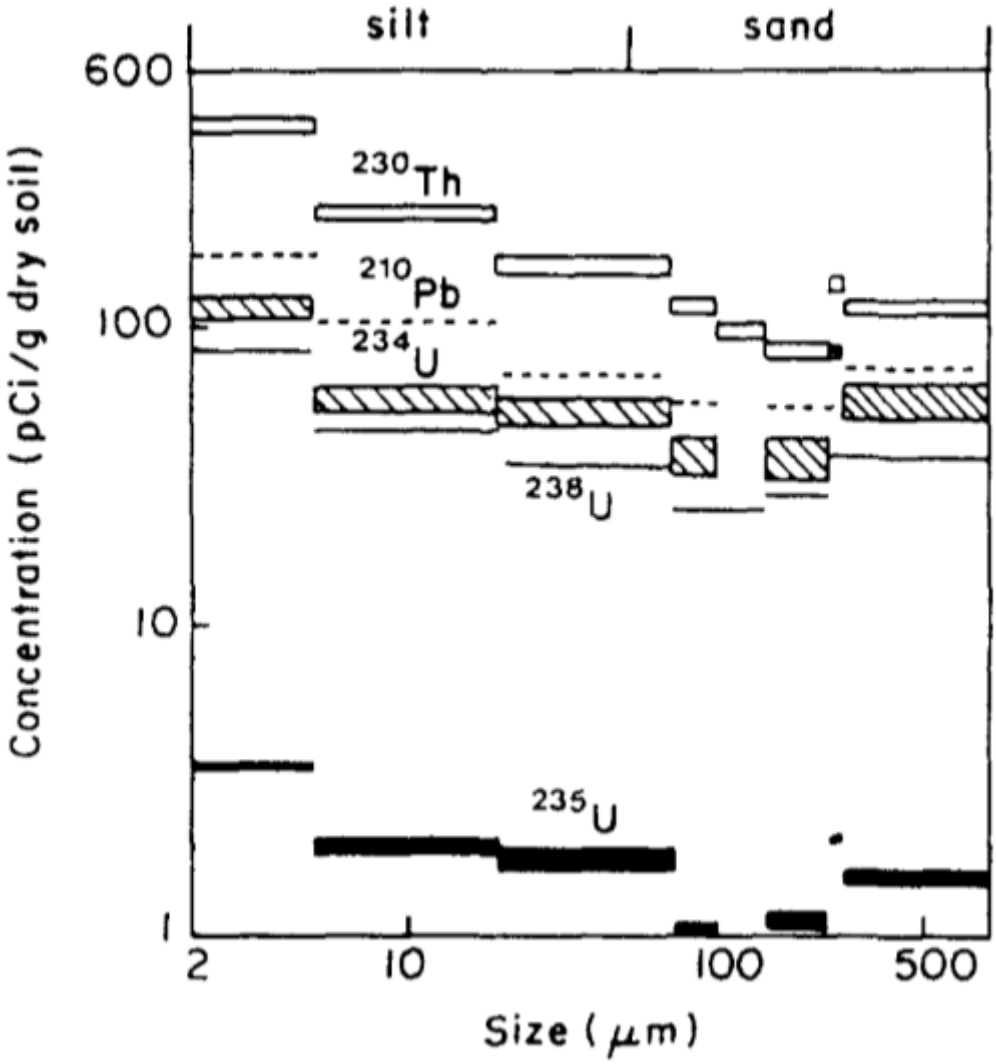

Figure 1.6. Concentrations of U-238, U-234, U-235, Th-230, and Pb-210 in various particle size fractions of a soil from Sheppard and Evenden (1988) (Originally from Megumi, 1979).

According to Sheppard (1980), and Taylor (1964), Th concentrations in soil can vary, with Powell et al. (2007) reporting the average concentration of U and Th in continental crust of being 2.7 and 9.6 ppm, respectively. To understand the significance of not only uptake but also movement in soils, scientists study it under variable conditions as Lee et al. (2002) and Finch and Murakami (1999) did in their studies. Typically, $(UO_2)^{2+}$, uranyl, found in nature is relatively mobile until reducing conditions lead to the oxidant + e- -> product, when the gain in e- losses from oxygen produce uranium minerals.

As previously discussed in the Radiometry Section, Van Gosen et al. (2009) is based on the research conducted by Mertie (1953; 1975) and Overstreet (1967). Combined, they support monazite as a placer deposit (fluvial). Supporting this placer deposit theory, Powell et al. (2007) report high uranium contamination in private wells ranging from 44.3 – 5570 μg/L, with isotopic ratios indicating natural sources of contamination. They also indicate that the levels found in samples from the O'Leary site are within range of those reported by UNSCEAR (United Nations Scientific Committee on the Effects of Atomic Radiation). These levels also indicate that monazite is not significantly affecting stream sediments. Powell et al. (2007) concluded that their ex-situ data are similar to previous in-situ data, suggesting that the soil uranium concentrations surrounding the creeks are close to the expected average values of the geologic material (granite) in area. Despite a high range of dates from published data, Mertile (1953) had U_3O_8 fraction percent that should have U activity from 20-100 kBq/kg. While this value is higher than reported by Powell et al. (2007), it supports the highly complex geologic area and placer deposit due to geographic location.

Due to similar physiochemical properties thorium can be studied as a surrogate to plutonium. In a natural environment plutonium is not found, thus naturally occurring thorium and uranium are studied to their relationship with crystalline and amorphous iron. Preliminary data from the study site found a positive correlation between iron concentrations and uranium and thorium concentrations in grass and blackberry plants (Ely et al., 2016). The current study delves further into this site by considering different plants and examinining the soil attatched to the roots. Based on chemical similarities between uranium and thorium, preliminary data, and soil geochemical properties, this work is motivated by two primary hypotheses:

1.) Uranium and thorium in the forms of UO_2^{2+} and Th^{4+} may be taken into plants indirectly due to their similar ionic potential to iron Fe^{3+} (4.57, 4.21, and 4.68, respectively)

2.) Strategy 2 (graminaceous) variable panicgrass will have higher concentration ratios and element to element ratios than Strategy 1 (non-graminaceous) given that both plants are under conditions favoring plant growth.

A corollary to the similar ionic potentials through this commonality of abundance is that hypothesis 2 is dependent on the difference between Strategy 1 versus Strategy 2 plants.

CHAPTER TWO

Methods

Six locations at the study site were selected for collection of soil and plant samples. The primary criteria for selecting a sampling location was that a loblolly pine and variable panicgrass plant were within approximately 24 inches of each other. All samples were collected along the roadbed of an old logging road used during timber operations many years ago. To explore the relationship between Fe, U, and Th, soils from the study site was characterized using particle size analysis, crystalline and amorphous iron extractions, and pH analysis in addition to X-ray powder diffraction (XRD). Then samples of loblolly pine and variable panicgrass were digested, and inductively coupled plasma mass spectrophotometry (ICP-MS) was used to determine the concentrations of relevant elements (potassium, calcium, uranium, thorium, and iron) within the shoots, roots, and soil. Additionally, the water content and organic matter content were determined for the soils and plants using methods described below. All data and analyses were conducted, saved, and graphed in Microsoft Excel.

Because of the area's varied topography and complex geology, a number of small pockets of well eroded areas are appropriate for sampling as they have bank-like formations, potentially exposing monazite and eroded metamorphosed/igneous rocks from the Paleozoic Era. Based on previous, unpublished research using an array of field and laboratory based methods in the Clemson University course EE&S 813: Environmental Radiation Protection Laboratory, the general area has been evaluated and several "hot spots" with naturally occurring radioactivity have been identified. More than

80% of this area, which is an abandoned logging roadcut, exhibits dense forest coverage. The segment close to the highway registers higher radiation, while in the area further away past an engineered berm, less radiation is detected.

The plants for this study were selected based on their proximity and abundance in the roadbed, beginning from the distal part of the roadcut to the proximal of Highway 130. In addition, they were also chosen because of their different metabolic pathways and their abundance throughout the Piedmont and Blue Ridge. Pairs of plants were selected within a 2-foot range of each other, with the samples of the grass and pine species being labeled as Grass shoots or grass plant (GP), senesced shoots or Grass Brown Plant (GBP), Grass Root (GR), Pine shoots or pine Plant (PP), and Pine Root (PR). The GBP is the previous year's growth of grass which has died and turned brown but is still present with the primary plant. To evaluate potential differences with an actively growing plant, this growth was isolated from the primary plant and analyzed separately. Approximately a 6" diameter and 6" deep section of soil was removed with each plant and will be labeled as Pine Soil (PS) and Grass Soil (GS). The soil was removed with a large shovel then the plant roots were separated by carefully breaking up the soil aliquot on the surface. The total length of exposed area sampled for this study was approximately 200 feet with a road bed width of 5 to 7 feet. The following methods outlined in US EPA 3052 and based on various soil techniques documented in research were used for soil and plant sample preparation (EPA, 1996).

Autoradiography

During sample collection, care was taken that the samples were of a weight both suitable for analysis and representative of the plant, with the aim of collecting 30 grams of organics and approximately 250 grams of corresponding soil for the root samples. The first analysis conducted was autoradiography imaging, its results being a qualitative evaluation of the distribution of radiation within the sample.

pH and Particle Size Analysis Methods

Soil is frequently characterized through pH and particle size analysis, with the former being measured using a typical electrode probe inserted into a mixture of equal parts of soil and deionized (DI) water, and then well stirred/shaken for 30 minutes (Thomas, 2009). To ensure consistent results, the pH was read with the Thermo Scientific Orion Star A214 probe within 2 minutes of stirring/shaking and at an equal depth for all 12 cases.

The particle size analysis (PSA) developed by Gee and Bauder (2009) is a nondestructive method performed by suspending 30.0 – 100.0 grams of the soil in deionized (DI) water and measuring the resulting density using a hydrometer. Forty grams of soil were soaked in 100 mL hexa metaphosphate (HMP) + 250 mL DI water to help dispersion. Then this mixture was stirred using an electric stirrer for 5 minutes before being poured into a 1-liter graduated cylinder. The remaining space, approximately 650 mL, was filled with DI water, and then the mixture was shaken for 1 minute using the hand-over-hand method. Immediately after shaking, the temperature was recorded and the R distance measured at intervals of 30 seconds, 1 minute, and 3, 10, 30, 60, 90, 120, and 1440 minutes. The R distance is the reading from the upper edge of

the meniscus surrounding the stem The R_L factor is recorded in a stock beaker filled with 100 mL HMP + 900 mL distilled water. The R_L factor can be used as a correction factor for solution viscosity and soil solution concentrations. After the 24-hour reading, the solution was filtered through a 53-micrometer sieve screen and dried at 105°C before being physically sorted using 1000, 500, 250, 106, and 53 micrometer sieves for 3 minutes. The sand, silt, and clay fractions can be calculated by determining the soil concentration (C), the oven dry weight of soil sample (C_o), and the summation percentage (P) at given time intervals, with equations 2.1 and 2.2 below:

$$\text{Soil Concentration}(C) = (R - RL), \quad \text{Eq. 2.1}$$

$$\text{Summation } (\%) = \frac{C}{C_o}, \quad \text{Eq. 2.2}$$

The sand fraction's percentage is calculated as (C_o – 1 minute C) / C_o, silt at (3 minutes – 1440 minutes) / C_o, and clay fraction as the (1440 minute reading / C_o).

Water Content and Loss-On-Ignition Methods

The analysis of the organics was separated into shoot, root, and soil of the samples harvested for the loblolly pine and variable panicgrass. A shoot was defined as exposed growth measuring approximately 1 cm above the ground surface, while everything else below was categorized as a root. Soil is the homogenized aliquot of soil which was dug up with the plants during collection. After harvesting, the samples were brought back to the lab and weighed. The roots were dipped into DI water and rubbed between fingers to thoroughly separate the soil from the roots. In order to obtain the best representative sample weight and obtain water content from all plant fractions (except

roots) they were weighed pre and post 7 weeks of air drying. Moisture content provided later for all plants was calculated by the weight lost between 7 weeks of air drying, followed by 72 hours at 50 °C in an oven. All other plant and soil samples were left to air dry for 7 weeks. Based on the ASTM D4638-11method, the dried plant and soil samples were re-dried for 72 hours at 50°C (Lee et al., 2002); then the moisture content was determined using Equation 2.3 below, also from the ASTM D4638-11 method.

$$\text{Water Content}(\%) = \frac{m_{wet} - m_{dry}}{m_{wet}} \qquad \text{Eq. 2.3}$$

where m_{wet} represents the wet mass in grams (g) and m_{dry} the dry mass after 72 hours in the oven (g).

To prepare the samples for LOI (Loss-On-Ignition), 150 mL borosilicate beakers were used as they can withstand temperatures up to of 800°C; these were covered with aluminum foil, which can withstand temperatures of approximately 900°C, to prevent cross-contamination from other samples. To ensure standardization of the beakers used here, they were tared and weighed after heating in a 400°C furnace for 2 hours and then air cooled. The air-dried samples were placed into the newly tared beakers to obtain their oven-dried weight to measure the water content. While plant samples can be dried for variable times and at various temperatures, ranging from 30-60°C and between 24-72 hours, this study dried the samples at a temperature of 50°C for 72 hours.

Next, the organic matter (OM) content was measured using the LOI method adapted from Ben-Dor and Banin (1989). LOI is essentially an ashing method in which the oven-dried samples are placed in borosilicate beakers to burn off their organic matter. This process assumes that the organic matter content is equal to the LOI. Following Ben-

Dor and Banin's (1989) method, the samples were initially exposed to 25°C, with the temperature being raised by 50°C every 30 minutes until it reached 400°C, where it was held for 4 hours. This process, which takes 20 hours overall, is referred to as a Ramp and Dwell Graph. The resulting value obtained from LOI can be corrected for dehydroxylation, which is the process of removing hydroxyl groups from an organic compound. The correction factor for dehydroxylation can be calculated using regression analysis but was not performed for this experiment. The equation used for organic matter content calculation is Equation 2.4 below.

$$\text{LOI}(\%) = \frac{m_{105} - m_{400}}{m_{105}} \qquad \text{Eq. 2.4}$$

where m_{105} represents the mass in grams (g) at temperature 105°C and m_{400} the mass in grams (g) at temperature 400°C.

Digestion and Dilution Methods

After ashing, samples can be digested with acid. To ensure complete digestion, this study used a microwave-assisted digestion technique modeled in EPA Method 3052 and Magnum (2009) using the MARS Multiwave 1000. This method uses high pressure teflon tubes and acid to completely dissolve biological elements including soil, sediment, botanical, or waste oil while maintaining high productivity and safety. Two acid mixture techniques were used here: 10.0 mL of HNO_3 + sample (g) and 10.0 mL HNO_3 + 2.0 mL H_2O_2 + sample (g) for both plants. The later acid mixture was used as a second attempt to digest the pine roots. To assist in the soil digestion, 9.0 mL of HNO_3 + 3.0 mL HF + 1.0 g sample (g) were used. The samples were first heated to 180°C for 5.5 minutes, remaining at this temperature for 9.5 minutes before being allowed either to cool overnight or cool

in a refrigerator for 30 minutes. The solution in the teflon tubes was then filtered through a 20 micrometer (μm) syringe filter to eliminate organics or particles that could potentially result in nebulizer clogging during the ICP-MS analysis.

Ashing and filtering the sample usually precludes any further issues; however, the loblolly pine root digestate after filtering remained very dark, suggesting the presence of left-over particulates or residual organics which are the most recalcitrant part of a plant. To ensure they contained no organics or ligands, the pine samples were microwaved again, this second attempt resulted with no apparent change. To eliminate possible interferences like HF, the samples (PP 1-6) were dried on a hotplate at 105°C during the day and at 50°C at night over the next 7 days. The material remaining on the hot plate was subsequently ashed (LOI) at a higher temperature of 550°C to make sure the samples were free of organics. After the LOI, the pine samples were a dry, vesicular light weight ash as seen in Figure 2.1. HNO_3 was again added to this material, and it was subjected to microwave-assisted digestion. The resulting samples were clear, allowing for them to be analyzed without clogging the ICP-MS.

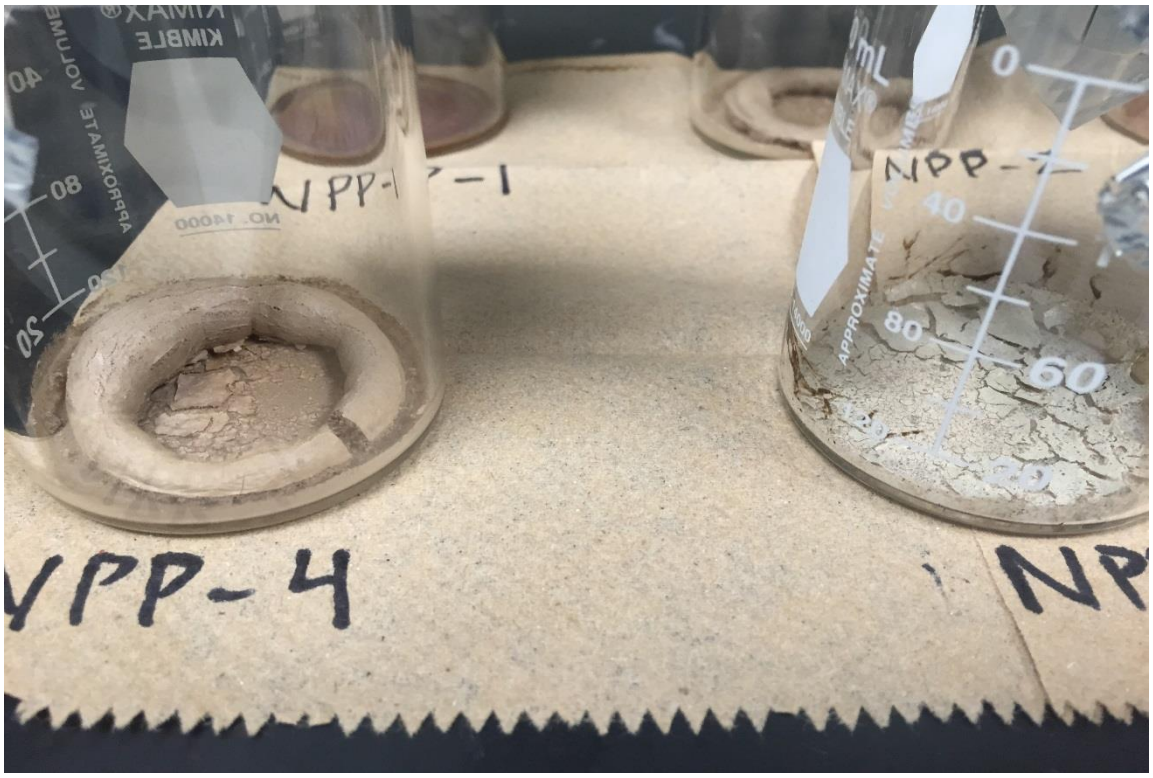

Figure 2.1. PR-4 (Pine Root 4) twice-ashed sample.

The solution remaining after filtering is a completely digested sample, or digestate, which is too concentrated for ICP-MS analysis. Thus, 1.0 mL of it is mixed with 9.0 mL of 2% HNO_3 which is the matrix of the ICP-MS standards.

X-ray Diffraction Methods

For the purpose of this study, x-ray diffraction, or XRD, was conducted on soil that was not exposed to acids, moisture, or water, or used in any other experiment following sample collection. Such samples can be pre-treated to remove such elements as carbonates, organics, sulfates, and iron oxides. Depending on the equipment used, the sample, which needs to be of a certain mass and powdered as finely as possible, was placed on a mount. This study used the Rigaku 5th gen. MiniFlex, which requires a

powdered sample to be placed on a glass slide as flat as possible. This was done by putting the powdered soil into a pre-indented slide and flattening it as evenly as possible. The goal of XRD analysis is to help determine the mineralogy of the soil, its monazite content being of interest for this research.

Analytical Method for Crystalline and Amorphous Iron Oxides

The crystalline and amorphous iron oxides were measured using a method similar to the total elemental analysis discussed later. This analysis is used to determine the iron concentrations in soils, allowing for scientists to know how much of this nutrient, which is key for plant growth, is being taken up and if it is freely available in the soil. Knowing these concentrations can also provide an indication of the soil--plant relationship.

The median of total Fe concentration in the Earth's soil is 3% (Murad and Fischer, 1988), and knowing the percentage of amorphous and/or crystalline iron oxide concentrations provides insight on their bioavailability and energy expenditure. The steps given below for determining iron availability are operationally defined, meaning while they do not give 100% accurate information, they are generally accepted to target amorphous (i.e., ferrihydrite) and crystalline (i.e., hematite, goethite) phases. Crystalline iron oxides, which typically include the minerals hematite, goethite, and lepidocrocite, are able to be extracted depending on environmental conditions. For instance, extracting crystalline iron oxides using citrate and dithionite reduces the system to allow Fe^{3+} to a more soluble Fe^{2+}, provided the temperature of the system remains below 80°C to prevent the formation of FeS. For the amorphous iron oxides, the system extracts water soluble iron, exchangeable iron, ferrihydrite, and a fraction of organically bound iron, then

adding acidified ammonium oxalate at pH 3 and limiting the exposure of the specimen to light. Because particle size and surface reactivity of the soils significantly affect the rates of reaction, a constant soil size less than 0.15 mm was used, put into variable dark 50 mL or 150 mL centrifuge tubes, and placed double-covered in a box.

The crystalline iron oxide requires a heated water bath constantly stirred as developed by Leoppert and Inkeep (2008), who modified the method originally introduced by Mehra and Jackson (1960) and Jackson et al. (1986). To separate the Fe^{2+} and Fe^{3+}, selective extractions were experimentally conducted using citrate-dithionite-bicarbonate (buffered at pH 7) to obtain crystalline iron oxides. For amorphous iron, acid ammonium-oxalate (pH 3) was used in the dark for poorly crystalline amorphous iron oxides. Crystalline and amorphous extraction techniques were developed by Holmgren (1967); Mehra and Jackson (1960); Schwertmann, (1964); McKeague and Day (1966); and Jackson et al. (1986), all of which were summarized and condensed in Loeppert and Inskeep's (2008) methods. These are also operationally defined based on specific extractions, not as an accurate measure of specific fraction of soil Fe, but providing a good basis for understanding. In all cases the digestate was diluted in 2% HNO_3 (1 mL of digestate into 9 mL of 2% HNO_3) for ICP-MS analysis of the Fe, U, and Th concentrations. Based on the hypothesis that U and Th concentrations are correlated with Fe, we have compared our results from these extractions in the discussion below.

Total Elemental Analysis – Inductively Coupled Plasma Mass Spectrometry

As the primary goal of this study is to investigate the relationship between iron and both thorium and uranium, a dilution factor for the digestate was used here to

normalized the measured concentrations of Fe, U, Th, and other analytes on the ICP-MS back to the solid phase concentrations based on the initial weight of sample added to the digestion tubes. In theory, the total measurable iron concentration should be the HF digested sample or the crystalline iron extraction, allowing for comparison across all values. However, the low levels of iron detected in the soils during the experiment did not seem plausible. We hypothesize that the fluoride is complexing with iron and interfering with the ICP-MS analysis. To attempt to address this situation, the original digestate solution from HF was then evaporated in glass beakers, resulting in improved values. However, there seemed to be an interference with low amounts of Th and U. To investigate if it came from the glassware and to address issues of high concentrations on the ICP, two separate experiments were conducted. One evaporated a 0.1 mL of the original digestate in a glass beaker, and the second evaporated similar solutions in Teflon beakers to see the change, if any. The final grass and pine shoot and root results reported below were from HNO_3 and H_2O_2 microwave assisted digestions. The final soil results reported below were 0.1 mL evaporated digestate samples in glass beakers with spiked internal standard consisting of neptunium, lithium, scandium, bismuth, gallium, indium, iridium, yttrium, and lead. These sets of results were used due to the least mechanical issues, best expected yields, and strong calibrations due to internal standard.

Concentration ratios are of importance to the study, and were based off the concentrations and dilutions from the ICP-MS results. To calculate the concentration ratios in tables presented below (Table 3.7 and 3.8) the average and standard deviation of a set of samples were reported. For instance, concentration ratio of uranium in pine plant

pair 1 to pine soil 1 from crystalline extraction: (U-PP-1 / U-PS-C-1) = CR_1. The average and standard deviation of CR_1 to CR_6 for uranium are were reported in the tables, along with thorium and iron CR's.

To evaluate the factors which may control the uptake of U and Th, comparisons were made between the total elemental analysis, extractable iron elemental analysis, and soil parameters (i.e., pH, organic matter content, particle size) were made to evaluate the correlations related to U and Th uptake. Also, comparisons were made with regards to the type of plant used and the location of the plants. In addition, knowing the previous metrics like %OM and/or the results from the particle size analysis, we hypothesized that under favorable growing conditions variable panicgrass will exhibit stronger positive correlations of radionuclides to iron than loblolly pine. A summary of the methods used here including their sources, goals, and the information they add to improve our understanding of the complex geochemical system investigated in this study.

Table 2.2. Summary of all experiments conducted.

Experiment	Objective	Knowledge Gained
Autoradiography Image Plate	First look at a sample if radiation is detectable.	Qualitative assessment of distribution of radioactive signatures.
Soil pH	First look at soil conditions (Thomas G.W., 2009).	General understanding of natural environment conditions. Correlate pH with Th/U uptake.
Particle Size Analysis	Understand the dominate clast/particle size present (Gee and Bauder, 2009).	Investigation of dominate particle size with correlations of Th/U uptake could result in the preferential uptake with smaller particle sizes.
Water Content (%WC)	Helps show the saturation level of the system (ASTM D4638-11).	Water content is necessary to know if the system is in healthy condition. Done to normalize concentration determination.
LOI (%OM)	Calculate the % organic matter of a sample by loss-on-Ignition (Ben-Dor and Banin, 1989).	Knowing %OM can decide how healthy the system was correlation between OM% and Th/U uptake.
XRD	Determine soil mineralogy.	Helps decide if the sample is exactly monazite, and possibly what other minerals are affecting the area.
ICP-MS	Obtain the elemental analysis of a sample.	Have a quantitative understanding of the system and helps find discoverable relationships between Fe, Th, U, and others. Gives a definitive answer if my samples contain radioactive elements and their concentrations.
"Free" Iron or Crystalline Iron	Find amount of "Free" iron oxide as an indicator of bounded Fe in soils (Mehra and Jackson, 1960; Jackson et al., 1986).	"Free" iron oxide counts are assumed to be with "Active" Iron Data. ICP-MS data allows for a more quantitative understanding of possible Fe in the soil that are bounded. Such "Free" iron are not easily accessible to organisms. Process uses Sodium Dithionite. Crystalline iron is only available through higher energy usage, chelators, exudates, reductants, ect.
"Active" Iron or Amorphous Iron	Find amount of "Active" iron oxide as an indicator of free iron within soils (Schwertmann, 1984; McKeague and Day, 1966).	"Active" iron oxide count allows a more quantitative understanding paired with "Free" and ICP-MS data for indications of the amount of irons being bound to the soil. Such "Active" or amorphous irons are more prevalent and can be taken up by plants or organism with less energy expenditure.

CHAPTER THREE

Results

The results obtained from this study include both site description and elemental analysis of the soils and plants: referred to as GBP (senesced shoots or grass brown plant), GP (grass plant shoots or grass plant) , GR (grass root), GS (grass soil), PP (pine plant shoots or pine plant), PR (pine root), and PS (pine soil).

Site Description Results

The site description results include the sampling and the autoradiography of plants from the research area. The sampling location, the Salem and Tamassee Quadrangle, is approximately 40 minutes north of Clemson, South Carolina. The study site seen in Figure 3.1 illustrates the longitudinal manner in which the sample pairs, numbered 1 through 6, were harvested. The location of each pair of variable panicgrass and loblolly pine sampled is shown in Figure 3.1. More specifically, Figure 3.2 shows an example of a sample, in this case pair 4, with the pine on the left marked by the black sharpie and the grass on the right with the red. The tape measure indicates the distance between the plants, showing that they share a similar environment.

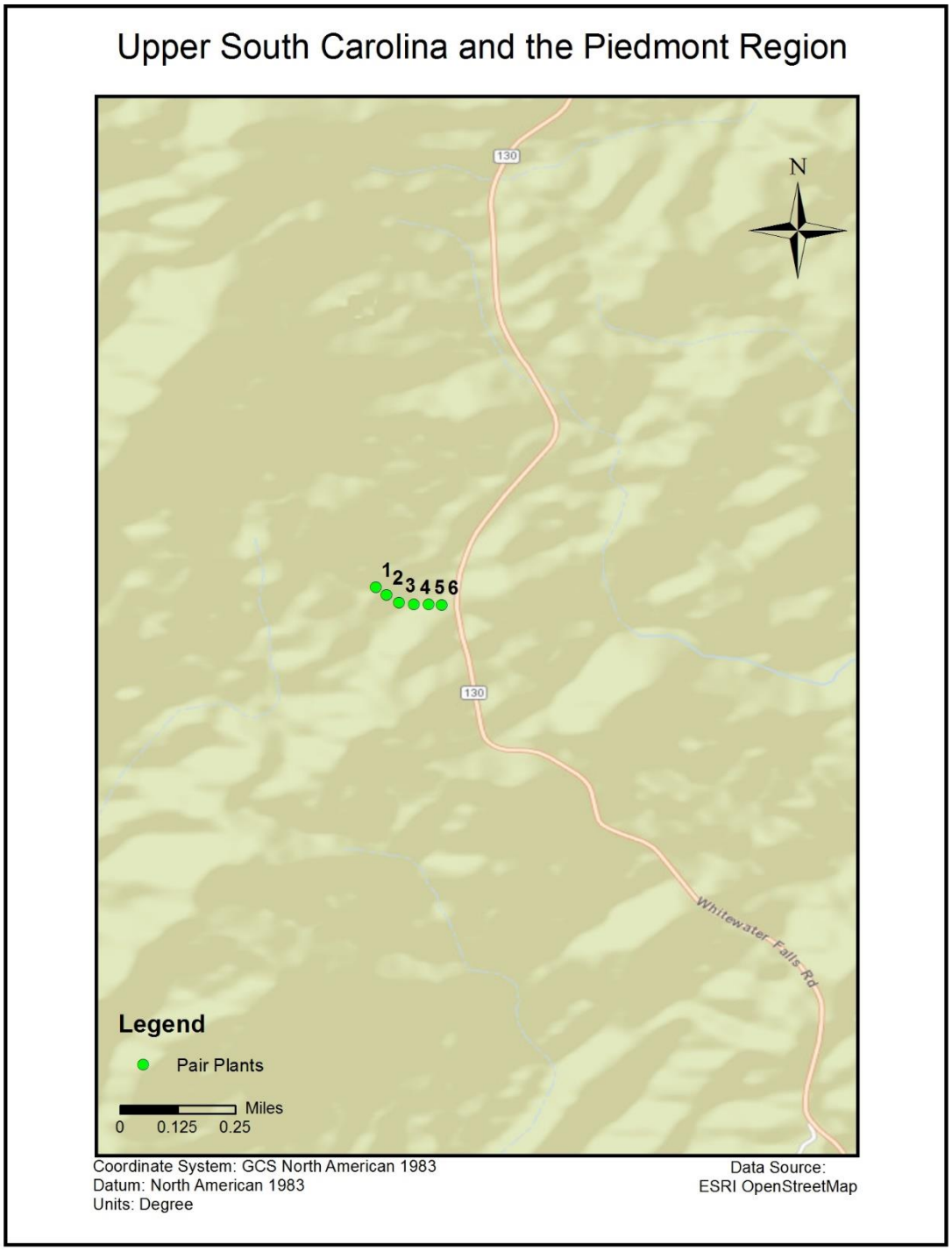

Figure 3.1. Study site pairs in longitudinal order and their respective locations in the Salem and Tamassee Quadrangle

Figure 3.2. Pair 4 of plants side by side (left - black sharpie = pine; right –red sharpie = grass).

The samples were placed on autoradiography plates to determine if the presence of radiation could be qualitatively detected. The grass plant sample-4 had detectable levels of radiation, while the loblolly pine-4 showed negative. Figure 3.3 below shows one example of a typical autoradiography plate from this study, comparing panicgrass GBP-4 and GP-4, with the smaller plate in the left showing the unexposed photo of the two and the larger the exposed plate. The darker leaves on the GBP image outlined in orange indicate the older growth, which has higher activity than newer growth (GP).

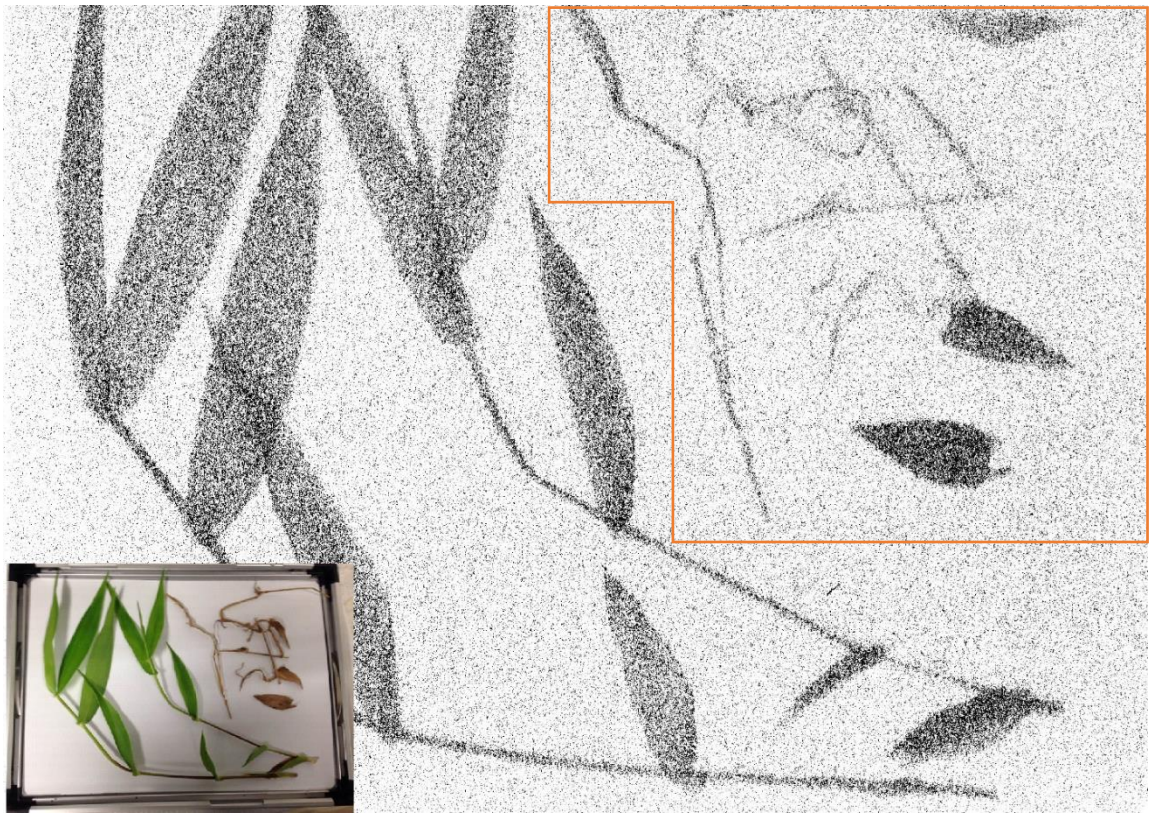

Figure 3.3. Autoradiography image of Variable panicgrass sample 4 (GP-4 & GBP-4 (orange)) where darker spots indicate more radioactivity. The unexposed photo of grass brown plant, and grass plant pair 4 on bottom left.

These qualitative results were verified using a field deployable NaI detector that detects gamma radiation (in counts per second, cps) from the surroundings (Canberra Inspector 1000). Table 3.1 below lists the measured cps for each pair, based on a five minute count time, showing all were fairly close in range with only one large spike of 1375 for GS pair-4.

Soils Results

Table 3.1 below summarizes the results from the methods used to help characterize the soils of the study site at GPS locations in Table 3.2

Table 3.1. Soils Results for pH, %OM, %WC, NaI detector, and particle size analysis.

Pair	Name	pH	%OM	%WC	Counts Per Second (cps)	%Sand	%Silt	%Clay
1	GS	5.12	6.10	1.70	800	86.67	3.33	10.00
1	PS	4.77	3.942	1.04		71.67	10.00	18.33
2	GS	5.12	6.185	1.56	752.5	81.67	13.67	4.67
2	PS	4.69	6.483	1.22		80.33	13.33	6.33
3	GS	4.93	5.187	1.38	795	81.67	13.67	4.67
3	PS	4.61	4.124	1.17		80.33	9.33	10.33
4	GS	4.48	5.623	1.33	1375	81.67	13.67	4.67
4	PS	4.47	5.911	1.29		73.67	12.67	13.67
5	GS	4.55	4.886	1.17	1050	66.67	16.67	16.67
5	PS	4.66	5.265	1.26		67.00	15.00	18.00
6	GS	4.37	4.635	1.11	900	73.33	10.00	16.67
6	PS	5.62	4.589	1.07		65.33	15.00	19.67

Table 3.2. Latitude and Longitude of sampling pairs 1 – 6.

Pair	Latitude	Longitude
1	34° 58’ 19.82”	83° 1’53.67”
2	34° 58’ 19.67”	83° 1’53.29”
3	34° 58’ 19.89”	83° 1’54.47”
4	34° 58’ 19.19”	83° 1’54.03”
5	34° 58’ 18.75”	83° 1’52.46”
6	34° 58’ 18.38”	83° 1’51.47”

As these results show, the pH, particle size analysis, %WC, and LOI did not change much from sample to sample; the average pH of the sampled soil was 4.78, with a standard deviation of 0.3. Similarly, %OM varied little among the sample plants. For a more quantitative understanding of the soil, particle size was divided into % sand, silt, and clay, the results indicating little variation in size overall as supported by the ternary diagram seen in Figure 3.4 below. As discused below, XRD of all samples confirmed the presence of monazite, quartz, vermiculite, ilite, and kaolinite. However, we were not able to perform a quantiative measure of each of these phases.

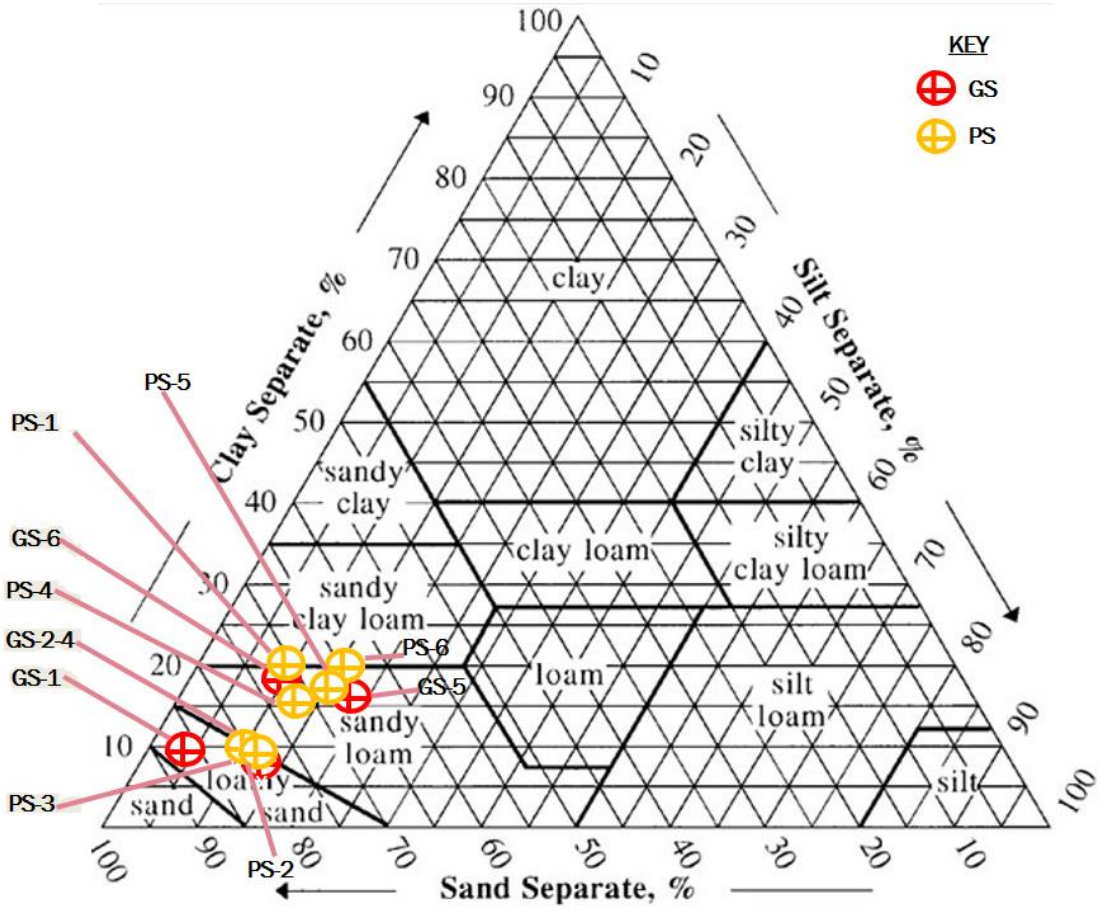

Figure 3.4. Summary of Table 3.1 particle size analysis shown on a ternary diagram. Averagely all the soils are a sandy loam.

Because of the lack of variation in particle size, it was not included as a factor in the analysis of variance. However, the pine soils appear to be slightly more clayey than the grass as the first 3 pairs in Figure 3.4 seem to contain more sands than the last 3, meaning the soil of the varaible panicgrass species has more sand by ± 5% and the loblolly pine species more clay by ± 5%.

To extend the examination of the soil characteristics, the soil samples were analyzed using XRD (Rigaku PDXL Program), with the results for sample GS-1 shown in Figure 3.5. All other XRD patterns are provided in the Appendix (A-25) and all showed similar features.

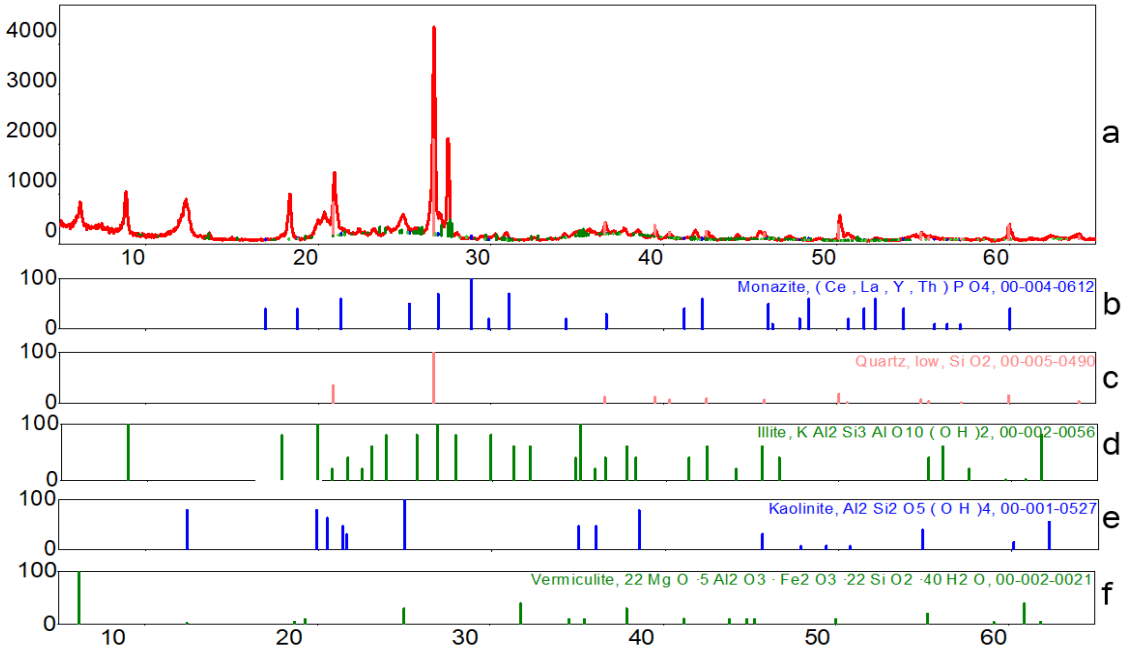

Figure 3.5. a.) XRD image of GS-1 sample with known peaks b.) Monazite, c.) Quartz, d.) Illite, e.) Kaolinite, and f.) Vermiculite spectra. The Y-axis is intensity (cps) and X-axis is 2-theta (deg).

The XRD peaks from the (a) soil sample match well with the peaks from the individual minerals, (b) monazite, (c) quartz, (d) illite, (e) kaolinite, and (f) vermiculite. For example, monazite matches fairly well at 28° – 30° peaks as well as at 42°. While peaks of other phyllosilicates are found, they are not as strong as the minerals of interest in this study. The remaining samples exhibited similar results with slight variations in the 2-theta (deg) axis of less than 3°.

To provide a more in-depth analysis of the soil of the study area, the elemental measurements reported as ppm dry soil for crystalline iron (C-Fe), amorphous iron (A-Fe), crystalline uranium (C-U), crystalline thorium (C-Th), aluminum, potassium, amorphous uranium (A-U), and amorphous thorium (A-Th) are listed in Table 3.4. Note that "crystalline" and "amorphous" U and Th are not meant to indicate the physical form of U and Th. Rather these are the concentrations of U and Th which were recovered during the crystalline and amorphous iron extractions. Table 3.3 show the values obtained from the total digestion of the soil. Results for Fe, U, and Th are not shown due to the interferences described previously. In the work described below, all reported values use the concentrations of U and Th based upon measurements of the crystalline iron extraction procedure. Similar correlations were found when comparing the U and Th concentration based upon the amorphous iron extraction.

Table 3.3. Soils Results for Total [Al], [K], and [Ca] mg / kg soil (ppm) during the first ICP-MS run.

Pair	Name	Al	K	Ca
1	GS	7.31×10^2	5.59×10^3	1.65×10^3
1	PS	8.36×10^2	6.07×10^3	1.82×10^3
2	GS	1.08×10^3	7.58×10^3	9.57×10^2
2	PS	4.42×10^2	5.68×10^3	1.66×10^3

3	GS	9.24×10^2	7.50×10^3	2.22×10^3
3	PS	5.03×10^2	5.74×10^3	1.75×10^3
4	GS	4.45×10^2	6.56×10^3	2.20×10^3
4	PS	7.84×10^2	6.13×10^3	1.92×10^3
5	GS	5.67×10^2	6.37×10^3	2.47×10^3
5	PS	2.31×10^2	3.58×10^3	2.22×10^3
6	GS	6.09×10^2	6.15×10^3	2.12×10^3
6	PS	4.35×10^2	5.84×10^3	3.86×10^3

Table 3.4. Soils Results for crystalline and amorphous extractions for [Fe], [U], [Th], and their respective %RSD in mg / kg soil (ppm). C = crystalline extraction, A = amorphous extraction, and RSD = relative standard deviation (calculated as the relative standard deviation of triplicate ICP-MS measurements of the same sample).

Pair	**Name**	**C-Fe**	**C-U**	**C-Th**	**C-Fe %RSD**	**C-U %RSD**	**C-Th %RSD**
1	GS	5.23×10^4	9.85	1.24×10^2	2.60	0.74	1.97
1	PS	3.39×10^4	4.23	7.01×10^1	0.85	1.19	0.39
2	GS	4.95×10^4	9.37	1.14×10^2	0.82	1.10	1.05
2	PS	3.24×10^4	4.79	7.10×10^1	0.42	0.90	0.51
3	GS	4.02×10^4	6.46	1.17×10^2	4.24	5.04	4.37
3	PS	2.69×10^4	3.96	7.53×10^1	0.41	1.08	0.44
4	GS	5.65×10^4	13.4	2.63×10^2	1.01	0.56	1.00
4	PS	3.56×10^4	5.37	9.04×10^1	1.97	2.40	2.74
5	GS	6.71×10^4	10.5	2.48×10^2	1.32	1.33	1.92
5	PS	4.89×10^4	6.70	1.49×10^2	0.85	2.1	0.91
6	GS	6.74×10^4	11.0	2.24×10^2	1.00	1.04	1.46
6	PS	4.87×10^4	5.46	1.18×10^2	3.51	4.28	4.09
Pair	**Name**	**A-Fe**	**A-U**	**A-Th**	**A-Fe %RSD**	**A-U %RSD**	**A-Th %RSD**
1	GS	2.66×10^4	9.44	1.17×10^2	0.86	1.31	0.42
1	PS	5.07×10^4	6.68	8.71×10^1	2.21	1.96	2.29
2	GS	3.10×10^4	9.36	1.09×10^2	0.96	1.72	0.56
2	PS	4.09×10^4	7.97	1.36×10^2	0.96	1.82	1.24
3	GS	1.89×10^4	6.59	9.04×10^1	0.71	0.54	0.67
3	PS	3.07×10^4	6.12	8.64×10^1	0.39	1.46	0.60
4	GS	2.14×10^4	14.8	2.77×10^2	0.54	0.86	0.37
4	PS	2.74×10^4	6.74	1.08×10^2	0.58	1.29	0.40
5	GS	2.48×10^4	10.9	2.50×10^2	0.06	0.43	0.35
5	PS	4.41×10^4	7.57	1.64×10^2	0.64	1.18	0.37
6	GS	2.44×10^4	11.6	2.31×10^2	0.13	0.97	1.02
6	PS	2.79×10^4	6.31	1.31×10^2	1.15	2.93	0.47

The soil concentrations from Table 3.4 were graphed with the characteristics from Table 3.1 in order to determine trends and relationships. The results reported here focus on the concentrations of thorium, uranium, and iron in relation to one another as these are of particular interest to this work. As most of these graphs showed minimal relationships, only one example showing the relationship among thorium, uranium, and organic matter is given in Figure 3.6 below; others showing similar relationships can be found in Appendix A. The lack of correlation between U and Th concentrations and the soil parameters pH, particle size, and organic matter content is thought to be due to the limited range of measured values. While greater variability was expected, all samples came from within approxiamtely 50 meters of each other. Therefore, these may be indicative of a fairly homogenous distribution at the site.

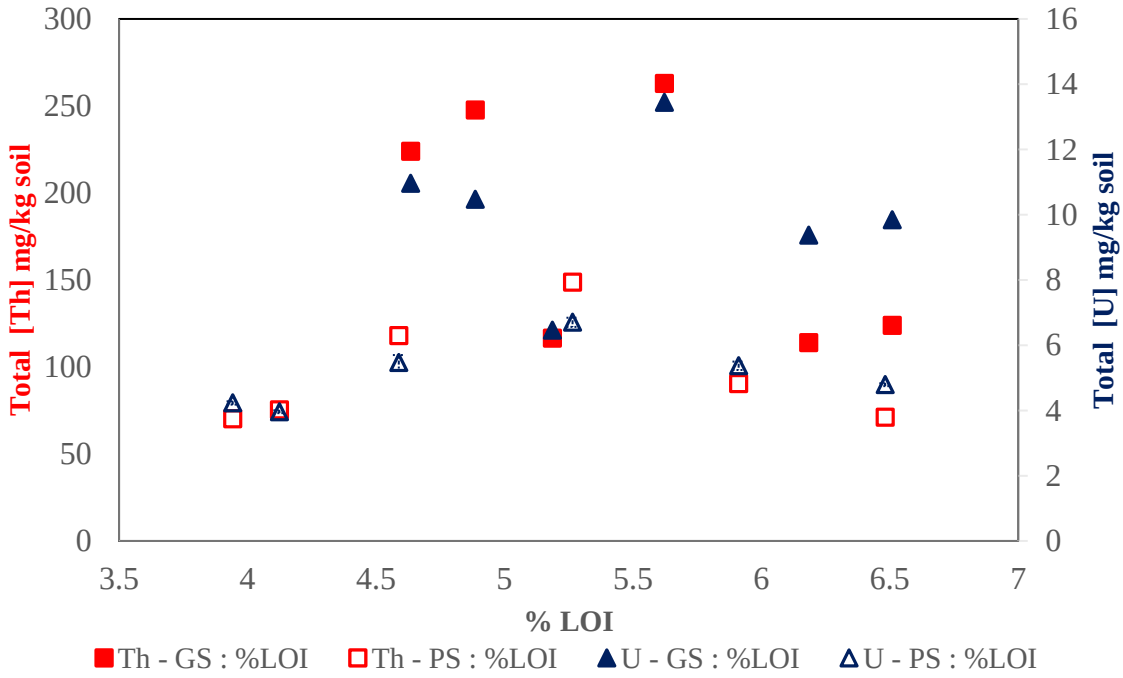

Figure 3.6. Total thorium and uranium in ppm to LOI of corresponding grass and pine soils.

The most noteworthy relationship found is that variable panicgrass soils generally measure higher thorium and uranium concentrations than the loblolly pine (Figure 3.6). This trend is also evident in the thorium and uranium soil concentrations in relation to particle sizes, and thorium, uranium, and iron. For the specific graphs see Appendix A-3, A-6, A-8, and A-9.

The most interesting trends were found between thorium and uranium and amorphous and crystalline iron. These relationships for the both soils are seen in Figure 3.7 and 3.8. Figure 3.7 shows thorium and uranium graphed to their corresponding amorphous iron soil. As this figure shows, as amorphous iron increases in the soil, the measured thorium and uranium decreases. However, the variable panicgrass soil does not exhibit this trend as obviously as the loblolly pine. Similarly, Figure 3.8 compares crystalline iron to thorium and uranium.

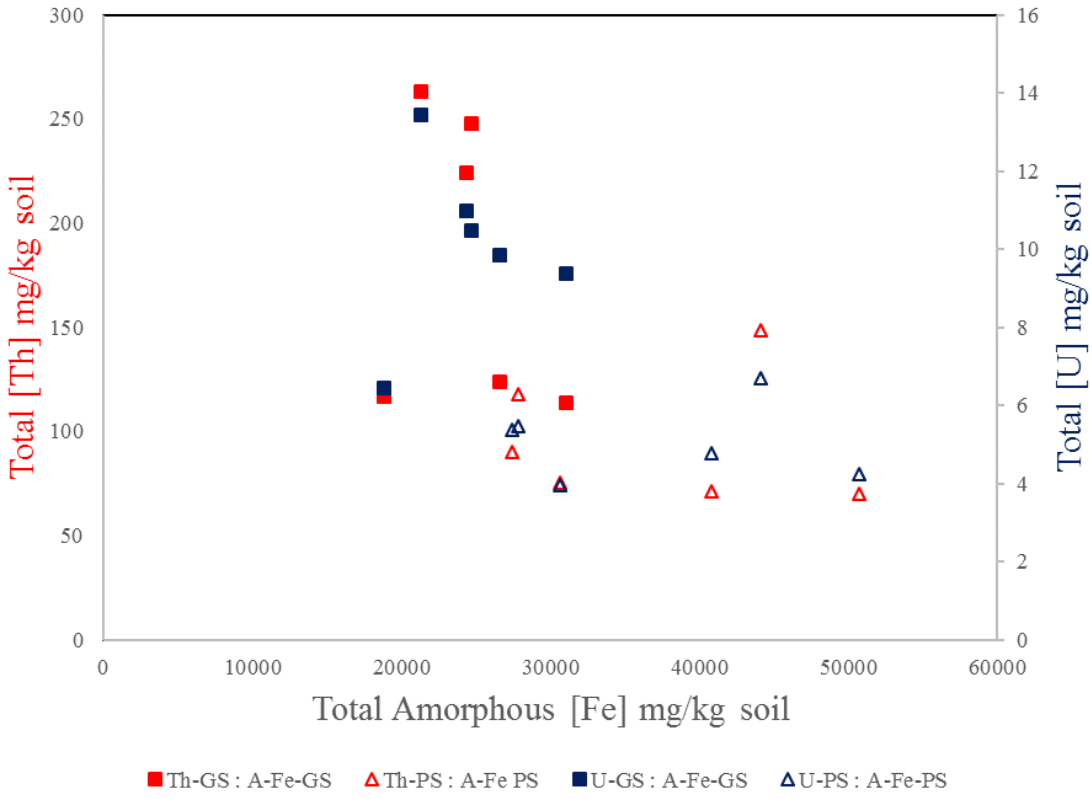

Figure 3.7. Total thorium and uranium (ppm) in all soils plotted against total amorphous iron (ppm) in corresponding soils.

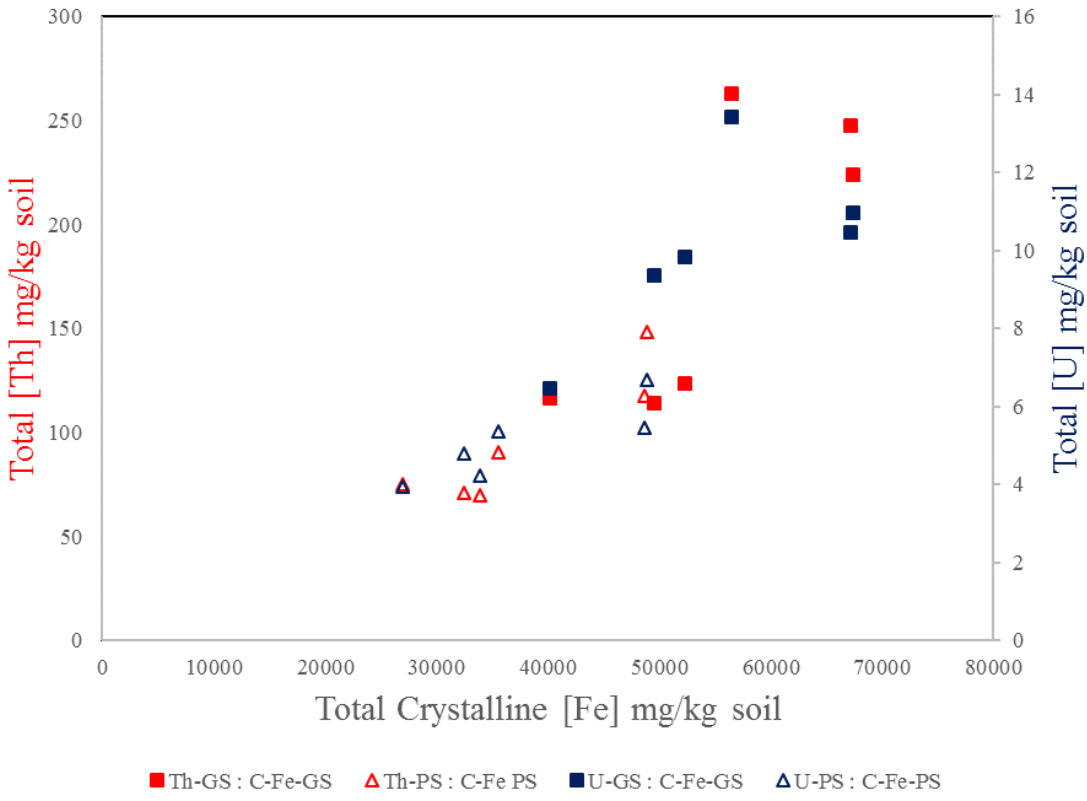

Figure 3.8. Total thorium and uranium (ppm) in all soils to total crystalline iron (ppm) in corresponding soils.

Looking closer at both Figures 3.7 and 3.8 they can be graphed similarly, to identify any trends. These relationships for the grass soils are seen in Figure 3.9. As this figure shows, the R^2 values of these trends are not acceptable (<0.8) although there seems to be a slight positive slope for thorium in variable panicgrass soils to the crystalline iron and a negative slope for both thorium and uranium in variable panicgrass soils to amphorous iron. The thorium and uranium concentrations in the pine soils graphed to these two types of irons also exhibited slightly positive for crystalline iron in pine soil,

while amorphous was practically no slope. The one exception is the relationship of thorium in pine soils to crystalline iron, which had an acceptable $R^2 = 0.8195$ and a moderately small positive slope (Appendix A-2).

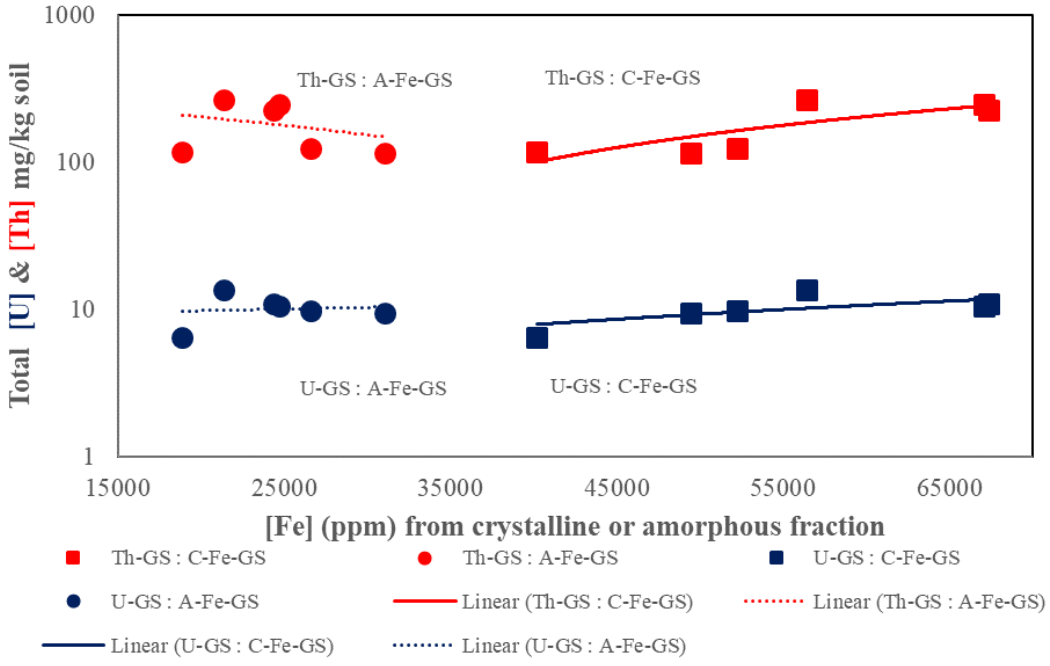

System	R^2 and Slope
Th-GS : A-GS-Fe	0.0883, -5.0×10^{-3}
Th-GS : C-GS-Fe	0.6215, 5.3×10^{-3}
U-GS : A-GS-Fe	0.0096, -5.0×10^{-5}
U-GS : C-GS-Fe	0.4291, 1.0×10^{-4}

Figure 3.9. Calculated Total [Th] and [U] mg/kg grass soil (ppm) to total crystalline (C) and amorphous (A) [Fe] mg/kg grass soil.

As crystalline iron increases in the soils, both the uranium and thorium also increase. These two graphs indicate higher thorium and uranium in the variable panicgrass soils than in the loblolly pine, results supported by the previous six analyses. However, there is no indication of the reason for this difference.

Plants Results

Table 3.5 below summarizes the elemental analysis of the plants including the %WC and organic matter content determined by LOI as well as the measured concentrations of iron, thorium, uranium, aluminum, potassium, and calcium. For a fuller understanding of these relationships, this study graphed the thorium, uranium, and iron to the pine and grass, comparing these values to their respected soils. We include a representative sample of the most pertinent graphs below. The remainder can be found in Appendix B-7 through B-13. Figure 3.10 below compares the total uranium on a log scale with the percentage LOI of the pine soils (PS), important because the initial stage of uptake is possible only from the ground. This graph indicates no strong positive or negative trends, the one possibility being the uranium concentration in pine root compared to the %LOI of PS, with an $R^2 = 0.66$. However, there is clear order of magnitude of difference between concentrations in pine shoot compared to the pine root, a result also seen in the thorium and iron in the pine samples (see Appendix B-1). Similarly, the grass shoots exhibited the same trends, with grass roots being higher in concentration in comparison to senesced shoots and grass shoots (Appendix B-2).

*Table 3.5. Plant Results for %WC, %OM, and Total [Fe], [U], [Th], [Al], [P], [K], [Ca] mg / kg dry plant (ppm). ** Indicates experiment error.*

Pair	Name	%WC	%OM	Fe	U	Th	Al	K	Ca
1	GBP	7.0	89.0	9.11×10^{2}	6.06×10^{-1}	3.41	2.92×10^{3}	5.43×10^{3}	3.16×10^{3}
1	GP	8.0	90.0	1.59×10^{2}	7.69×10^{-2}	4.94×10^{-1}	3.98×10^{2}	3.53×10^{4}	2.70×10^{3}
1	GR	23.5	**	1.91×10^{4}	1.38×10^{1}	8.03×10^{1}	4.53×10^{4}	1.40×10^{4}	6.36×10^{3}
1	PP	8.3	96.9	4.46×10^{1}	1.94×10^{-2}	1.12×10^{-1}	3.99×10^{2}	6.14×10^{4}	2.66×10^{3}
1	PR	14.2	72.6	1.40×10^{3}	1.43	8.07	3.45×10^{3}	1.86×10^{3}	1.50×10^{3}
2	GBP	7.0	90.2	3.83×10^{2}	2.15×10^{-1}	1.31	9.81×10^{2}	1.74×10^{3}	1.87×10^{3}
2	GP	8.5	89.8	1.86×10^{2}	7.85×10^{-2}	5.13×10^{-1}	4.79×10^{2}	4.36×10^{4}	3.13×10^{3}
2	GR	10.2	71.5	5.03×10^{3}	3.37	2.03×10^{1}	1.11×10^{4}	7.35×10^{3}	4.58×10^{3}
2	PP	8.9	91.5	2.86×10^{1}	8.16×10^{-3}	4.47×10^{-2}	2.66×10^{2}	3.50×10^{4}	2.68×10^{3}
2	PR	16.4	89.2	6.19×10^{3}	4.53	2.59×10^{1}	1.66×10^{4}	7.79×10^{3}	4.20×10^{3}
3	GBP	5.7	79.0	2.70×10^{3}	1.34	9.86	6.01×10^{3}	2.19×10^{3}	3.78×10^{3}
3	GP	7.8	88.8	2.02×10^{2}	9.55×10^{-2}	6.44×10^{-1}	5.17×10^{2}	2.84×10^{4}	2.08×10^{3}
3	GR	8.7	51.5	3.71×10^{3}	2.44	1.65×10^{1}	7.24×10^{3}	2.40×10^{3}	1.60×10^{3}
3	PP	8.8	95.9	4.39×10^{1}	1.82×10^{-2}	5.95×10^{-2}	1.56×10^{2}	7.04×10^{4}	2.08×10^{3}
3	PR	12.0	75.5	3.46×10^{3}	2.30	1.75×10^{1}	7.27×10^{3}	4.05×10^{3}	1.70×10^{3}
4	GBP	6.3	94.0	2.10×10^{2}	1.11×10^{-1}	1.27	5.79×10^{2}	4.73×10^{3}	3.15×10^{3}
4	GP	8.5	90.9	1.05×10^{2}	3.55×10^{-2}	4.17×10^{-1}	1.84×10^{2}	3.99×10^{4}	2.27×10^{3}
4	GR	12.6	57.7	4.90×10^{3}	4.11	4.04×10^{1}	1.06×10^{4}	5.00×10^{3}	1.83×10^{3}
4	PP	7.8	91.8	5.47×10^{1}	1.25×10^{-2}	8.02×10^{-2}	1.45×10^{2}	3.31×10^{4}	1.94×10^{3}
4	PR	13.1	67.2	4.31×10^{3}	4.30	2.91×10^{1}	9.31×10^{3}	2.09×10^{3}	1.55×10^{3}
5	GBP	7.0	91.4	6.78×10^{2}	3.47×10^{-1}	4.66	1.64×10^{3}	2.39×10^{3}	1.70×10^{3}
5	GP	10.0	86.1	1.99×10^{2}	8.68×10^{-2}	1.13	4.82×10^{2}	4.02×10^{4}	2.12×10^{3}
5	GR	11.8	68.4	4.26×10^{3}	3.13	3.97×10^{1}	9.01×10^{3}	6.44×10^{4}	1.28×10^{3}
5	PP	8.3	78.3	1.29×10^{1}	6.77×10^{-3}	6.20×10^{-2}	5.35×10^{1}	9.92×10^{3}	4.59×10^{2}
5	PR	13.8	82.8	2.65×10^{3}	1.88	2.16×10^{1}	5.79×10^{3}	1.93×10^{3}	7.39×10^{2}
6	GBP	6.8	94.6	2.25×10^{2}	9.86×10^{-2}	1.15	5.83×10^{2}	4.98×10^{3}	1.94×10^{3}
6	GP	7.6	92.4	7.17×10^{1}	3.01×10^{-2}	3.25×10^{-1}	1.74×10^{2}	1.64×10^{4}	9.24×10^{2}
6	GR	13.2	63.9	5.16×10^{3}	3.68	4.08×10^{1}	1.13×10^{4}	2.89×10^{3}	1.36×10^{3}
6	PP	8.6	76.2	5.68	2.45×10^{-3}	1.45×10^{-2}	4.94×10^{1}	5.69×10^{3}	4.27×10^{2}
6	PR	10.7	76.8	4.51×10^{3}	3.26	3.26×10^{1}	9.77×10^{3}	1.98×10^{3}	9.56×10^{2}

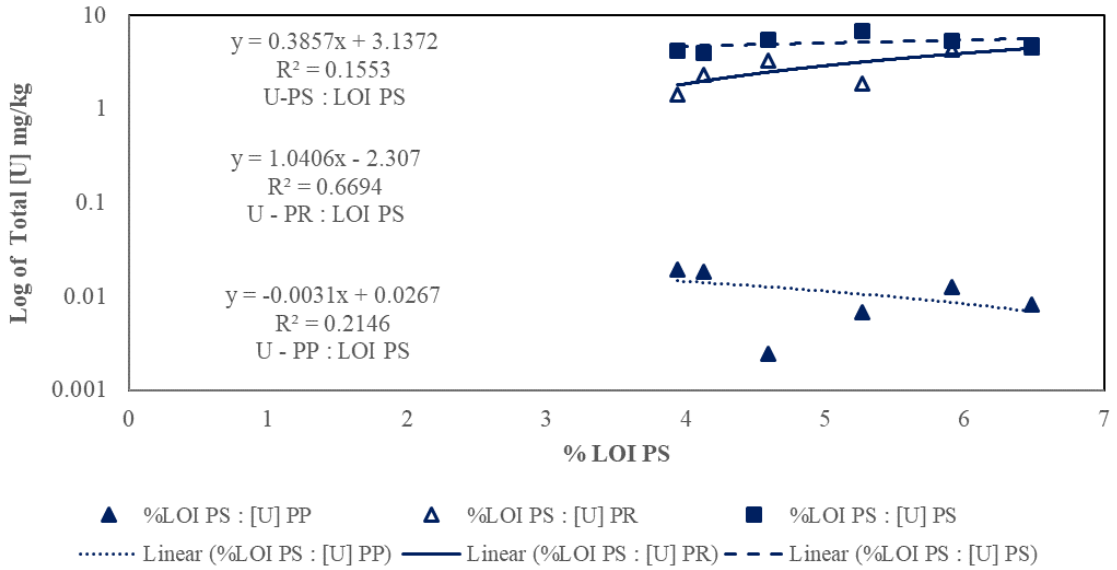

Figure 3.10. Total [U] mg / kg soil (ppm) to %LOI in pine soil for pine plant and pine root.

A plot of U and Th concentrations in the pine roots versus amorphous and crystalline iron in the soil is shown in Figure 3.11. None of the relationships graphed in Figure 3.11 exhibit an acceptable R^2 value. However, uranium in the pine root exhibits negative slopes for both types of iron while thorium exhibits a positive slope with crystalline iron and a negative one for amorphous. Moreover, as the iron concentration in soil increases, there is no evidence of an increase in uranium or thorium in pine roots.

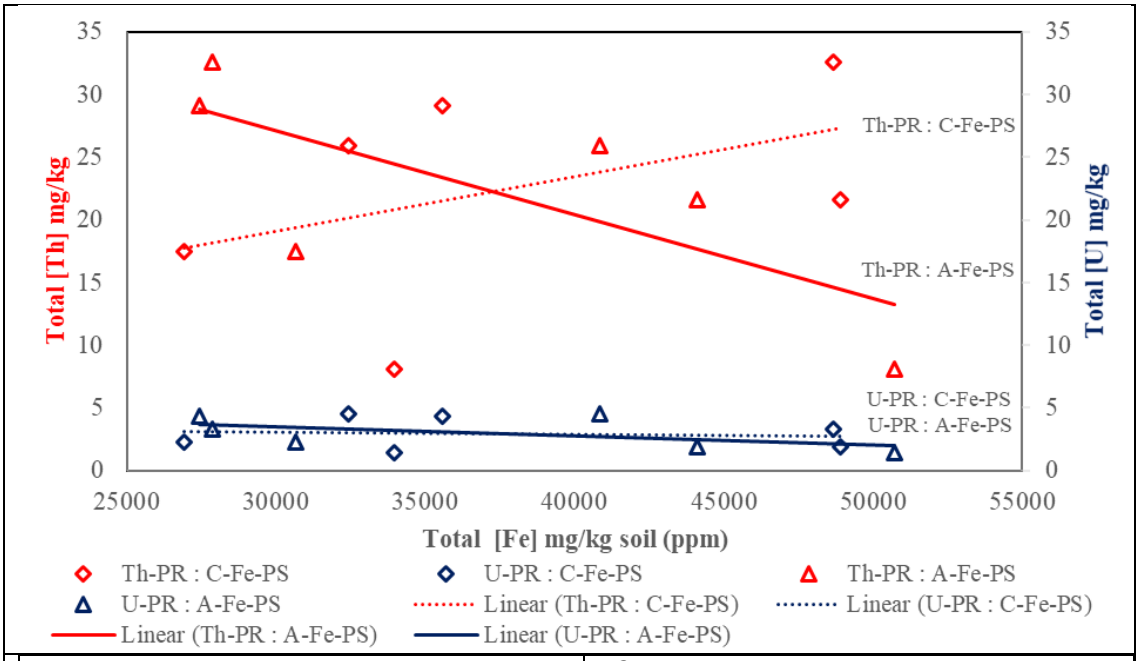

System	R^2 and Slope
Th-PR : C-PS-Fe	0.1953, 4.0×10^{-4}
Th-PR : A-PS-Fe	0.5413, -7.0×10^{-4}
U-PR : C-PS-Fe	0.0148, -2.5×10^{-5}
U-PR : A-PS-Fe	0.2966, -7.0×10^{-5}

Figure 3.11. Total [Th & U] mg/kg root against total crystalline and amorphous [Fe] mg/kg soil.

Comparing thorium and uranium within the pine shoot to iron in the pine root, and thorium and uranium in the pine root to iron in the pine root yielded similar trends to Figure 3.9 in soils. Figure 3.12 indicates a positive slope when graphing uranium and thorium in the pine root versus iron, with a R^2 value of 0.8463 for uranium. Thus, there may be a relationship between iron and uranium associated with the roots. This could be due to uranium adsorbing onto the iron associate with the roots or due to some physiological phenomena.

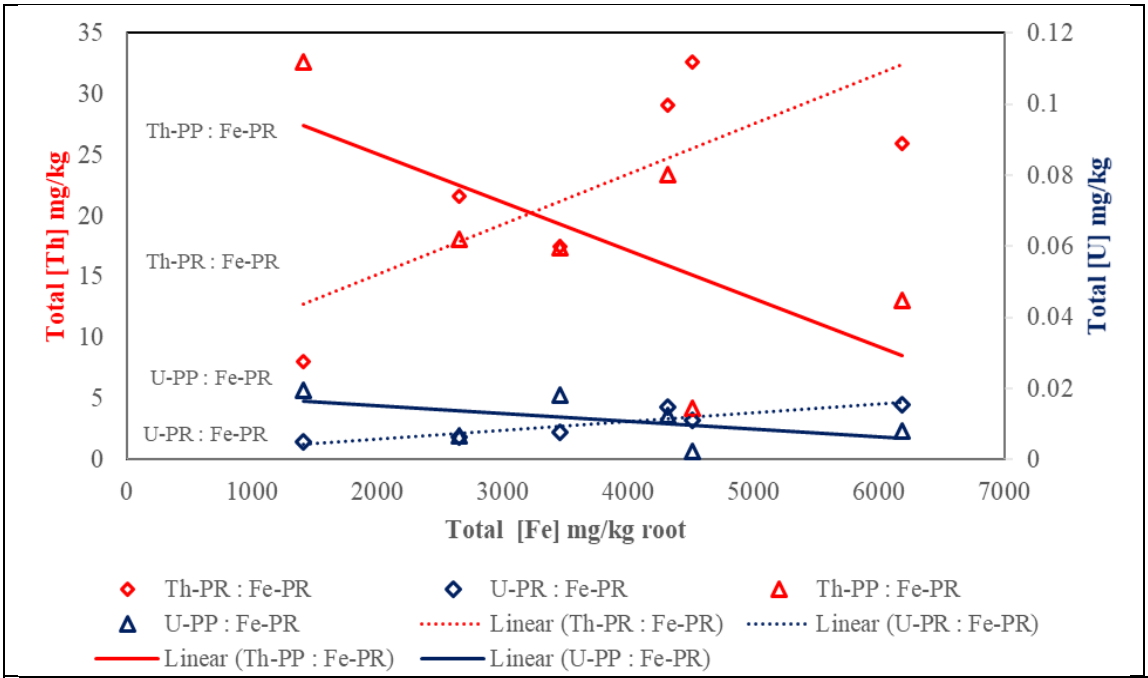

System	R^2 and Slope
Th-PP : Fe-PR	0.4634, -1.0×10^{-5}
Th-PR : Fe-PR	0.5888, 4.1×10^{-3}
U-PP : Fe-PR	0.2909, -2.0×10^{-6}
U-PR : Fe-PR	0.8463, 7.0×10^{-4}

Figure 3.12. Graph shows the Total [U] mg/kg plant (ppm) and Total [Th] mg/kg plant (ppm) against Total [Fe] mg/kg soil (ppm) in soil for pines.

Figure 3.13 shows the relationship between thorium and uranium in grass roots and iron in grass roots and thorium and uranium in the grass root to iron in the grass soil. The largest R^2 value is found for the comparision of uranium in the grass root with the iron in the grass root. In addition, there are positive slopes for thorium and uranium in grass roots compared to iron in grass roots of amorphous iron in the grass soil. However, there is not a strong R^2 value for thorium and uranium compared to amphorous iron in the grass soil (see Appendix B-3 for the comparison with crystalline iron). The similar relationships for pine can be found in Appendix B-4.

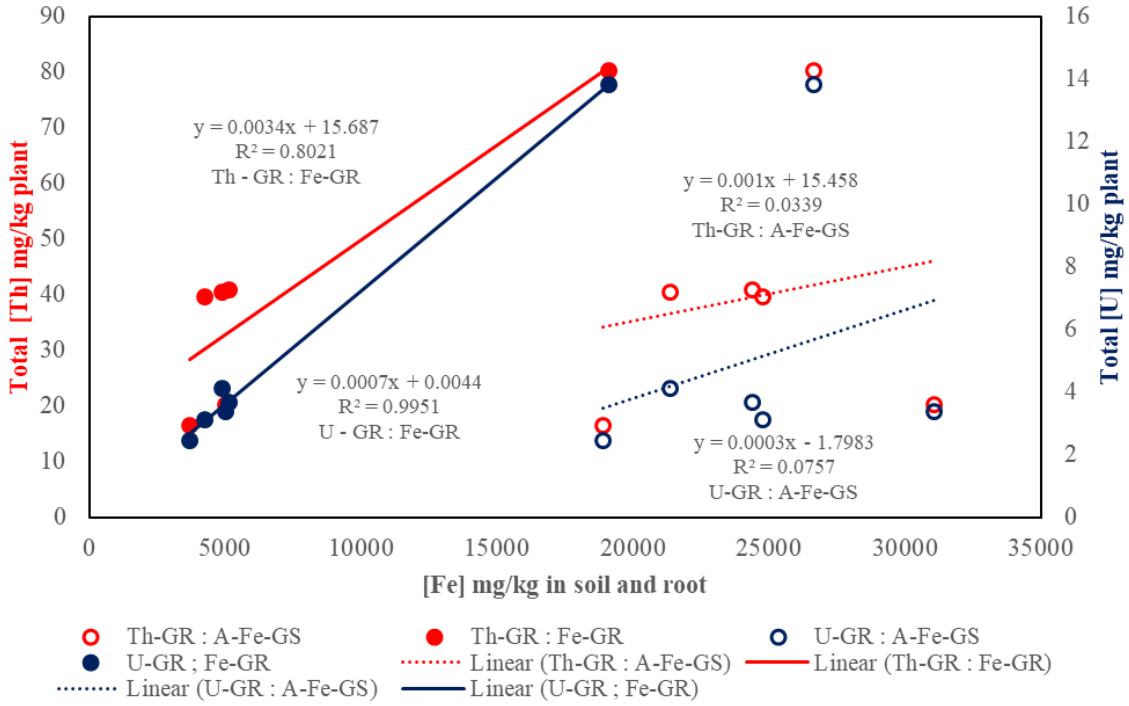

Figure 3.13. Graph shows the Total [U] mg/kg plant and Total [Th] mg/kg plant against Total [Fe] mg/kg root.

Figure 3.14 compares thorium and uranium in the shoots versus iron in the shoots for both the grass and pine plants. The relationship between the thorium and iron in the grass shoot, and thorium and uranium to iron in the pine all have weak R^2 values even though the slopes are positive. Uranium compared to iron in the grass shoot exhibited the strongest R^2 value, $R^2 = 0.95$, as well as a positive slope. Because all fours slopes are positive, an increase in iron in the shoots of the plants increases the thorium and uranium in both grass and pine plants. The stronger relationship between uranium and iron for the grass shoot could indicate a correlated uptake mechanism for uranium in the grass (discussed below).

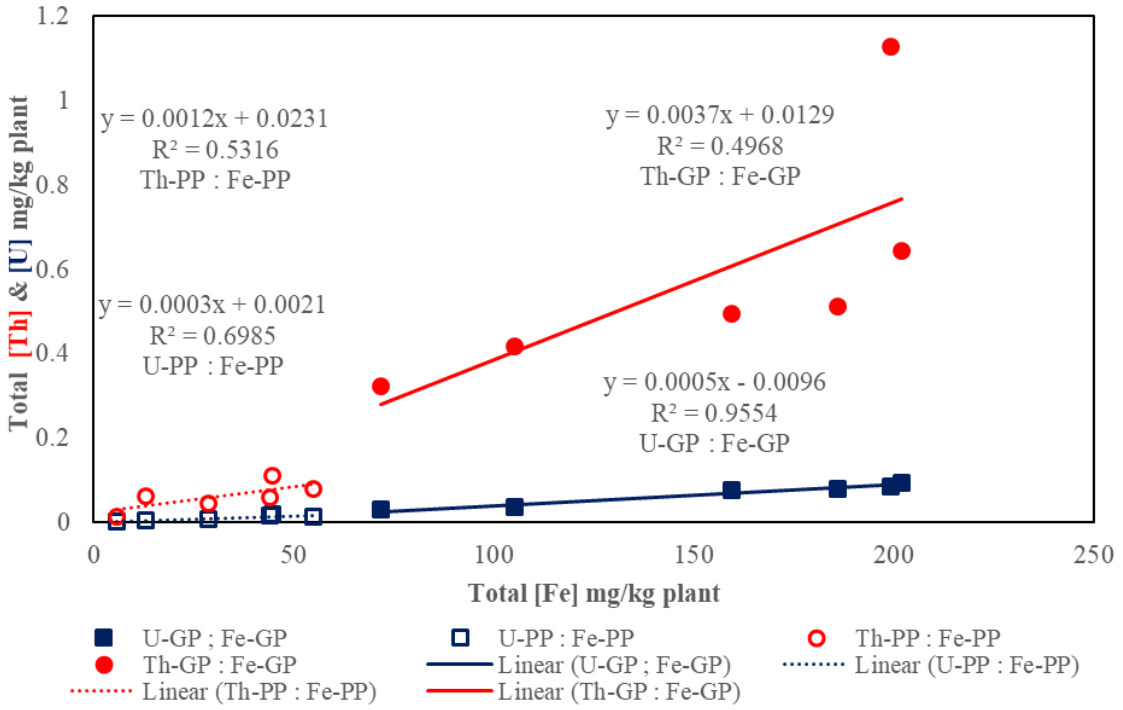

Figure 3.14. Graph shows the Total [U] mg/kg plant and Total [Th] mg/kg plant against Total [Fe] mg/kg plant.

Table 3.6 below summarizes the relationships between thorium and uranium graphed to iron and themselves, as a element to element ratio. These ratios are calculated by the slope of an element of interest to iron (in this case) in the same plant section. All relationships have positive slopes and are within the same magnitude, even across the different order of magnitudes of iron. Thus, there does appear to be a relationship between uranium and thorium concentrations in the plant and iron.

Table 3.6. Element to element ratio s of uranium and thorium in plants and roots by iron indicated by R^2 and slope for the different plant types.

	Uranium			Thorium		
Phase	**R^2**	**Slope**	**Standard Error**	**R^2**	**Slope**	**Standard Error**
GBP / Fe-GBP	.9826	5.0×10^{-4}	6.95×10^{-2}	.9392	3.5×10^{-3}	9.32×10^{-1}
GP / Fe-GP	.9554	5.0×10^{-4}	$6.50\ 10^{-3}$	.4968	3.7×10^{-3}	2.26×10^{-1}

GR / Fe-GR	.9951	7.0×10^{-4}	3.39×10^{-1}	.8021	3.4×10^{-3}	1.13×10^{1}
PP / Fe-PP	.6983	3.0×10^{-4}	4.10×10^{-3}	.5316	1.2×10^{-3}	2.51×10^{-2}
PR / Fe-PR	.8463	7.0×10^{-4}	5.65×10^{-1}	.5888	4.1×10^{-3}	6.34

The average and standard deviation of the concentration ratios (CR) for thorium, uranium, and iron in GBP, GP, and GR in relation to the crystalline and amorphous iron in the GS are shown in Table 3.7 (Calculated using Equation 1.1 for each element of interest). As this table shows, the grass takes up and translocates more uranium and thorium than iron across GBP/GS, GP/GS, and GR/GS as indicated by the comparative CRs. There is an order of magnitude difference in the concentrations of elements when comparing the grass root to senesced shoots, which is manifested in the higher CR for the senesced grass shoots compared to the grass plant, indicating signs accumulation.

Table 3.7 The average and standard deviations of concentration ratios for each grass type (GBP/GS) for both Crystalline and Amorphous iron digestion techniques.

Element	Phases for CR	Avg CR and Std Dev for crystalline iron	Avg CR and Std Dev for amorphous iron
Uranium	GBP/GS	$5.7 \times 10^{-2} \pm 7.6 \times 10^{-2}$	$5.6 \times 10^{-2} \pm 7.5 \times 10^{-2}$
	GP/GS	$7.4 \times 10^{-3} \pm 4.5 \times 10^{-3}$	$7.3 \times 10^{-3} \pm 4.5 \times 10^{-3}$
	GR/GS	$5.1 \times 10^{-1} \pm 4.4 \times 10^{-1}$	$5.1 \times 10^{-1} \pm 4.7 \times 10^{-1}$
Thorium	GBP/GS	$2.5 \times 10^{-2} \pm 3.0 \times 10^{-2}$	$3.0 \times 10^{-2} \pm 4.0 \times 10^{-2}$
	GP/GS	$3.6 \times 10^{-3} \pm 1.7 \times 10^{-3}$	$3.9 \times 10^{-3} \pm 2.2 \times 10^{-3}$
	GR/GS	$2.4 \times 10^{-1} \pm 2.0 \times 10^{-1}$	$2.6 \times 10^{-1} \pm 2.1 \times 10^{-1}$
Iron	GBP/GS	$1.8 \times 10^{-2} \pm 2.5 \times 10^{-2}$	$3.9 \times 10^{-2} \pm 5.2 \times 10^{-2}$
	GP/GS	$3.0 \times 10^{-3} \pm 1.4 \times 10^{-3}$	$6.4 \times 10^{-3} \pm 2.7 \times 10^{-3}$
	GR/GS	$1.3 \times 10^{-1} \pm 1.2 \times 10^{-1}$	$2.8 \times 10^{-1} \pm 2.1 \times 10^{-1}$

Table 3.8 shows the average and standard deviation of the concentration ratios of thorium, uranium, and iron in the pine shoot and root in relation to amorphous and crystalline iron in the pine soil. Appendix Figures B-5 and B-6 show visual representations of Tables 3.7 and 3.8. The small CR and standard deviation in the pine plant for thorium indicates little to no uptake into the shoots. In addition, higher concentrations of all three elements are found in the root than in the shoot. In contrast, the grass shoot exhibit a slightly higher CR average in the crystalline extraction than the amorphous. While the standard deviation is low, both the pine root and grass root CR are relatively similar, only differing from their corresponding shoots.

Table 3.8. The average and standard deviations of concentration ratio's for each pine type (PP/PS) for both Crystalline "C" and Amorphous "A" digestion techniques.

Element	Phases for CR	Avg CR and Std Dev for crystalline iron	Avg CR and Std Dev for amorphous iron
Uranium	PP/PS	$2.4 \times 10^{-3} \pm 1.8 \times 10^{-3}$	$1.7 \times 10^{-3} \pm 1.1 \times 10^{-3}$
	PR/PS	$5.9 \times 10^{-1} \pm 2.6 \times 10^{-1}$	$4.3 \times 10^{-1} \pm 1.7 \times 10^{-1}$
Thorium	PP/PS	$7.4 \times 10^{-4} \pm 5.0 \times 10^{-4}$	$5.9 \times 10^{-4} \pm 4.1 \times 10^{-4}$
	PR/PS	$2.4 \times 10^{-1} \pm 9.8 \times 10^{-2}$	$1.9 \times 10^{-1} \pm 6.7 \times 10^{-2}$
Iron	PP/PS	$9.6 \times 10^{-4} \pm 6.5 \times 10^{-4}$	$9.2 \times 10^{-4} \pm 6.9 \times 10^{-4}$
	PR/PS	$1.0 \times 10^{-1} \pm 5.5 \times 10^{-2}$	$1.1 \times 10^{-1} \pm 5.6 \times 10^{-2}$

CHAPTER FOUR

Elemental Analysis Discussion

The averages and standard deviations of CRs from the variable panicgrass and loblolly pine show three important results. First there is a greater concentration of thorium, uranium, and iron in the root versus the shoot for both plants. Secondly, there is an indication of accumulation due to higher concentrations of thorium, uranium, and iron in the senesced shoots compared to the grass shoot (GBP to GP). Third, when comparing both CR from crystalline and amorphous iron, the shoot systems decreased in CR from GBP, GP, to PP. However, these CRs could change due to a strong influence of amorphous and crystalline iron. The results also showed with an increasing amorphous iron concentration in soil that less thorium and uranium were measured, oppositely of crystalline iron fraction. To highlight and compare these results we discuss them similarly to chapter three result's soil and plant discussion to support, deny, or not confirm our hypothesis.

Soil Discussions

Identifying the various possible trends in the soil parameters the %WC, organic matter content, particle size, pH, mineralogy, and elemental concentrations of: calcium, potassium, and aluminum in the soils are all relatively similar indicating a relatively high degree of homogeneity in the site. Thus, hypothesis 1 could not be fully evaluated because there is not a large enough variation of the parameters of interest to indicate the presence of a trend. Figures A-3 through A-26 exhibit how these variables were similar without being controlled through benchtop experiments.

Sheppard and Evenden (1988) showed that micro, meso, and macro scales exist affecting thorium and uranium concentrations. Possible macro-scale scenarios are the upward migration of radionuclides in water going through the plant roots and to the leaves. This study has a similar macro to meso scale which exhibited little interference with the surroundings. These few interferences are assumed because the plant was healthy, continuously growing, and metabolically active. Through the homogeneities in amorphous and crystalline iron concentrations this study focuses on investigating the possible relationships of uranium and thorium uptake into the plants. With few variations across %WC, LOI, pH, XRD, and radioactivity, both plants have less possibilities to uptake their nutrients thus, the environment became the controlling factor. The potentially influencing factors and their homogeneity can be seen in Figures A-3 – A-26.

On the micro scale organic matter content of soils could have been a better indicator, if it exhibited higher organics possibly eluding to more specialized phytosiderophores or chelators within the soil. Similarly, within Figure 3.6 the uranium and thorium graphed against their corresponding organic matter content shows no strong indicator of increased thorium or uranium to higher organic matter. We concluded that from this graph there was little change in organic matter content between these soils, and showed no particular effect for thorium and uranium uptake. Our hypothesis is that the organic matter fraction contains strongly complexing ligands which could solubilize urnaium and thorium and lead to greater plan uptake. If soil was rich in organic matter there could be potentially be enhanced uptake into the root. For example, the use of a bacterial siderophores like DFOB (Desferrioxamine B) in root studies showed larger

upward mobility into the root xylem (Ely et al., 2016). However, using LOI as a proxy for organic matter content does not have sufficient resolution to determine if such reactive ligands are influencing this system.

Part of hypothesis 1 can be evaluated by Figure 3.7. The figure compares thorium and uranium in grass soil to crystalline and amorphous iron in corresponding soil, showing thorium and uranium fit better to crystalline iron. There were large differences in measured concentrations of amorphous iron and crystalline iron in grass soils when compared to very similar crystalline and amorphous iron in pine soils (A-21-22). Both soils have very similar pH, XRD, and particle sizes, thus there should be some other factor outside the geology and chemistry roles affecting different iron, thorium, and uranium concentrations. The difference in iron concentrations are most likely from the microenvironments of the soils though it is also possible that the plants have impacted the iron availability, potentially by depleting the more soluble amorphous iron fraction. For example, the microenvironment is most likely due to the difference of strategy 1 versus strategy 2 plants. The graminaceous strategy 2 plant (variable panicgrass) is more effective at uptaking iron instead of the chelators and reductases' of strategy 1 plants. However, Figure 3.7 showed thorium and uranium fit more positively to crystalline iron regardless of it's uptake strategy.

Figure 3.8 and 3.9 exhibit two unique trends regarding the uptake strategy of graminaceous versus non-graminaceous plants. Figure 3.8 exhibited a negative sloping trend for both thorium and uranium in grass and pine soils to the amorphous iron in those corresponding soils. The negative trend shows as we increased in amorphous iron less

thorium and uranium would be found. However, looking at the variable panicgrass soils versus the loblolly pine soils, the variable panicgrass almost exhibits an undefined slope, while loblolly clearly shows a more negative trend. Overall, for both strategies to exhibit this trend, amorphous iron might be a limiting factor for the microenvironment.

Total thorium and uranium in both soils compared to extracted amorphous iron in soil showed a overall negative trend (Figure 3.7), almost exactly opposite of 3.8. The correlation between crystalline iron concentration with thorium and uranium concentration in variable panicgrass and loblolly pine soils is strongly positive (Figure 3.8). Crystalline iron is far less soluble than iron in the "amorphous" fraction and thought to be a higher energy expenditure for organisms to obtain. Variable panicgrass still shows higher thorium and uranium concentrations in soil against the loblolly pine, but both exhibits that higher crystalline iron measured higher thorium and uranium could be measured as well. As a strategy 1 (non-graminaceous) plant uses chelators and reductases to obtain iron (less efficient and possibly more energy), they have just as large of a potential for thorium and uranium uptake versus the strategy 2 (graminacous) plant. All the soil properties besides elemental analysis were roughly the same, thus it can be said that there are other factors not covered by these properties that could explain why thorium and uranium concentrations vary in these soils.

The correlations between iron, thorium, and uranium concentrations in the soil indicate similar geochemical behavior of these ions which is similar to hypothesis 1 pertaining to plants. These two systems are related and not perfectly understood. Specifically, there is a stronger correlation between uranium and thorium concentrations

in soil with the crystalline extractable iron compared to amorphous extractable iron within the soils. The correlation with the less soluble form of iron could be related to the relatively low solubility of uranium and thorium bearing minerals, or that plant uptake could be possible if ionic potential is close enough to a main nutrient.

Plant Discussions

Element to element correlations compare thorium and uranium concentrations to iron concentration within the same plant fraction (Table 3.6). There is a stronger correlation for uranium/iron in respect to thorium/iron across all plant types and fractions. Using Excel's Data Analysis Add-in, a regression analysis was used to calculate the uncertainty which supports the strong R^2 values. The table also shows a decrease in correlation from GBP, GP, GR, PP, to PR; this trend could be an indication of the different metabolic processes between the variable panicgrass and loblolly pine. These strong R^2 values support our ionic potential hypothesis.

Similar to the element to element correlations, we investigated the possible trends with concentration of uranium and thorium plotted against iron concentrations in the corresponding roots or soils across all plant types and fractions (Appendix B-14). From this investigation, uranium concentration in grass roots is the only trend to directly correlate with increasing iron concentrations in the grass roots ($R^2 = 0.9951$). Therefore, as iron concentrations in roots increase so does uranium concentration in the grass roots. The correlation with the thorium cation is weaker because the ionic potential of the uranyl ion is closer to Fe^{3+}. All other trends explored by this method exhibit poor correlations with no apparent slopes or negative slopes regarding the increase in iron

concentrations in roots and soils. Although one plant fraction does show a positive correlation between uranium concentrations and iron concentrations, the majority of the samples do not support our hypothesis.

Like element to element trends, CRs are a quantitative investigation of a system. Uranium generally has higher CRs than thorium and iron as discussed with regards to Table 3.7 and 3.8 and Appendix B-5 and B-6. Caldwell et al. (2011) reports iron CRs in their vegetation as low as 0.03 mg kg^{-1} and as high as 0.59 mg kg^{-1} and plutonium CRs as low as 0.003 mg kg^{-1} and as high as 0.10 mg kg^{-1}. If thorium can be considered as a proxy for plutonium because both elements have a stable tetravalent oxidation state, then both variable panicgrass and loblolly pine can be used as accumulators due to the higher CRs for thorium of 0.26 and 0.24 mg kg^{-1} for variable panicgrass and loblolly pine, respectively. Variable panicgrass appears to have a higher CR than loblolly pine and thus could be a better accumulator. Average amorphous iron content in this work was twice as high as the iron concentrations reported by Caldwell et al. (2011).

The International Atomic Energy Agency (IAEA, 2010) has reported CRs for thorium in grasses and pines (min to max) as 1.6×10^{-3} to 2.7 and 1.0×10^{-5} to 3.1×10^{-3} and uranium in grasses and pines as 7.7×10^{-5} to 5.5 and 1.4×10^{-5} to 3.2×10^{-2} (Bq kg^{-1} of fresh weight to dry kg of soil). This study compared calculated values of thorium in grass and pine (average min to average max) as 1.0×10^{-3} to 0.5 and uranium in grasses and pine average min to average max as 3.2×10^{-3} to 1.0 in the same units through correction with the known water content. The average %WC for each plant type was used, except for the root fractions which are assumed to be 50 percent water (GP, 0.82;

GBP, 0.20; GR, 0.50; PP, 0.65; PR,0.50). This direct comparison shows that this study's average CRs are on the upper 50th percentile and roughly one order of magnitude from the highest reported by IAEA. This study exhibits higher CRs in grasses than pines but only by a small fraction. This is mirrored in the results by IAEA. Values reported by this study could be higher due to the larger range and greater amount of crystalline iron fraction in the system.

The usage of diethylenetriaminepentaacetic acid (DTPA) is a known multidente chelating agent (similar to Ethylenediaminetetraacetic acid (EDTA)) to increase the mobility of insoluble cations for plant uptake (Lee et al., 2002b). Concentrations of DTPA and EDTA can also be calculated due to being closely related to soil pH (Hornburg and Brummer, 1993). Therefore, any DTPA or EDTA found would be expected to have similar concentrations in samples with similar soil pHs. This study had an average pH value of 4.78, closely matching the acidic soils in Crowley soil in Lee et al. (2002a). The Crowley soil exhibited higher exchangeable plutonium, which is a good indication of the extricability of thorium from samples. However, Lee et al. (2002a) did note that the increase in exchangeable plutonium was limited to the soil's incubation time. If DTPA was used for this study, both the variable panicgrass and loblolly should have exhibited increased correlation ratios, uptake, and CR in thorium.

Synthetic DTPA can help improve CRs because of the increase in plant uptake; however, plants have natural ways to break down nutrients. These variations in decomposition are described as uptake mechanisms by Marschner and Romheld (1994) and Barker and Pilbeam (2016). Non-graminaceous plants use chealtors and reductase to

reduce Fe^{3+} into more soluble Fe^{2+} (i.e. acidification at the plasma membrane/cell wall interface) as a Strategy 1 plant; whereas, graminaceous plants typically use enhanced synthesis and secretion of phytosiderophores and a high-affinity transport system in the plasma membrane (Strategy 2 plants). Despite different uptake strategies, our results show that there is similar CRs for both uranium and thorium in respect to measured crystalline and amorphous iron in soils.

Although this study exhibited relatively stable environmental variables which resulted in similar amorphous and crystalline iron CRs for the plants, other studies show different environmental variables that could affect CR. Zhang et al. (1991) hypothesizes that the difference in growing conditions could affect the plant due to higher amounts of nutrients during the seed stage. This is difficult to evaluate for this study, but the age of the pine is certainly older than that of grass. Thus, the initial growing stage for pines could have contained positively loaded apoplasmic conditions for growth. Morrissey and Guerinot (2009) add to this complexity of variables by reporting several factors affecting the chelation of iron: specific chelators, iron transport genes, and surrounding microbial communities Therefore, it is difficult to correctly determine the cause of preferential uptake of iron.

These sections have discussed correlation ratios, translocation, CRs, cross comparison of CRs, and possible increases to CR through DTPA. This study and findings from literature, show that several factors, both internal and external in relation to the plant, can affect the plant CR. Increases in crystalline iron concentration corresponds to increasing concentrations of thorium and uranium in soil; however, the CR of both pine

and grass for crystalline and amorphous iron are similar. These outcomes show that additional experiments could be done to further analyze this complex system

CHAPTER FIVE

Conclusion

Initially our intent was to evaluate changes in uranium and thorium uptake in plants based on the assumption of the presence of areas with “high” and “low” uranium and thorium concentrations at the study site. These were evaluated using a field deployable NaI detector. However, statistical analysis indicated that no significant differences existed between the means of these measurements. Further analysis and measurements were taken for %WC, organic matter content, pH, particle size, iron content and mineralogy to examine trends with respect to uranium and thorium uptake in plants. The analysis and measurements all resulted in relatively similar data except for iron content. Concentrations of iron in the soil, roots, and shoots of plants exhibited sufficient variability for comparison with thorium and uranium concentrations. Therefore, the focus on this work has been on examining correlations between uranium and thorium uptake with iron uptake. The focus on iron correlations is consistent with hypothesis 1 implying similar behavior of Fe(III), U(VI), and Th(IV). The summary below discusses this concept with respect to 1) correlations of uranium, thorium, and iron within the plant shoots and roots, 2) the influence of the iron mineralogy on uranium and thorium uptake, and 3) comparison of the CR values for grasses and trees.

The element to element trends or correlations ratios between (1) uranium and iron and (2) thorium and iron in plant shoots exhibit moderately positive slopes, thus indicating a direct relationship between uranium and thorium in the plant shoots with iron in the plant shoot. A similar observation was made for the plant roots. The average ratios of uranium

to iron concentrations in the plant shoots and roots were more strongly correlated for the grass plant system (GBP, 0.9826; GP,0.9554; and GR, 0.9951) than the pine plant system (PP, 0.6983; PR, 0.8463). Relative to these uranium values, the thorium to iron ratio in plant shoots and roots within the same plant types decrease in R^2 compared to uranium. Additionally the magnitude of the uranium to iron ratio in plants was greater than that for the thorium/iron concentration ratio. These data indicate that:

- Uranium is more strongly correlated to iron uptake in grass and pine plants than thorium.
- Uranium and thorium uptake in grass shootsis more strongly correlated to iron than pine shoots.
- There are higher concentration ratios of uranium, thorium and iron in the senesced shoots of grass (GBP) indicating accumulation over time.

Thus it appears iron, uranium, and thorium cycling are closely related indicating similar biogeochemical behavior. This supports our primary hypothesis that the similar ionic potentials of U(VI), Th(IV), and Fe(III) lead to similar chemical behavior.

The concentration of extractable crystalline and amorphous iron in soils were measured and different concentrations of uranium and thorium were found in these extraction solutions. Thus, uranium and thorium are possibly associated with different pools of iron within the soil. There is a strongly negative slope for measured thorium and uranium concentrations in soil relative to increasing amorphous iron content in soil. Additionally, there is a steeper slope for the relationship between uranium and thorium in the grass soil relative to amorphous iron in soil versus uranium and thorium in pine soil

relative to amorphous iron in soil. Conversely, measured thorium and uranium concentrations in plants increased with respect to increasing crystalline iron content (i.e., a strongly positive sloping trend). There was also no distinction between the grass and pine soils as both were clearly linearly correlated. The stronger association of uranium and thorium with the crystalline iron fraction of the soil could be an indication of the more refractory nature of the uranium and thorium bearing solids, as the crystalline iron extraction procedure uses an inherently more aggressive digestion solution. These two pools of iron seem to influence the concentration of thorium and uranium in the soil. (i.e., could be a limiting factor with regards to uranium and thorium bioavailability to plants). The limiting factor between the two iron pools seems to be the range of concentration of amorphous and crystalline iron. When looking at a selective range of amorphous iron content (30,000 to 50,000 ppm) there is not as strongly of a negative slope.

The amount and ratio of radionuclides as they are being taken up into the plant shoot in respect to the soil is an important factor. Previously discussed uranium has a stronger correlation to grasses than pines, and that different iron pools can positively or negatively affect thorium and uranium concentrations. Both directly relate to the apparent decreasing CR for thorium and uranium across GBP, GP, and PP. However, between uranium and thorium for grass and pine systems (shoot and root) the crystalline and amorphous iron concentration did not exhibit any apparent affect on the CR. In respect to uranium CR behavior, pine and grass root CRs are higher than all other plant types. Pine roots are higher than grass roots by less than 0.1 ppm. In respect to thorium CR behavior, pine and grass root CRs are very similar with a difference also less than 0.1 ppm. Both

plants exhibit CRs within detectable measures and within the International Atomic Energy Agency (IAEA) values. However, due to the grass plant having the senesced (last years growth) plant component the grass plant system is better at accumulating thorium and uranium. The IAEA (2010) reports CRs for thorium in grasses and pines (min to max) as: (1.6×10^{-3} to 2.7) and (1.0×10^{-5} to 3.1×10^{-3}), and uranium in grasses and pines as: (7.7×10^{-5} to 5.5) and (1.4×10^{-5} to 3.2×10^{-2}) (Bq kg^{-1} of fresh weight to dry kg of soil). The reported CRs (for uranium in pine plant are 2.6×10^{-3}, and grass plants are 8.9 x 10^{-3} for grass plants) in this study are within these ranges found by IAEA, and show accumulation of more radionuclides in the roots than shoot of a plant, accumulation in last years senesced shoot over grass plant, and measured crystalline and amorphous iron in soils did not have an impact on CR.

Table 5.3. Review and summary of all experiments conducted.

Experiment	Knowledge Gained and Supported	R^2	Reason
Autoradiography Image Plate **NaI Detector**	Qualitative assessment of distribution of radioactive signatures.	Uranium in Grass Soils to detected Gamma/sec showed a .8563 R^2 value better than uranium in pine soils (< 0.5000).	Figure 3.3, A-5,A-6
Soil pH	General understanding of natural environment conditions. Correlate pH with Th/U uptake.	The average value of pH in the pine and grass soils are both ~4.81. Th and U are not changing by pH. (0.0965 (U-GS) ; 0.2456 (U-PS))	Figure A-12
Particle Size Analysis	Investigating dominate particle size with correlations of Th/U uptake could result in the preferential uptake with smaller particle sizes.	Soils are mostly a Sandy Loam, but boarder Loamy Sands also. Th and U are not changing by particle size.	Figure 3.4
LOI (%OM)	Knowing %OM can decide how healthy the system was correlation between OM% and Th/U uptake.	Consistent throughout samples and only 1 weight error causing very skewed point. %LOI in soil does not correlate to higher concentrations.	Figure 3.6

XRD	Helps decide if the sample is exactly monazite, and possibly what other minerals are affecting the area.	Samples contain monazite, illites, muscovite, quartz, kaolinite, vermiculite, and montmorillonite.	Figure 3.5
ICP-MS	Have a quantitative understanding of the system and helps find discoverable relationships between Fe, Th, U, and others. Gives a definitive answer if my samples contain radioactive elements and their concentrations.	ICP-MS helped calculate the concentrations of Fe, U, Th, Ca, K, P, Al. With concentrations in each type CR values can be calculated (Table 3.7 and 3.8).	Table 3.2 – 3.5
"Free" Iron Or Crystalline Iron	Crystalline iron oxide count paired with amorphous and ICP-MS data allows for a more quantitative understanding of possible free Fe in the soil not bounded. Such crystalline iron only available through higher energy usage, chelators, exudates, reductants, ect.	Similarly, to the ICP-MS results we have better results for Th, U, and Fe from the crystalline iron extraction. R^2 varies depending on the comparison.	Table 3.4, Figure 3.8
"Active" Iron Or Amorphous Iron	Amorphous iron oxide count allows a more quantitative understanding paired with crystalline and ICP-MS data for indications of the amount of irons being bound to the soil. Such amorphous iron is easily accessible to organisms using	Similarly, to the ICP-MS results we have better results for Th, U, and Fe from the crystalline iron extraction, but amorphous was helpful in showing differences between the two. R^2 varies depending on the comparison.	Table 3.4, Figure 3.7

CHAPTER SIX

Future Work

Future work should more systematically study the role of iron on uranium and thorium uptake in plants. For example, in an iron deficient system, would the variable panicgrass still show better uptake due to more efficient chelation of Fe(III)? Future work could validate the current results with a wider range of soil parameters and add an experiment by growing the same species in hydroponic solutions paired with high resolution CT scanning. The goal for the development of high resolution CT scanning is a qualitative look as a tracer in the plant and root structure for possible ions. This would help to better compare the translocation of uranium and thorium in a naturally occurring site, and for remediation purposes could help inform the identification of specific uptake mechanisms. This would give a better understanding of the plant system, which can be repeated for hydroponic studies.

Future sample preperation should carefully define sampling criteria. For instance, if the same study was repeated only pine trees up to 12.0 inches should be sampled. This would minimize error during the digestion process. Error can also be minimized for the evaporation of soil digestate using only 0.1 mL in a teflon beaker. Teflon beakers cause less interference than glass beakers.

Future sampling collection should be cautious of the botanical life and size. Future samples could involve larger tree samples by homogenizing large sections of the plant for digestion, but also in terms of specific translocation. Specific translocation through a tree trunk can be divided into sections for analysis. A list of possible

suggestions are: segments of the core or branches, leaves, senesced shoots (GBP), roots, and soil again. Larger trees would be interesting to test sections by needles, branches, bark, segments of the core, roots, and soils. Pairing all of these with autoradiography would show if there is long term possible attenuation within the trees. Additionally, a new tree of interest could be red maple, due to it being the most common tree by stem in the U.S. (NCSU, 2015). Red maple can also be used to help wetlands as Snow et al. exhibited (2008).

Another more plausible task is to gain an understanding at different locations. An ideal different sampling location is another large thorium bearing deposit, Lemhi Pass district in Montana and Idaho (Van Gosen et al., 2009). The Lemhi Pass district has approximately 64,000 metric tons of ThO_2 in reserve, in comparison to our study area which has approximately 4,800 tons. Similar site characterization done in this study should be repeated at the Lemhi Pass district to find vegetation growing on or near the outcroppings. Ideally repeating this current study again, sampling both a strategy 1 and strategy 2 plant to confirm their different uptake mechanisms, and their relationships to amorphous and crystalline iron. Overall, validating results by using a CT scanner method for roots, caution for new and old plant samples, and repeating the study in a new location would help support or deny this current work.

APPENDICES

Appendix A

Field Study and Soil Results Appendix

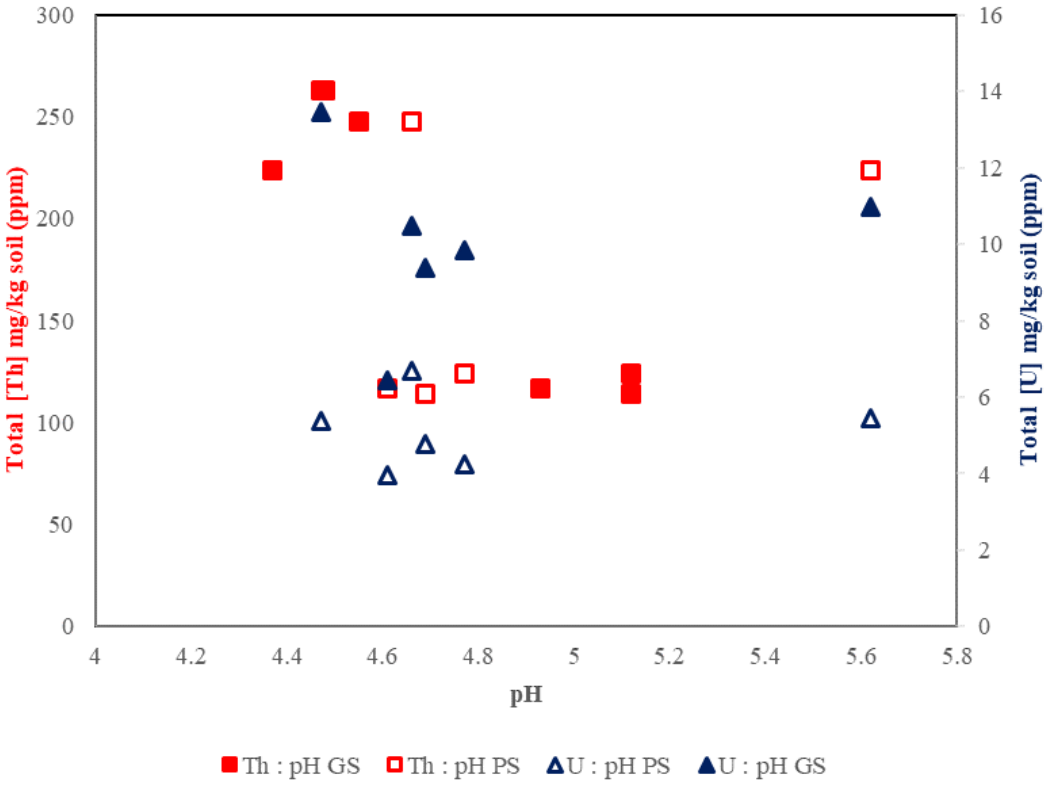

Figure A-1: Total measured Th and U in ppm to pH of soils.

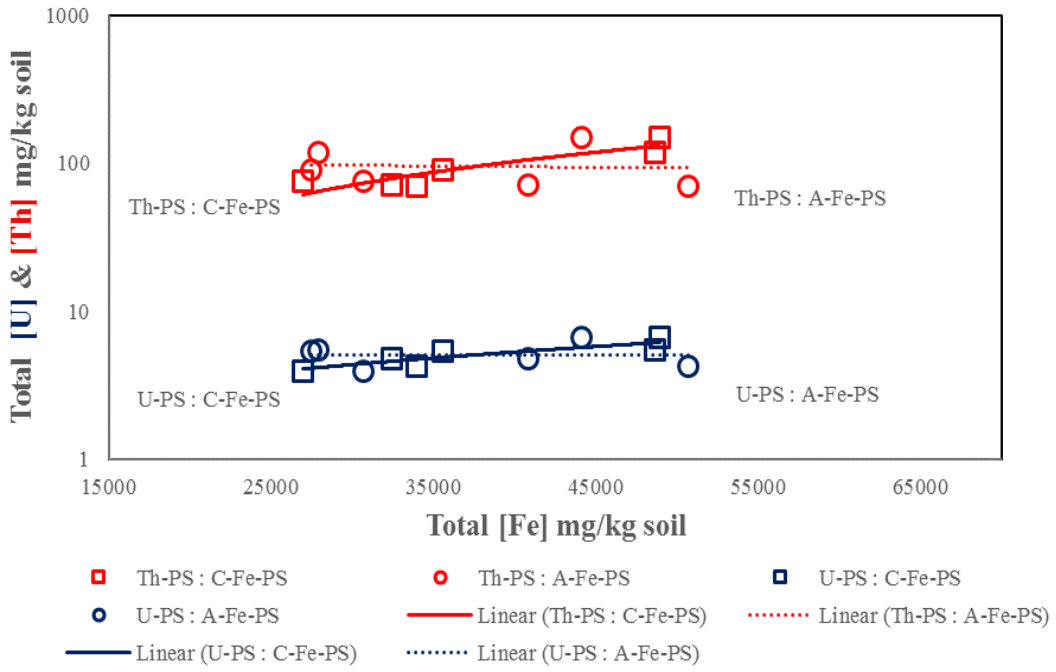

System	R^2 and Slope
Th-PS : C-PS-Fe	0.8195, 3.2×10^{-3}
Th-PS : A-PS-Fe	0.0037, -2.0×10^{-4}
U-PS : C-PS-Fe	0.7398, 9.0×10^{-5}
U-PS : A-PS-Fe	9.0×10^{-5}, -1.0×10^{-6}

Figure A-2: Calculated Total [Th] and [U] mg/kg pine soil (ppm) to Total Crystalline and Amorphous [Fe] mg/kg pine soil (ppm).

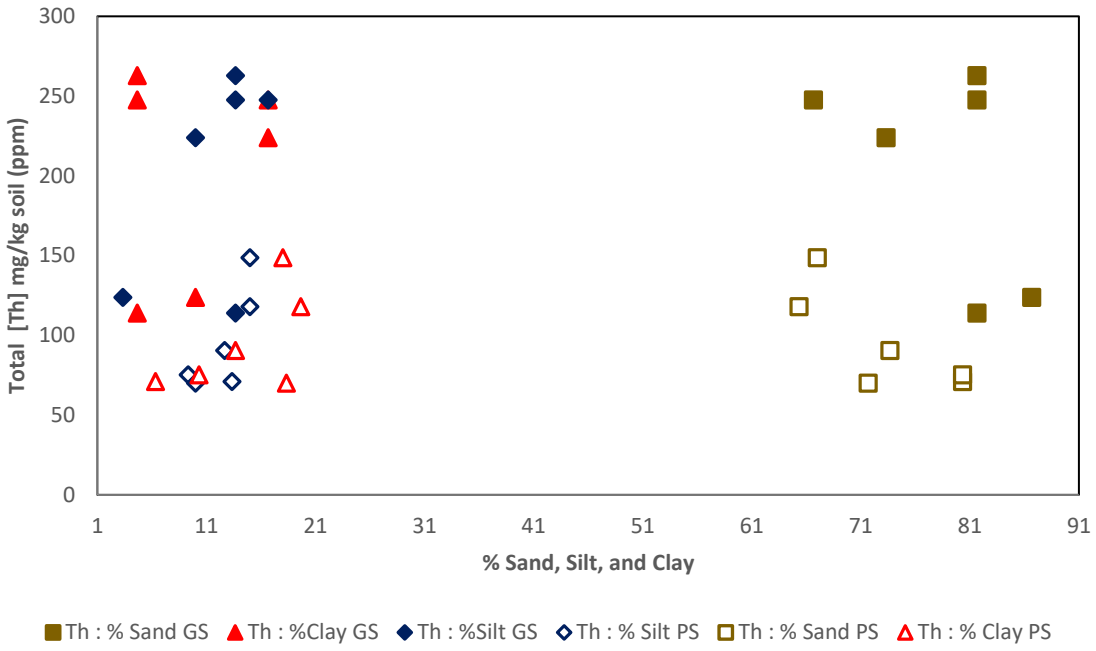

Figure A-3: Graph of Total Th concentrations to percent sand, silt, and clay in both Grass and Pine soils.

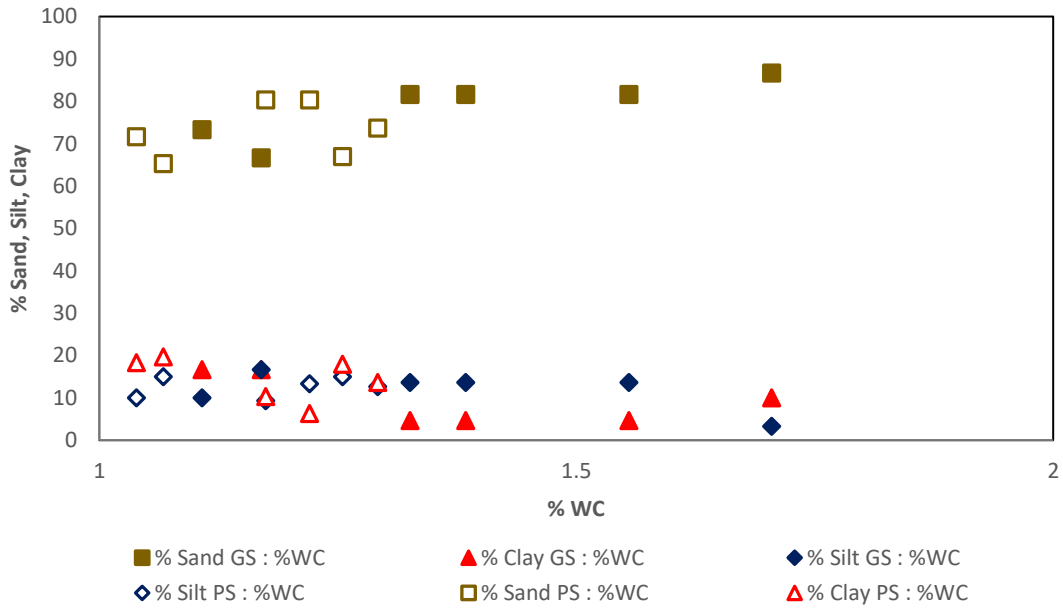

Figure A-4: Fractions of % sand, silt, and clay to %WC in soils.

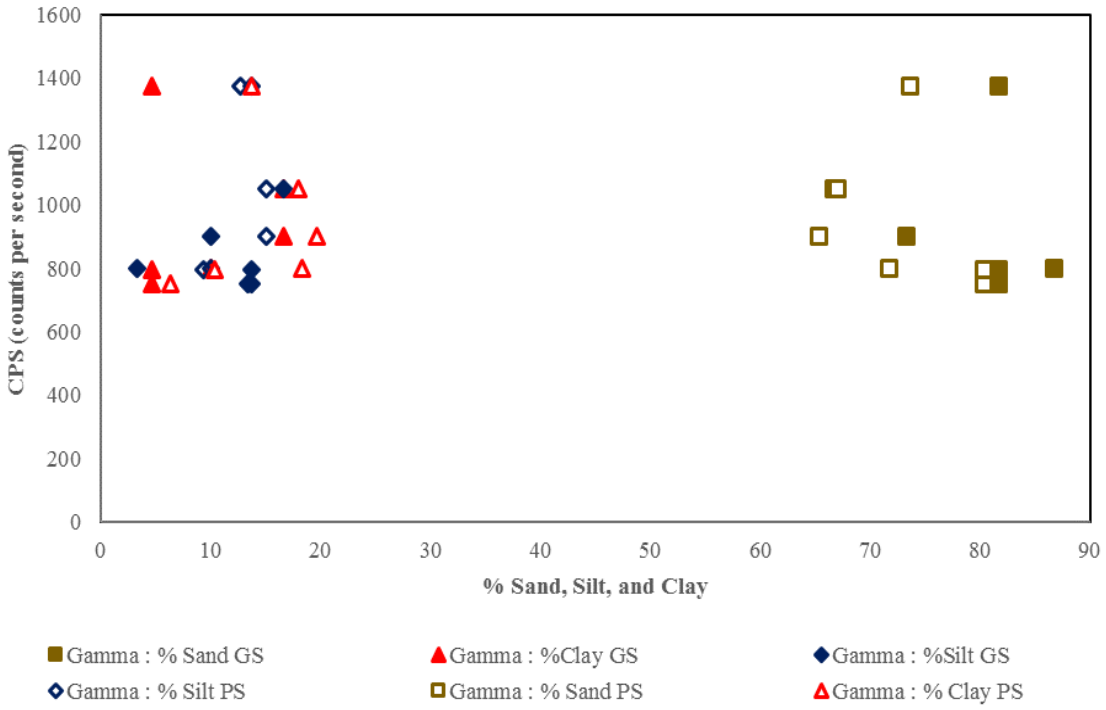

Figure A-5: Shows CPS to total %Sand, total %silt, and total %sand per soil.

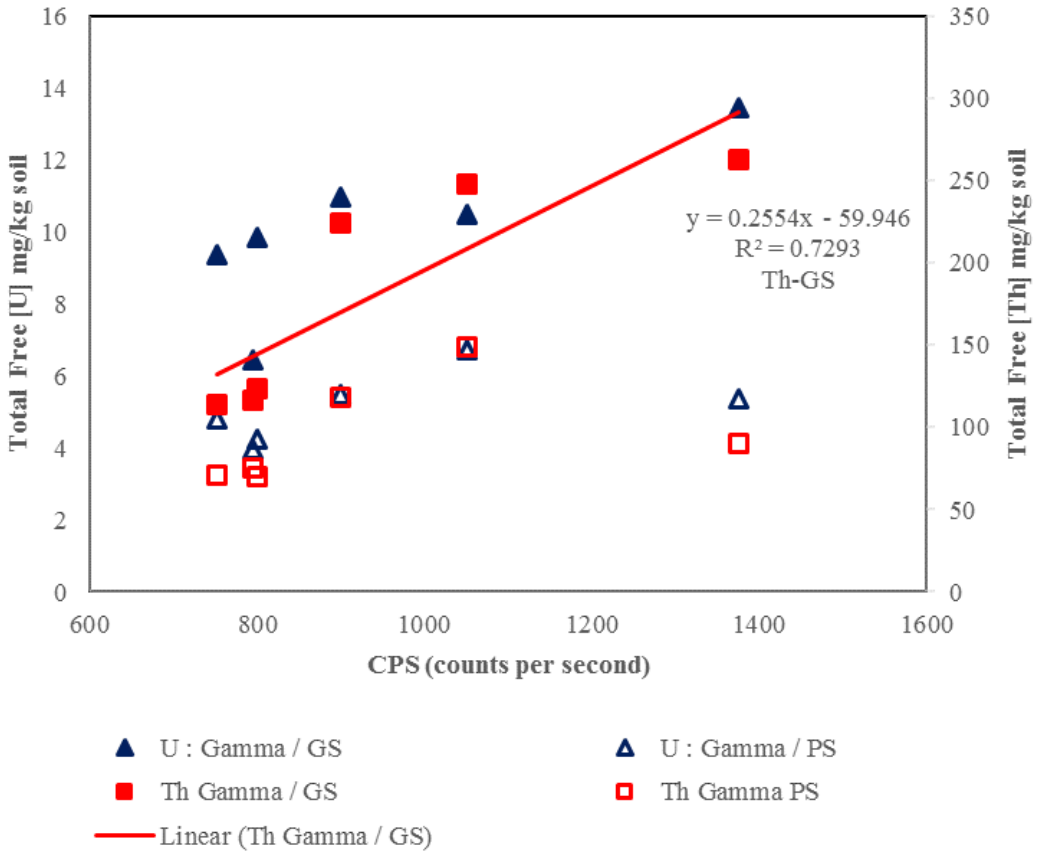

Figure A-6: Shows Crystalline [U] and [Th] mg/kg soil (ppm) to detected CPS.

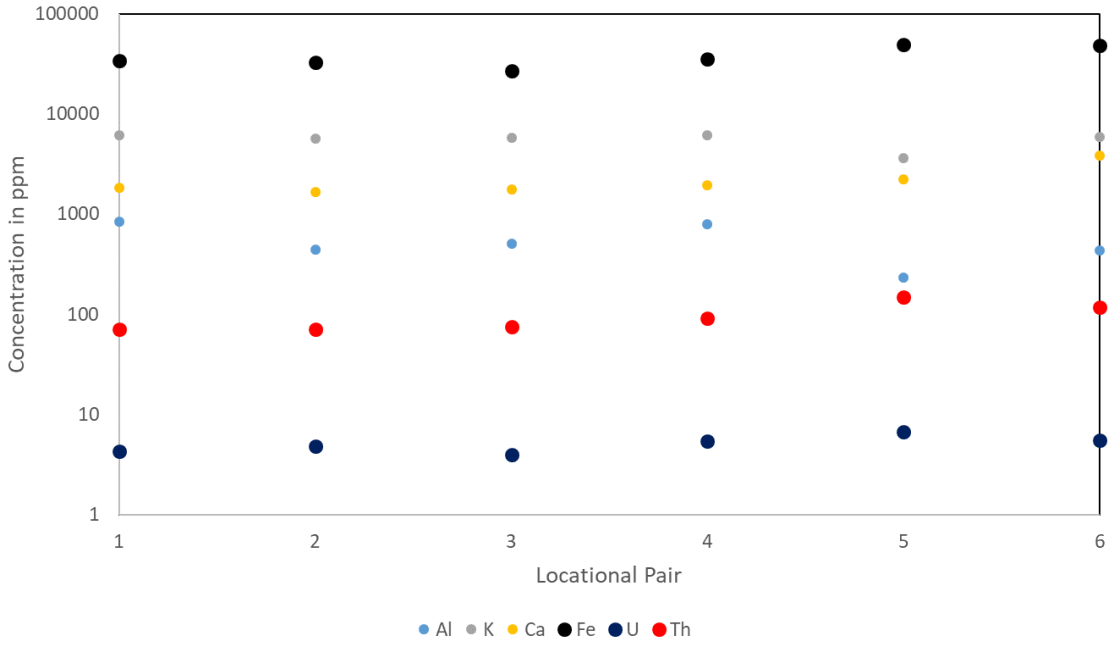

Figure A-7: Graph of Total [Al], [K], [Ca], [Fe], [U], and [Th] in pine soils by location pair.

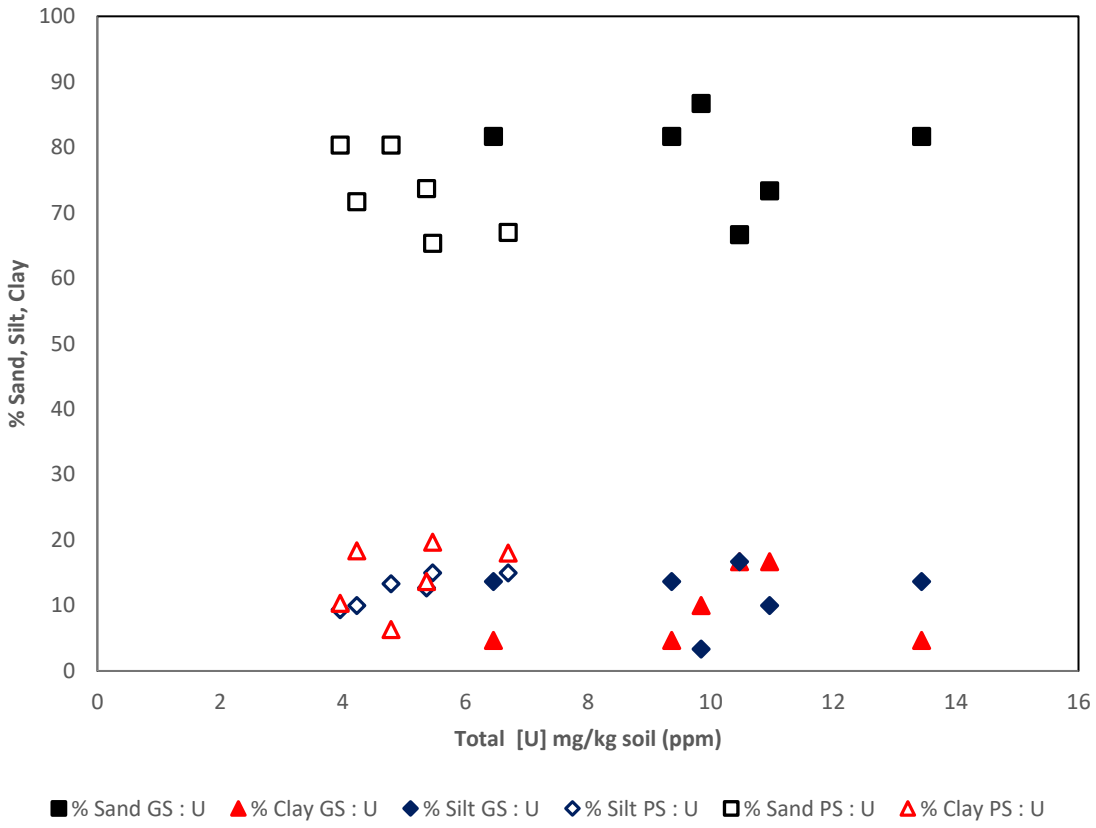

Figure A-8: Graph of Total U concentrations to percent sand, silt, and clay in both Grass and Pine soils.

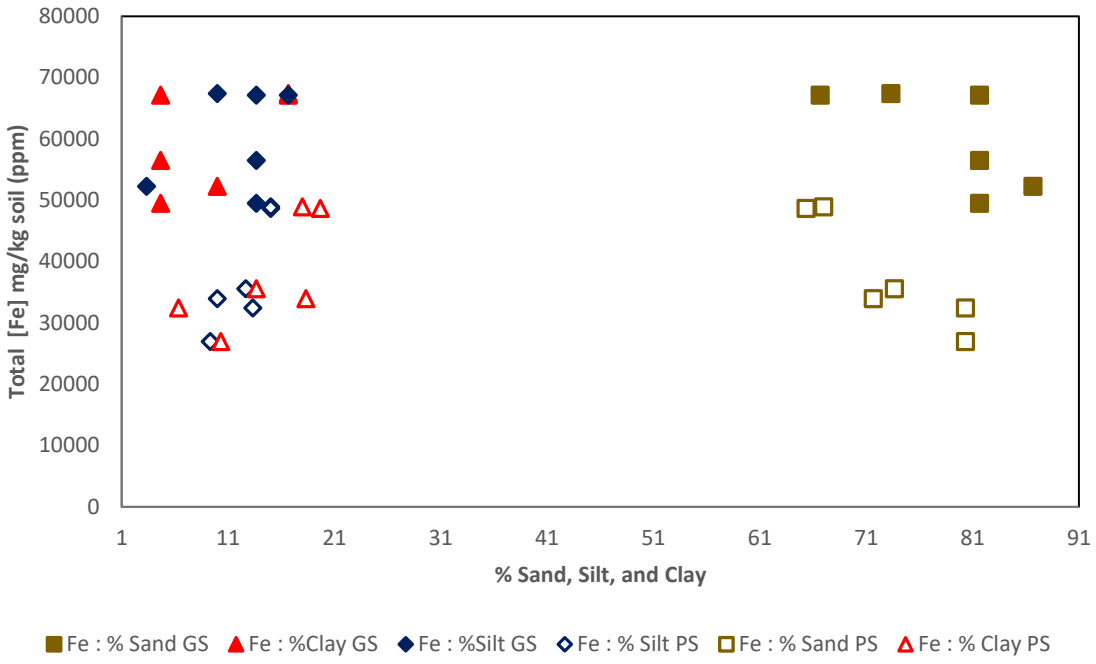

Figure A-9: Graph of Total [Fe] ppm to percent sand, silt, and clay in both Grass and Pine soil.

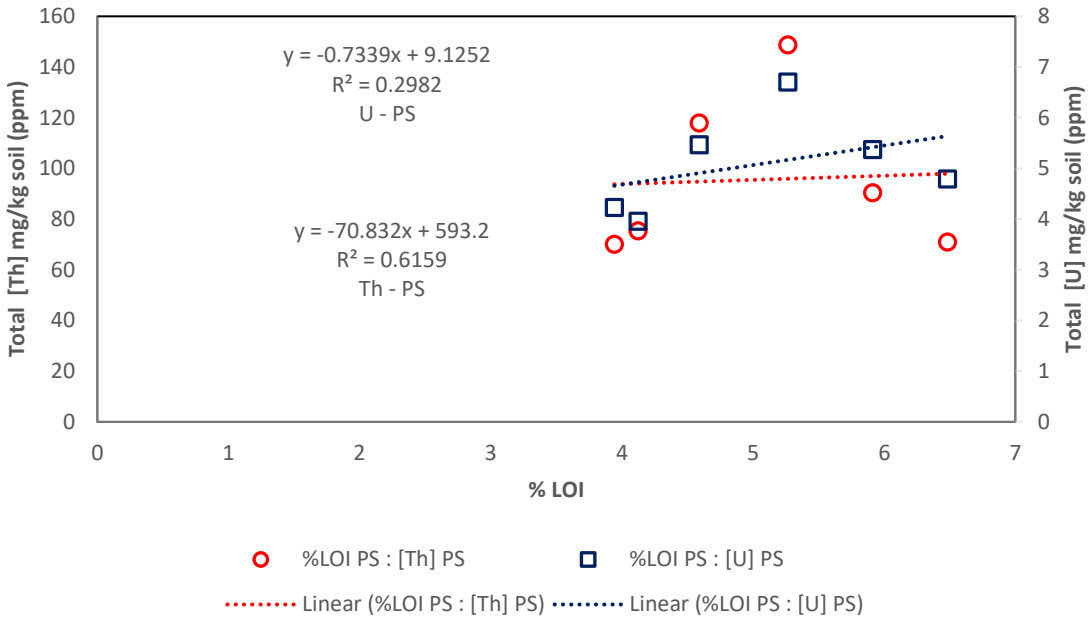

Figure A-10: Total [Th] and [U] in Pine soils to organic matter content in corresponding soils.

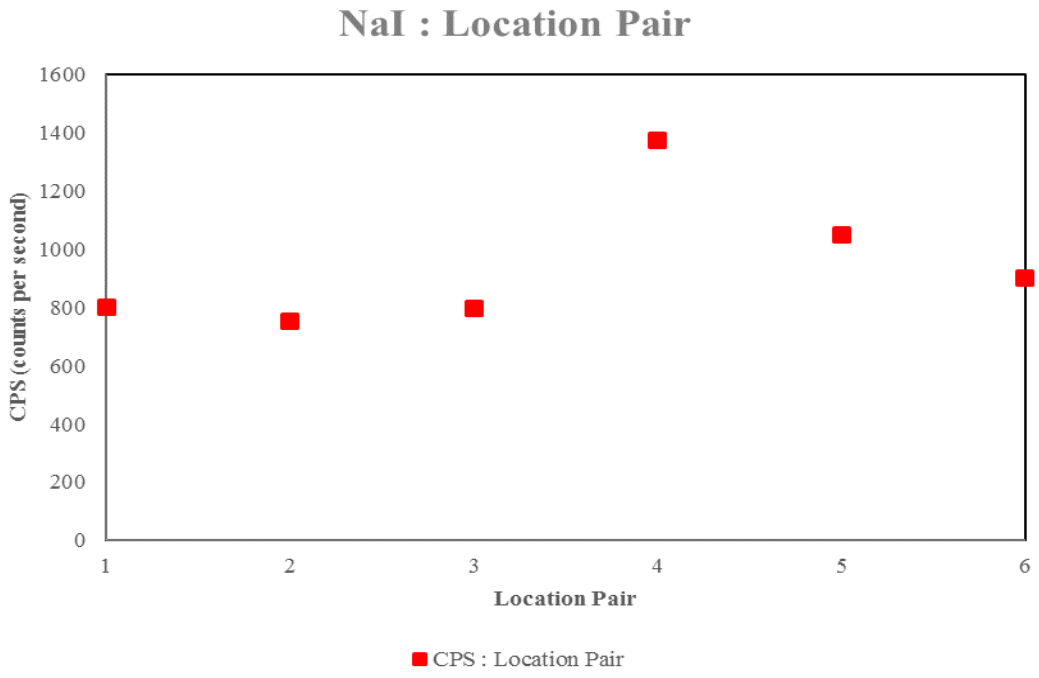

Figure A-11: Total gamma detected from NaI detector by location.

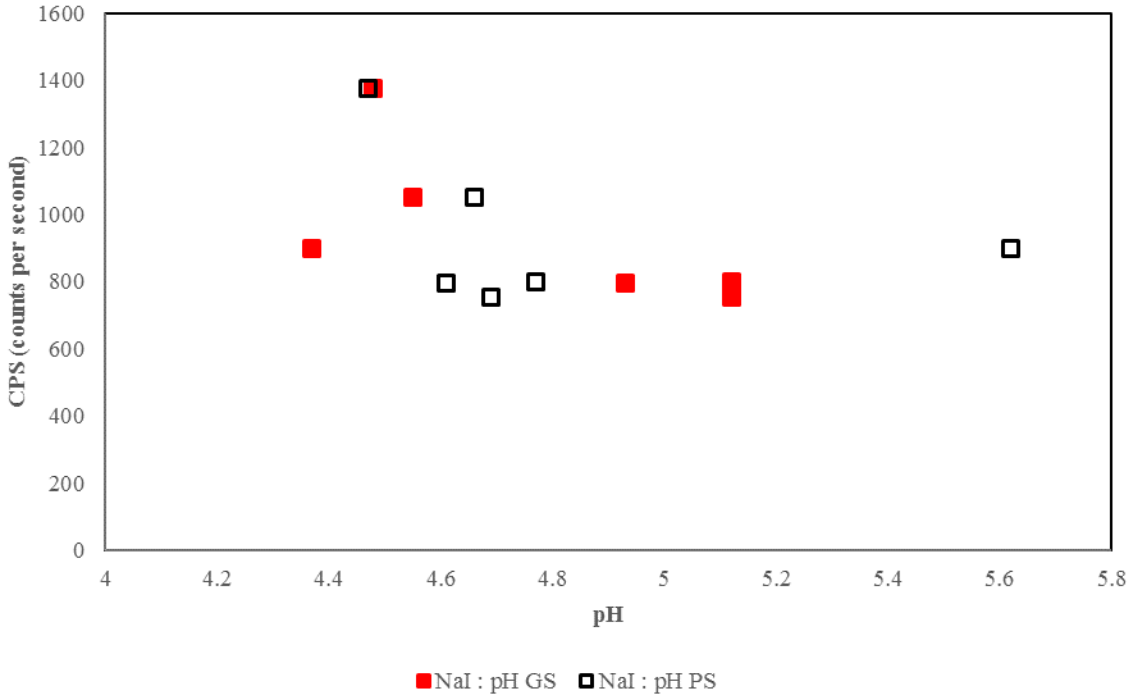

Figure A-12: Total gamma detected from NaI detector to pH in grass and pine soils.

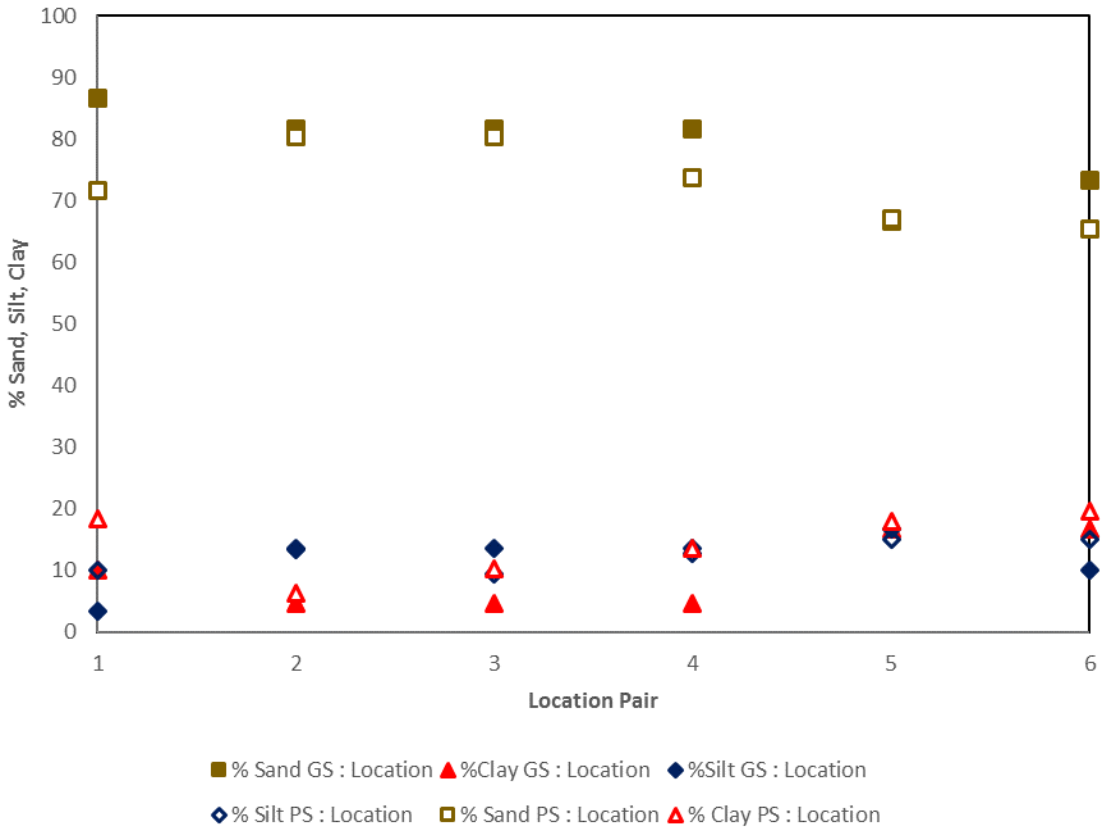

Figure A-13: Percent sand, silt, and clay to location pair for corresponding soil.

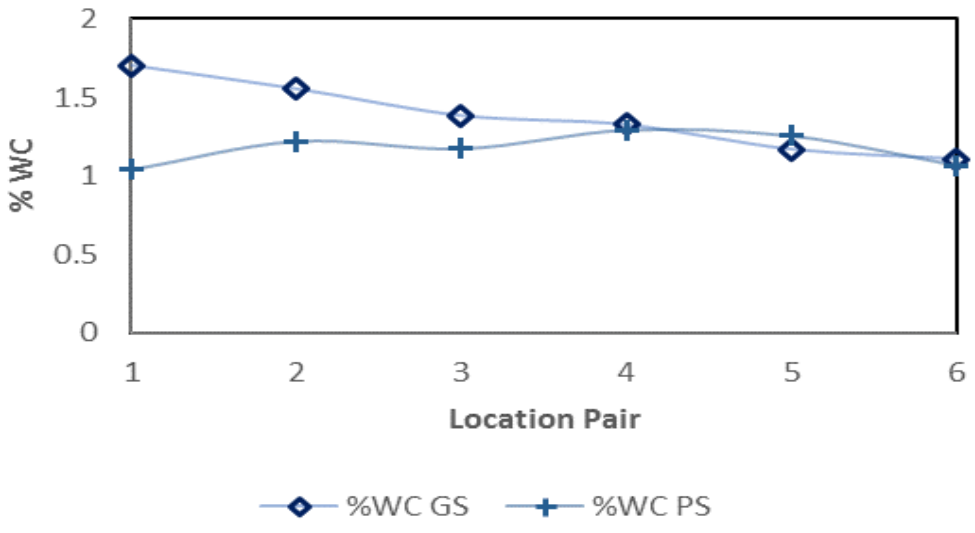

Figure A-14: Percent water content to corresponding soil by locational pair.

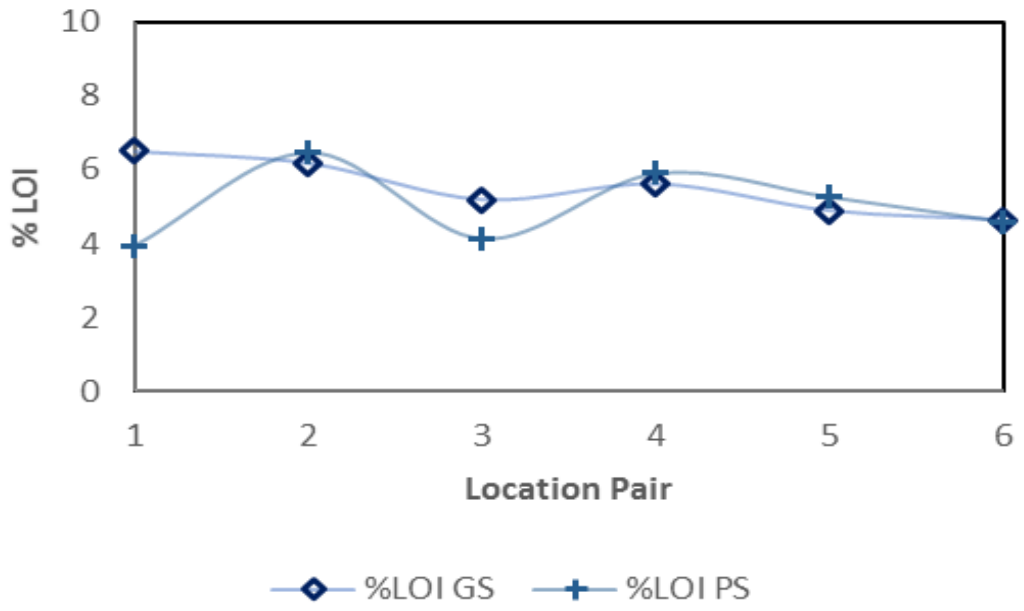

Figure A-15: Percent organic matter content of corresponding soil by locational pair.

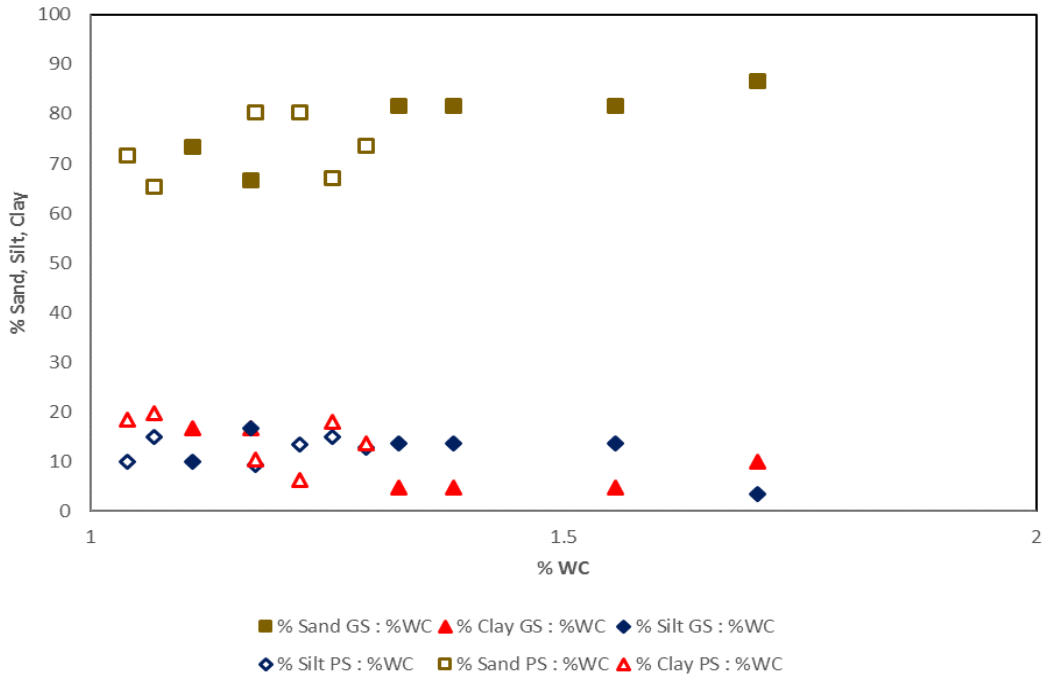

Figure A-16: Percent sand, silt, and clay fractions to percent water content of corresponding soil

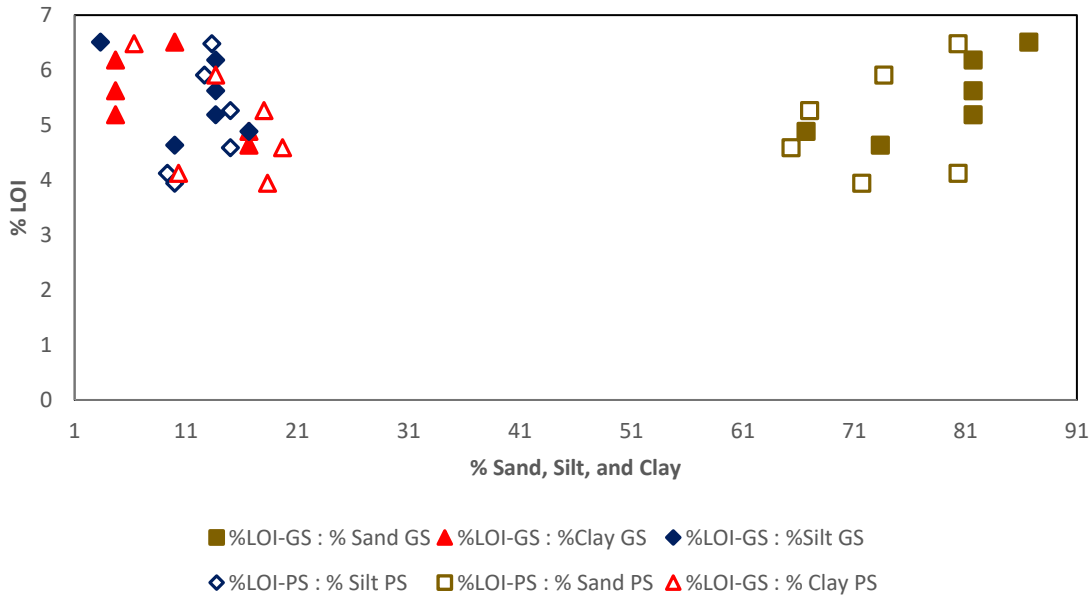

Figure A-17: Percent organic matter content to corresponding soil of percent sand, silt, and clay.

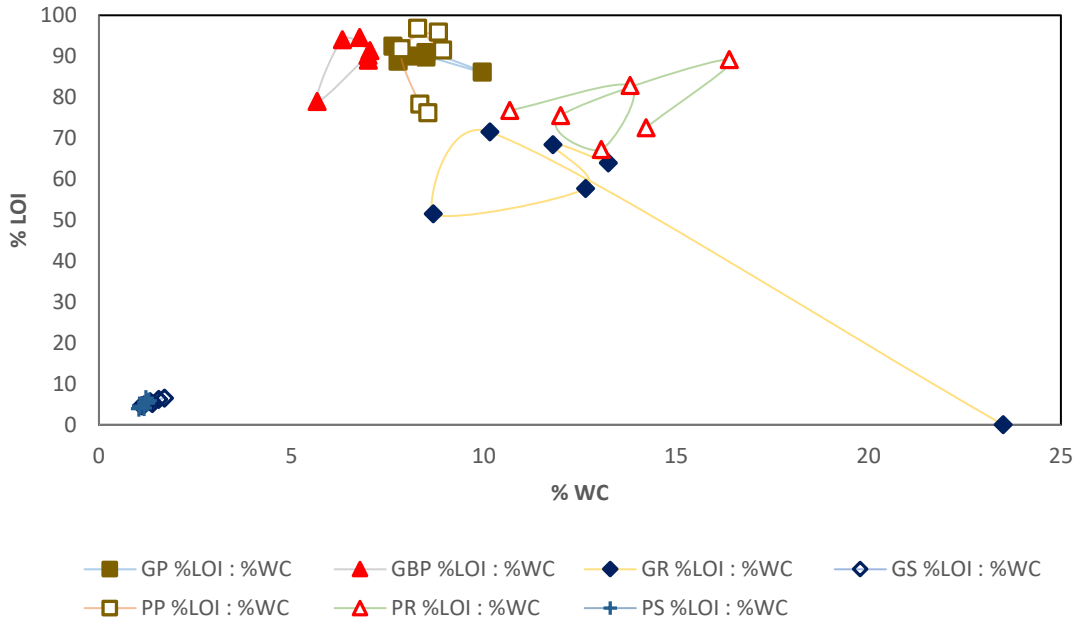

Figure A-18: Percent organic matter content to percent water content for each plant fraction including soils.

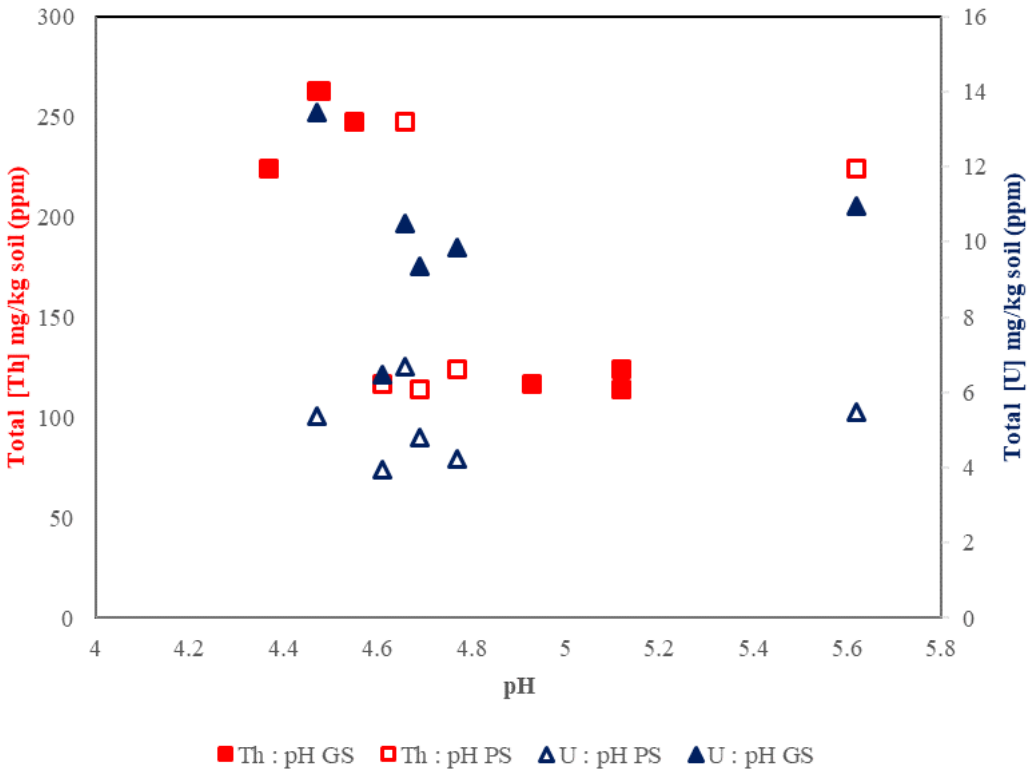

Figure A-19: Total [Th] and [U] in ppm to pH of corresponding soils.

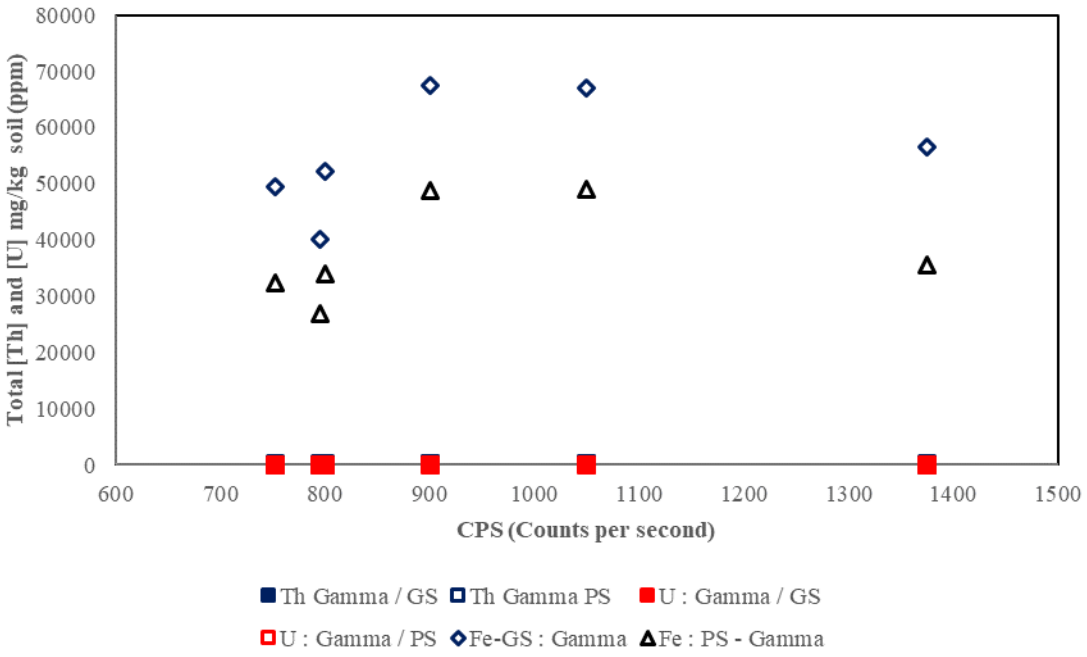

Figure A-20: Total [Th] and [U] in ppm to detected CPS of NaI detector by pair and plant soil.

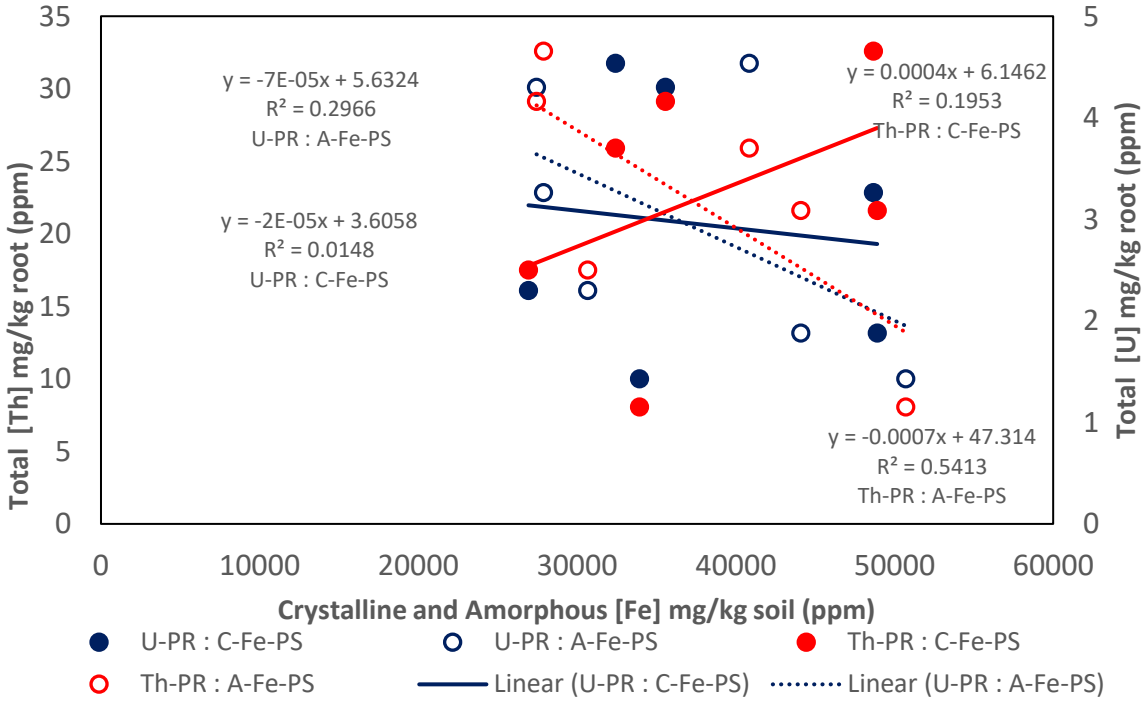

Figure A-21: Total [Th] and [U] pine root to crystalline and amorphous[Fe] in pine soil.

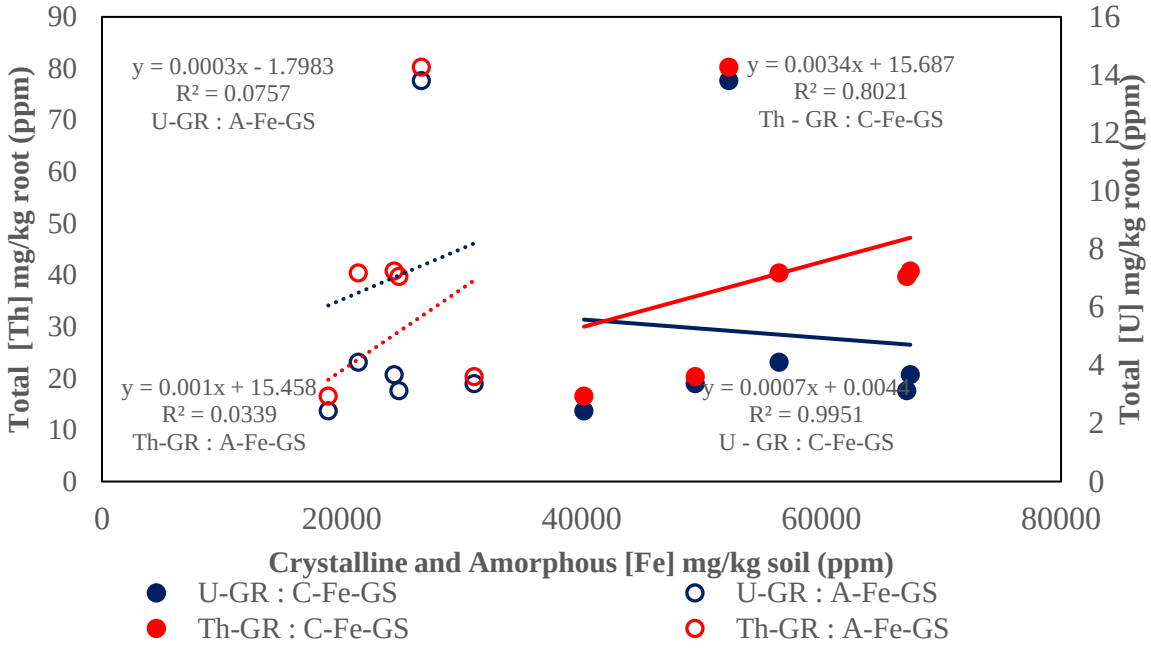

Figure A-22: Total [Th] and [U] grass root to crystalline and amorphous[Fe] in grass soil.

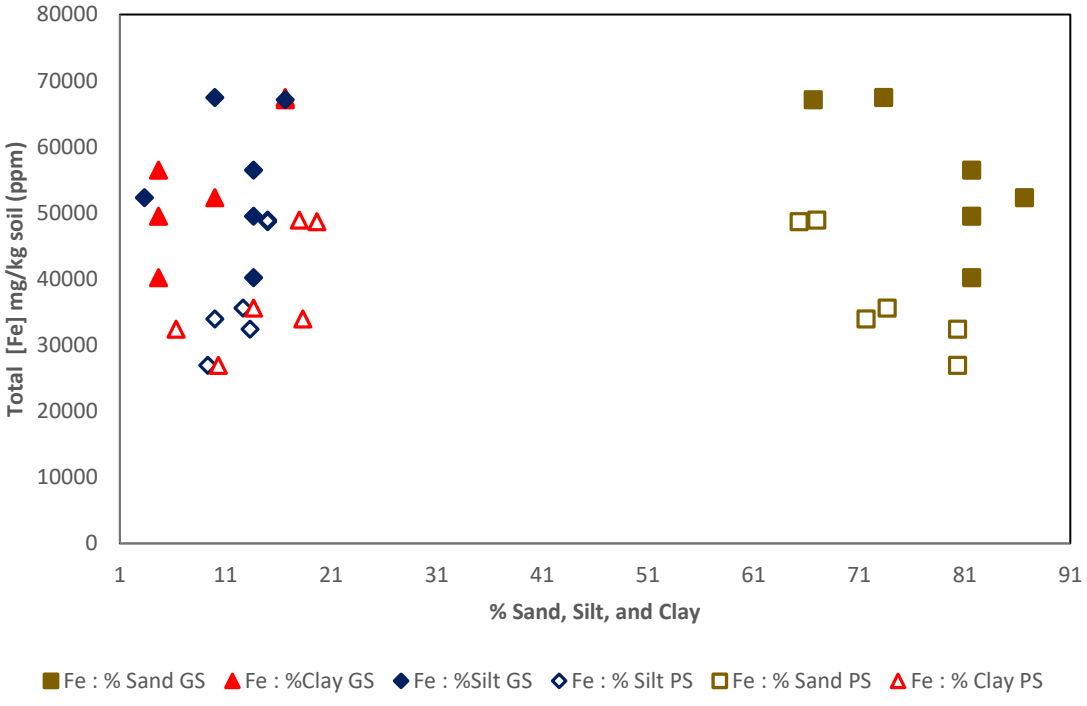

Figure A-23: Total [Fe] in ppm to percent sand, silt, and clay for corresponding soils.

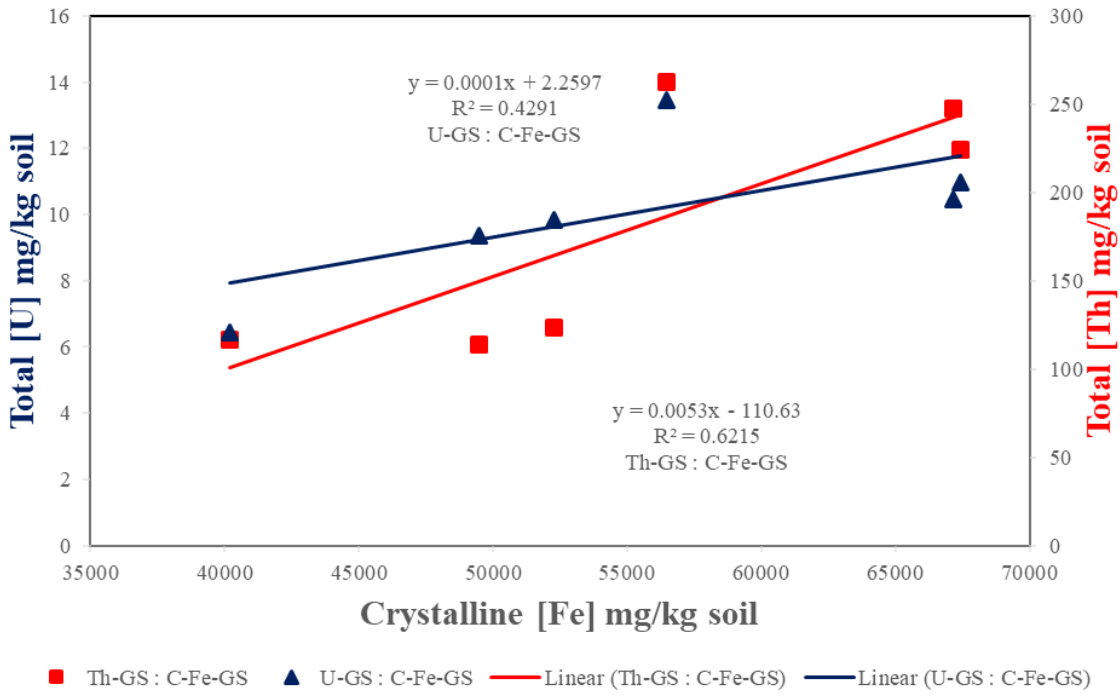

Figure A-24: Total [Th] and [U] (ppm) in grass soils to total crystalline iron (ppm) in corresponding grass soils.

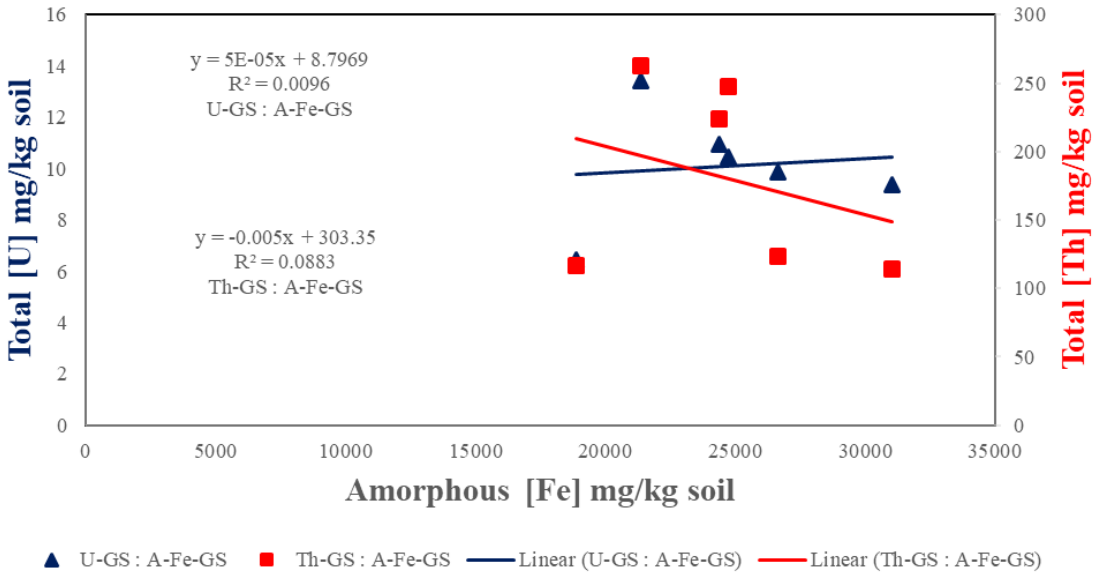

Figure A- 25: Total thorium and uranium (ppm) in grass soils to total amorphous iron (ppm) in corresponding grass soils.

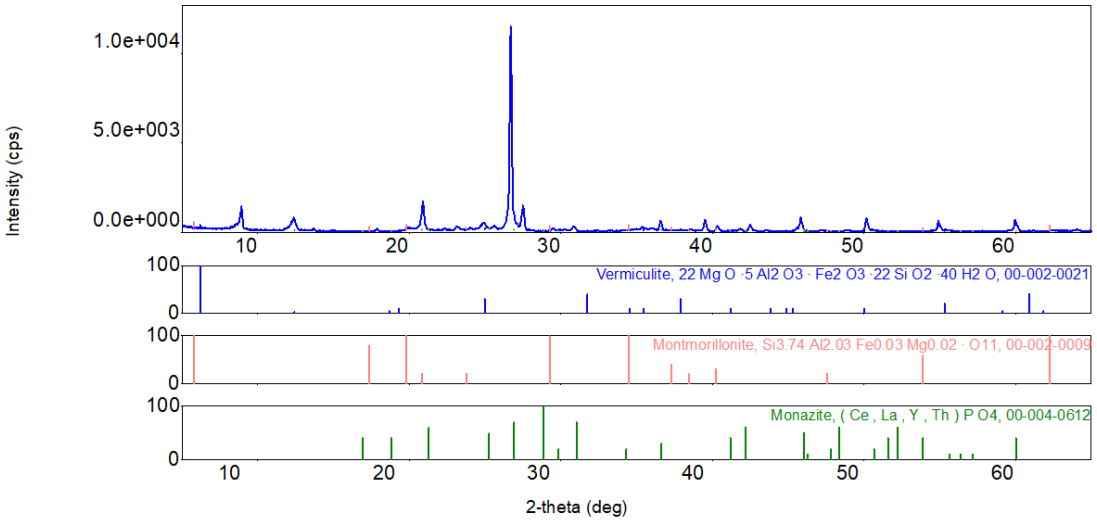

Figure A- 26: GS-1-500 XRD of vermiculite, montmorillonite, and monazite.

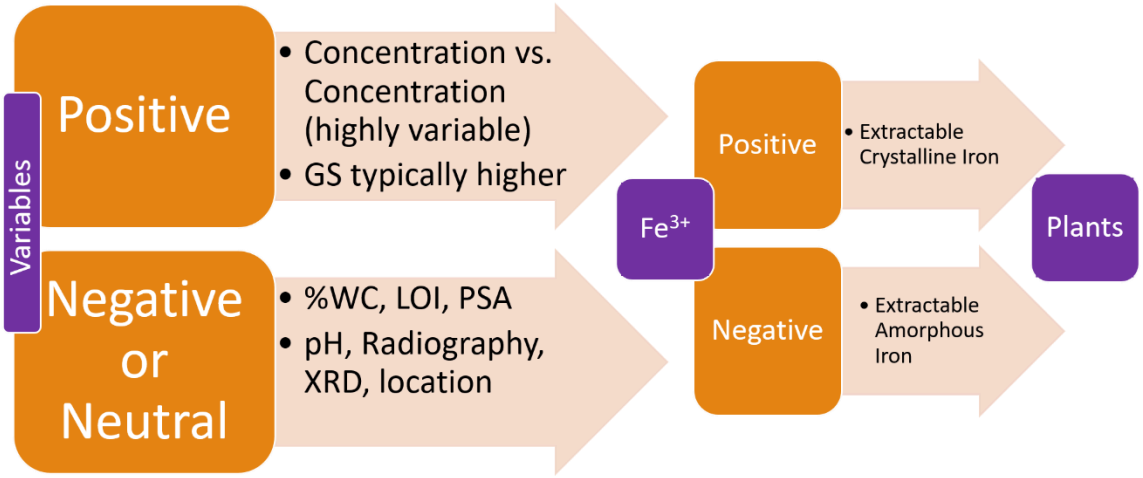

Figure A- 27: Flow chart showing soil variables compared against each other, then comparisons to Fe(III) for crystalline and amorphous extractions. Lastly showing how the variables than need to be compared across the different plant shoots and roots.

Appendix B

Plant and Soil Results Appendix

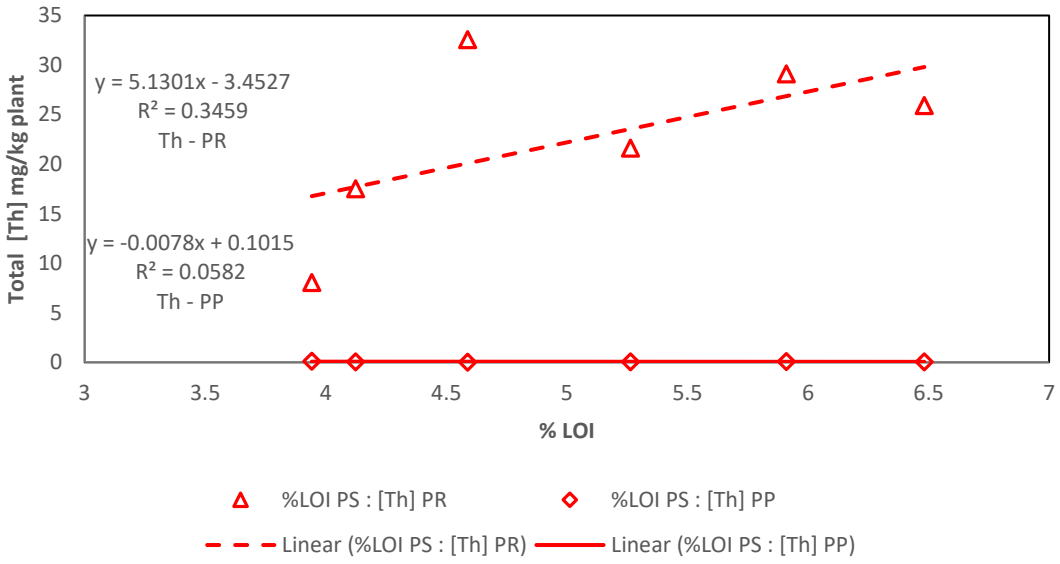

Figure B-1: Total [Th] mg / kg soil (ppm) to %LOI in pine soil for pine plant and pine root.

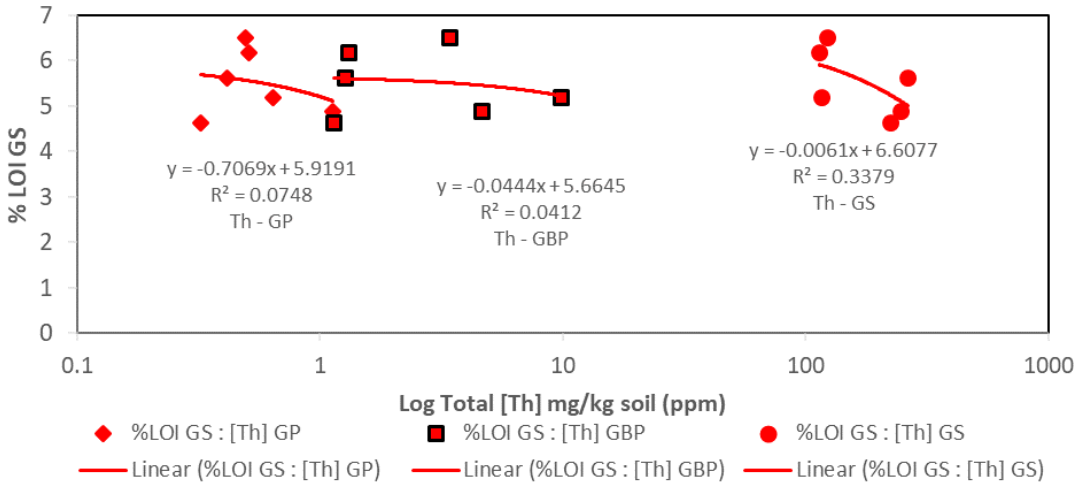

Figure B-2: Total [Th] mg / kg soil (ppm) to %LOI in grass soil for pine plant and pine root.

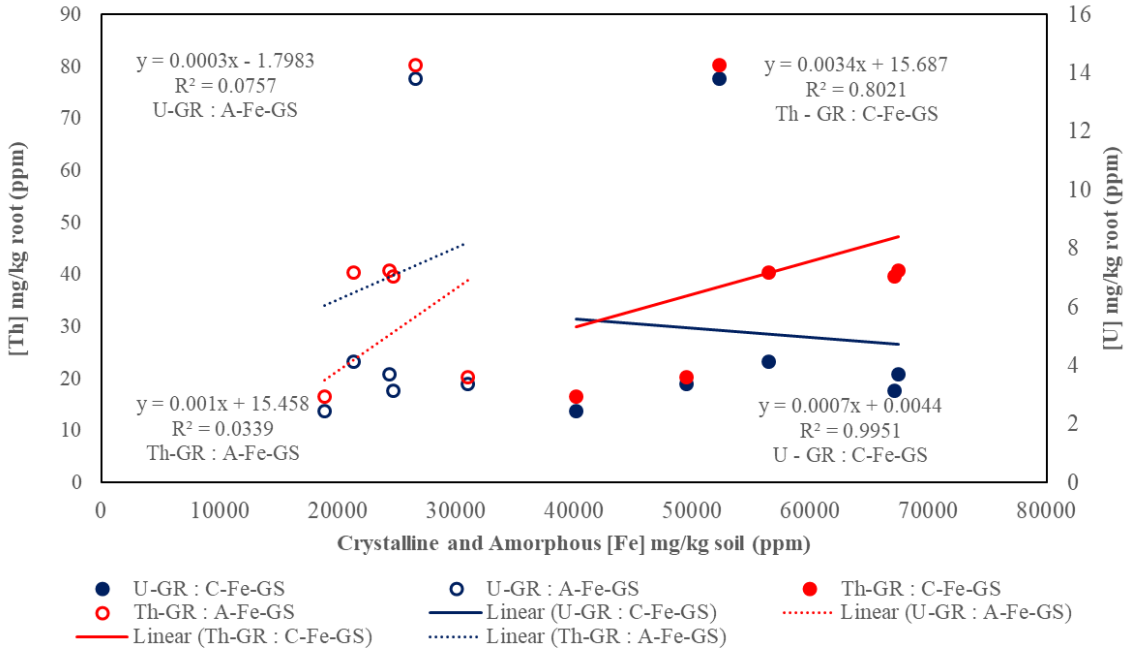

Figure B-3: Graph shows the [Th] and [U] for grass roots to crystalline and amorphous grass soils in (ppm).

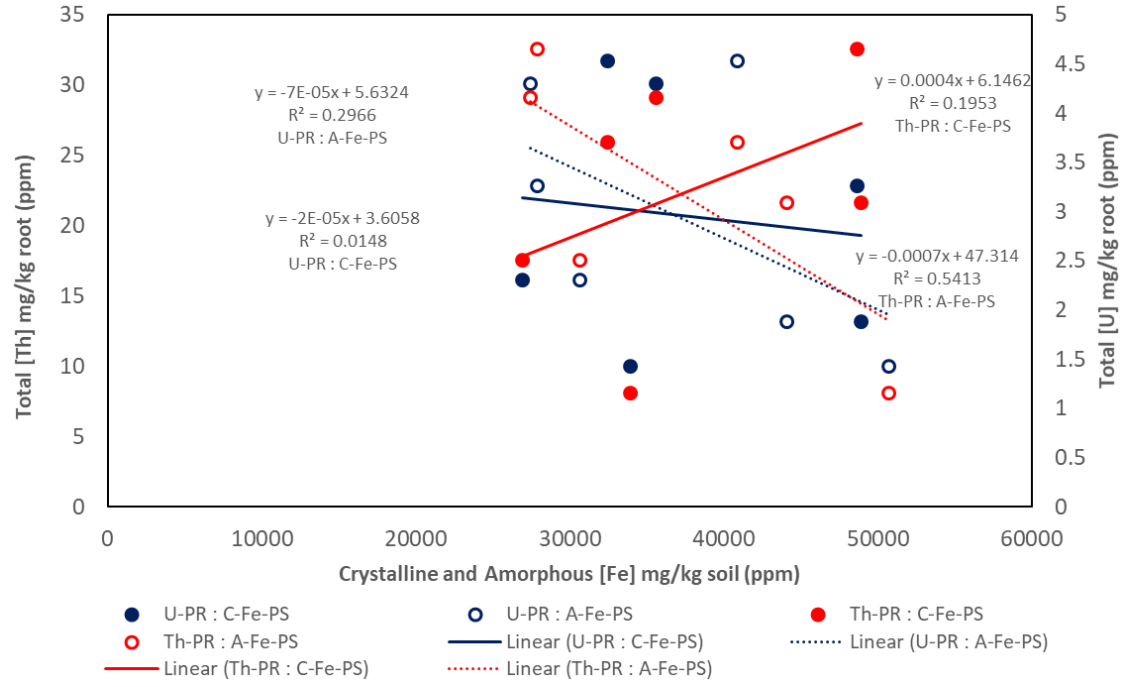

Figure B-4: Graph shows the Total [U] mg/kg plant (ppm), Total [Th] mg/kg plant (ppm) against crystalline and amorphous [Fe] mg/kg soil (ppm) in soil or root for pines.

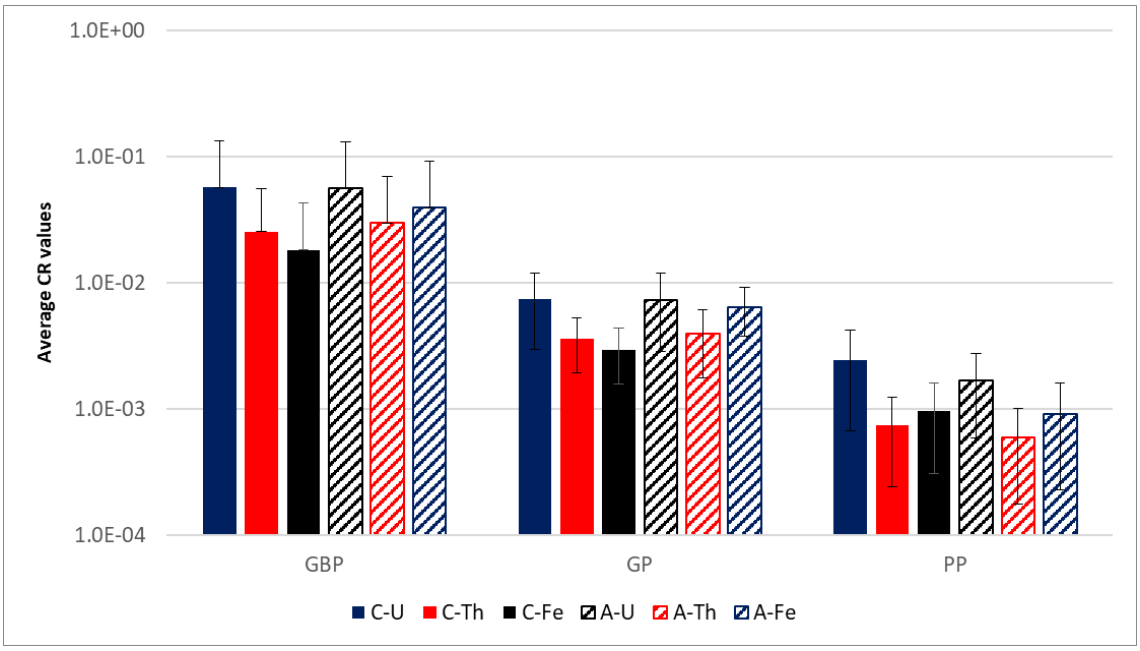

Figure B-5: Log scale of the average and standard deviations of concentration ratio's for each plant shoot type (PP/PS) for both Crystalline "C" and Amorphous "A" digestion techniques.

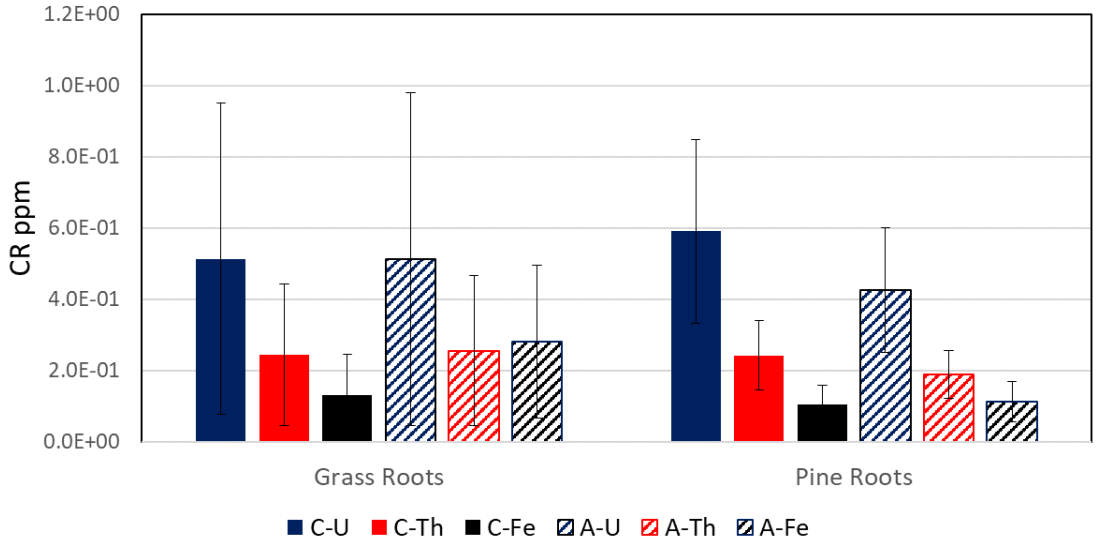

Figure B-6: The average and standard deviations of concentration ratio's for each plant root type (PR/PS) for both Crystalline "C" and Amorphous "A" digestion techniques.

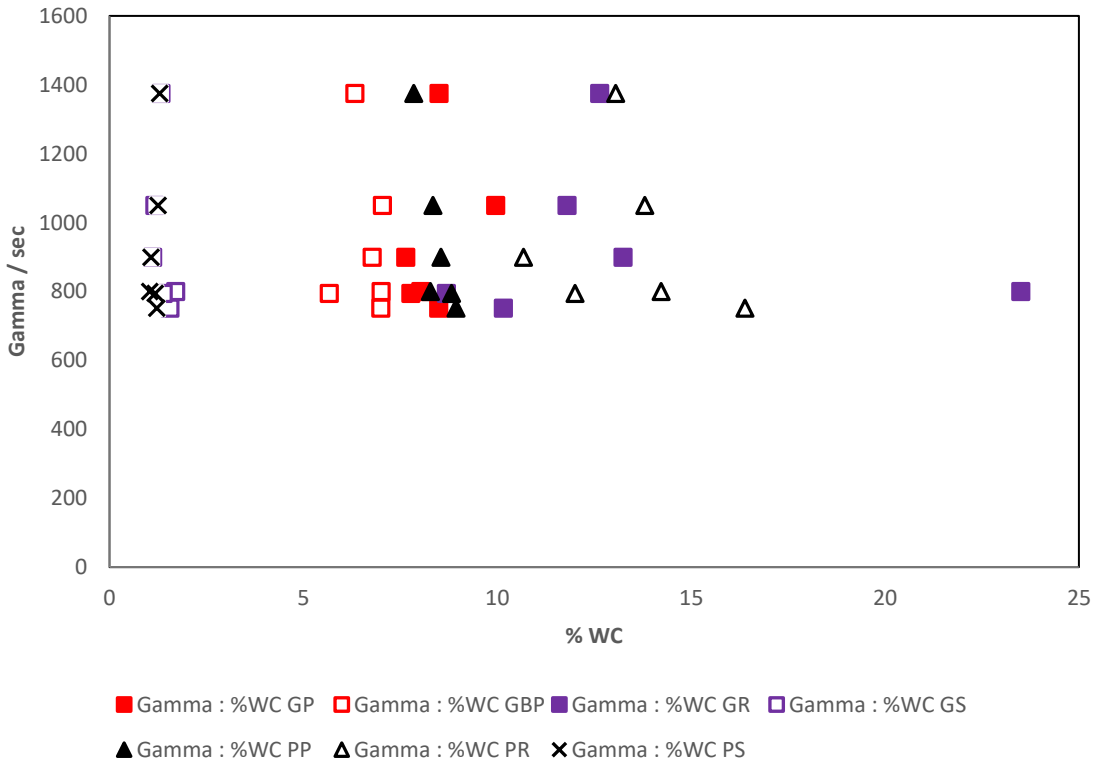

Figure B-7: NaI Detector (CPS) by pair to %WC of GP, GBP, PP, GR, PR, GS, and PS.

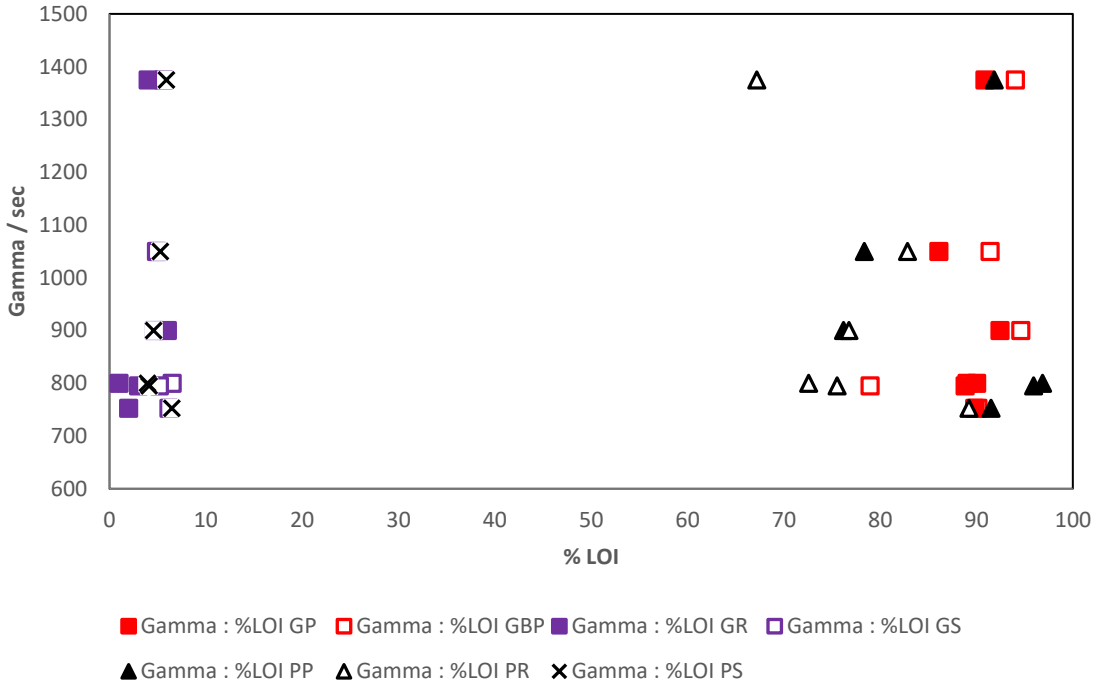

Figure B-8: NaI Detector (CPS) by pair to %LOI of GP, GBP, PP, GR, PR, GS, and PS.

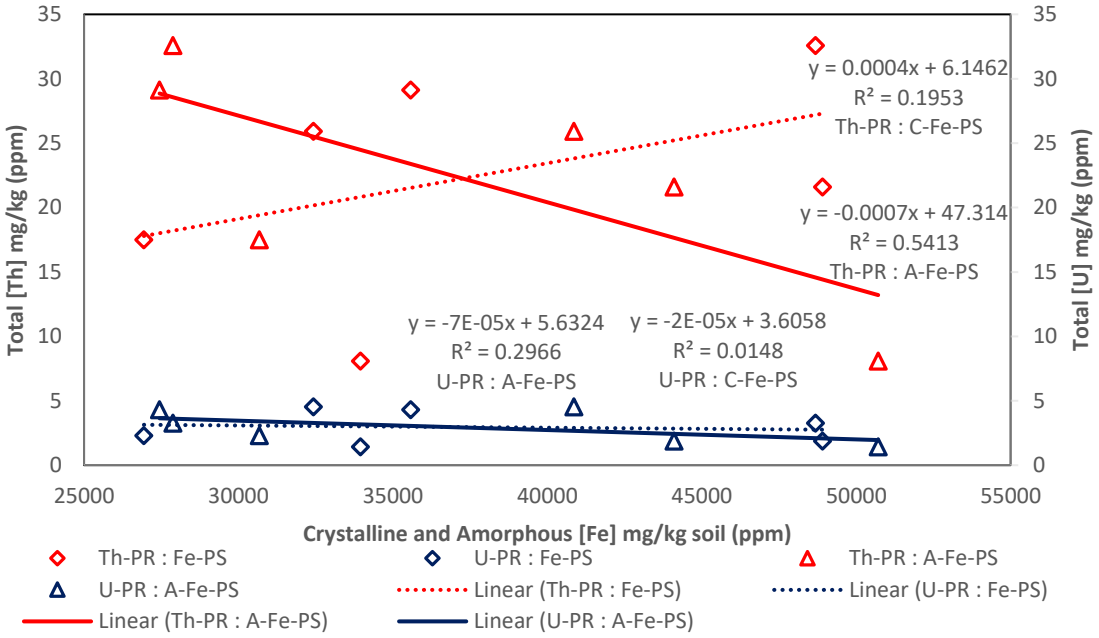

Figure B-9: Total [Th & U] mg/kg Root (ppm) against Crystalline and Amorphous [Fe] mg/kg Root (ppm) in pine roots.

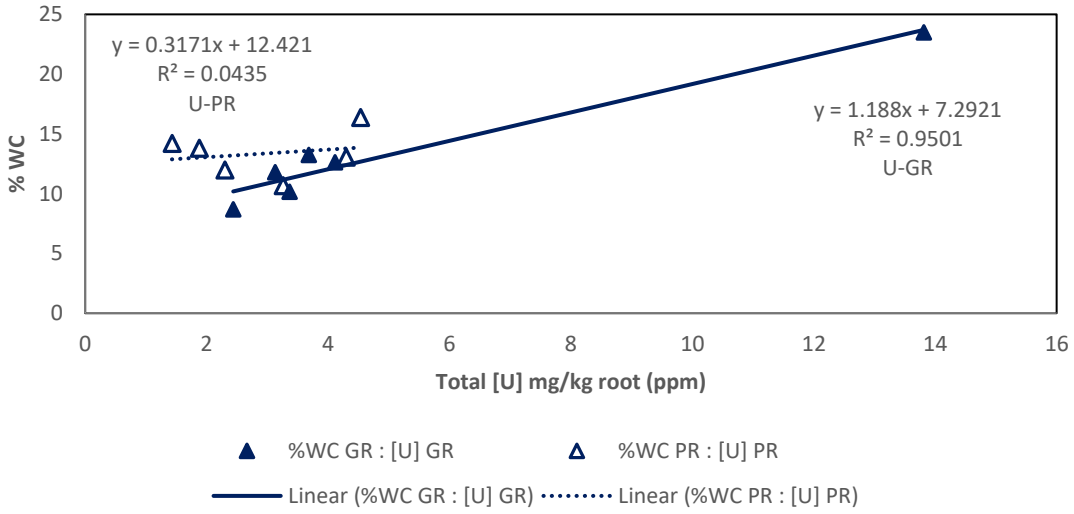

Figure B-10: %WC against Total [U] mg/kg soil (ppm) for Grass and Pine root.

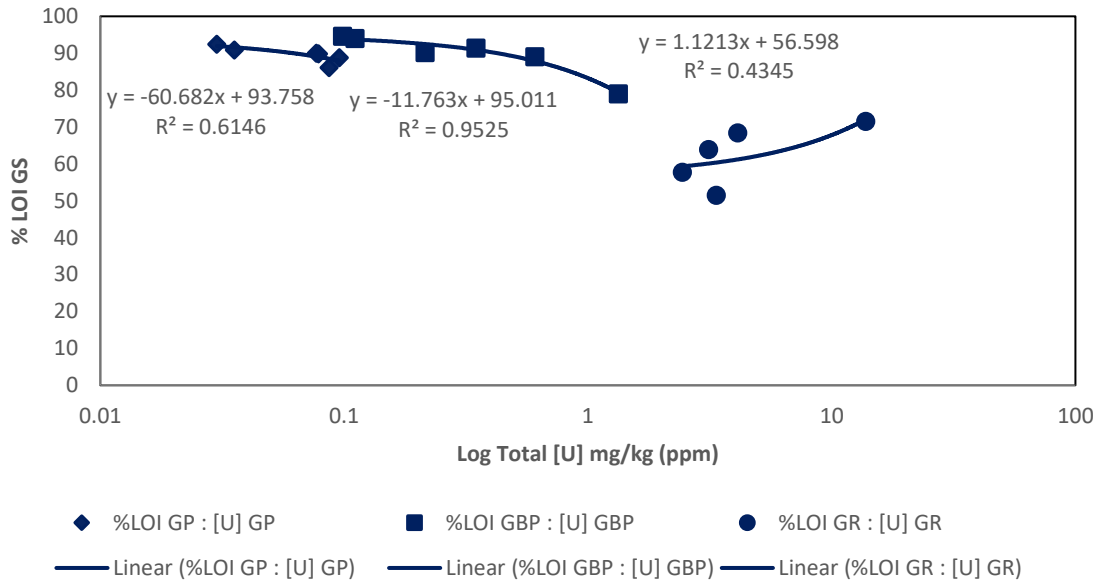

Figure B-11: %LOI against Log Total [U] mg/kg soil (ppm) in GP, GBP, and GR.

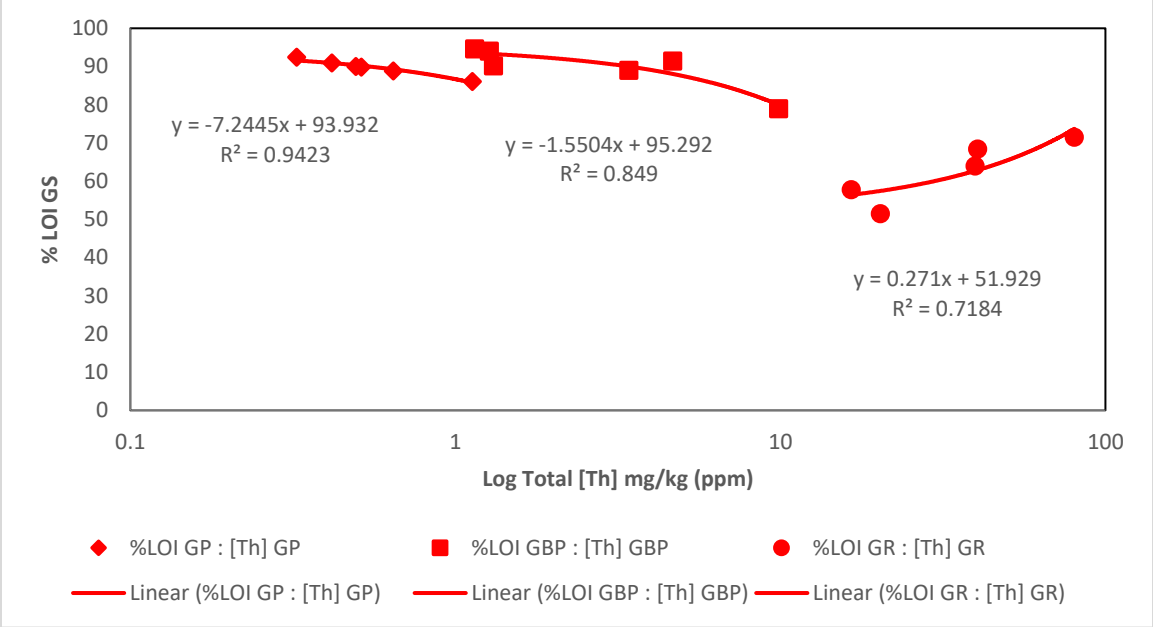

Figure B-12: %LOI of GS against Log Total [Th] mg/kg soil (ppm) in GP, GBP, and GR.

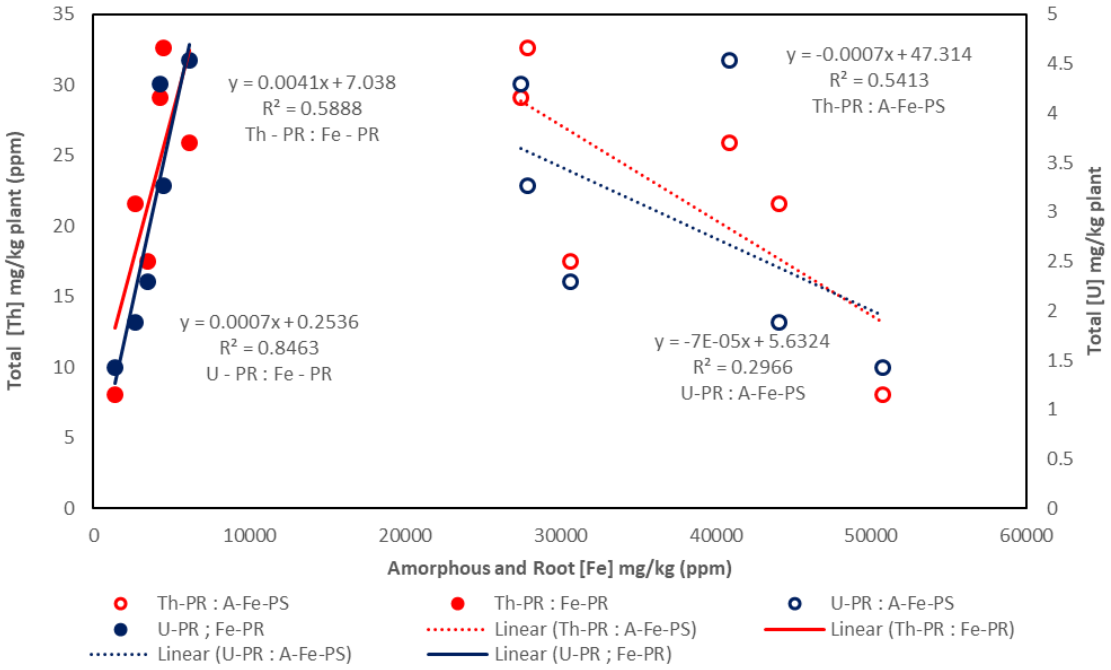

Figure B- 13: Total [Th] and [U] in pine roots to amorphous iron in pine soil and iron in pine root.

	Fe-Soils Relationship	R^2	Fe-Root Relationship	R^2
Th-GBP	-	0.2368	-	0.014
Th-GP	0	0.1405	-	0.0458
Th-GR	-	0.0835	+	0.8021
U-GBP	0	0.0782	0	0.0059
U-GP	-	0.0002	0	0.0104
U-GR	-	0.2524	+	0.9951
Th-PP	-	0.1807	-	0.4634
Th-PR	0	0.1953	0	0.5888
U-PP	-	0.624	-	0.2909
U-PR	-	0.0148	0	0.8463

Figure B-14: Table showing the positive (+ & green), negative (- & red), or neutral (yellow) trends and the corresponding R^2 value for Types and element to Fe in soils or Fe in root.

Work Cited

Albertson. P.N., 2003., Naturally Occurring Radionuclides in Georgia Water Supplies: Implications for Community Water Systems., Proceedings of the 2003 Georgia Water Resources Conference.

Arbor Day Foundation., 2016., Loblolly Pine *Pinus taeda*., Web: https://www.arborday.org/trees/treeguide/TreeDetail.cfm?ItemID=899

Back. W., LeGrand. H.E., 1988., Region 21, Piedmont and Blue Ridge., The Geology of North America - Hydrogeology., Vol. 2 O-2.

Barker, A., Pilbeam, D., (2016)., *Handbook of Plant Nutrition*., CRC Press.

Ben-Dor, E., Banin, A., 1989., Determination of organic matter content in arid-zone soils using a simple “loss-on-ignition” method., Commun., Soil Sci. Plant Anal. 20;1675-1695

Buckhout, T. J., Bell, P. F., Luster, D. G., & Chaney, R. L. (1989). Iron-Stress Induced Redox Activity in Tomato (Lycopersicum esculentum Mill.) Is Localized on the Plasma Membrane. *Plant Physiology*, *90*(1), 151–156.

Camobreco, V.J., Richards, B.K., Steehuis, T.S., Peverly, J.H., McBride, M.B., 1996., Movement of heavy metals through undisturbed and homogenized soil columns., Soil Science., 161:740 – 750.

Ce´line M.D., Francoise D.V., Julie D., Fabien C., Laure G., Suzuki A., 2009., Nitrogen in agricultural plants., Annals of Botany., 105: 1141–1157., doi:10.1093/aob/mcq028

Chapman. M.J., Cravotta. C.A., Szabo. Z., Lindsey. B.D., 2013., Naturally Occurring Contaminants in the Piedmont and Blue Ridge Crystalline-Rock Aquifers and Piedmont Early Mesozoic Basin Siliciclastic-Rock Aquifers, Eastern United States, USGS.

Davis. J.C., 2002., Statistics and Data Analysis in Geology (3rd)., John Willey and Sons.

Donahue. J.C., Kibler. S.R., 2007., Ground-water Quality in the Piedmont Blue Ridge Unconfined Aquifer System of Georgia., Georgia Environmental Protection Division., Circular 12U.

Ebbs, S. D., Norvell, W. A., & Kochian, L. V. (1998). The Effect of Acidification and Chelating Agents on the Solubilization of Uranium from Contaminated Soil. *Journal of Environmental Quality*, *27*(6), 1486–1494. https://doi.org/10.2134/jeq1998.00472425002700060027x

Ely, S., Powell, B. A., Molz, F.J., Tharayil, N., 2016., Examination of Actinide and Nuclear Fission Product uptake in graminaceous and nongraminaceous plants., Thesis

EPA., 1996., Method 3052 - Microwave assisted acid digestion of siliceous and organically based matrices., Web: https://www.epa.gov/hw-sw846/sw-846-test-method-3052-microwave-assisted-acid-digestion-siliceous-and-organically-based

Finch, R., Murakami, T., 1999., Systematics and paragenesis of uranium minerals. In: Burns, P.C., Finch, R., (Eds.), Reviews in Mineralogy Uranium: Mineralogy, Geochemistry and the Environment, vol 38. Mineralogical Society of America, Washington DC, pp. 91 – 179.

Gee, G.W., Bauder, J.W., 2008., Methods of Soil Analysis Part 5 – Mineralogical Methods. SSSA Book Ser. 5.5.

Hansen. R.O., Stout, P.R., 1968., Isotopic Distributions of Uranium and Thorium in Soils., Soil Science., V.105: 1.(44-50)

Holden, M. J., Luster, D. G., Chaney, R. L., Buckhout, T. J., & Robinson, C. (1991). Fe^{3+}-Chelate Reductase Activity of Plasma Membranes Isolated from Tomato (Lycopersicon esculentum Mill.) Roots: Comparison of Enzymes from Fe-Deficient and Fe-Sufficient Roots. *Plant Physiology*, *97*(2), 537–544.

Hornburg, V., Brummer, G.W., (1993)., Behaviour of heavy metals in soils. 1. Heavy metal mobility., 2. Pflanzenernahr. Bodenk., 156,467-477

Hughes, L. D., Powell, B. A., Soreefan, A. M., Falta, D., & DeVol, T. A. (2005). Anomalously High Levels of Uranium and Other Naturally Occurring Radionuclides in Private Wells in the Piedmont Region of South Carolina. *Health Physics Society*, *88*(3), 248–252. https://doi.org/10.1097/01.HP.0000146580.29977.f4

IAEA.,2010., Handbook of Parameter Values for the Prediction of Radionuclide Transfer in Terrestrial and Freshwater Environments - Vienna., Technical reports series, ISSN 0074–1914 ; no. 472

Jackson, M.L., Lim, C.H., Zelazny, L.W., 1986., Oxides, hydroxides, and aluminosilicates. Methods of soil analysis. Part 1., A. Klute (ed)., Agron. Monogr. 9. 101 – 150.

Kucks, Robert P., 2005, Terrestrial Radioactivity and Gamma-ray Exposure in the United States and Canada: Gridded geographic images., Web: http://mrdata.usgs.gov/radiometric/

Lakshmanan, A. R., & Venkateswarlu, K. S. (1988). Uptake of uranium by vegetables and rice. *Water, Air, and Soil Pollution*, *38*(1–2), 151–155. https://doi.org/10.1007/BF00279593

Lazof, D., Linton, R.W., Volk, R.J., Rufty, T.W., 1991., The application of SIMS to nutrient tracer studies in plant physiology., Biol Cell., 74:127 – 134.

Lee, J. H., Hossner, L. R., Attrep Jr., M., & Kung, K. S. (2002a). Comparative uptake of plutonium from soils by Brassica juncea and Helianthus annuus. *Environmental Pollution*, *120*(2), 173–182. https://doi.org/10.1016/S0269-7491(02)00167-7

Lee, J.H., Hossner, L.R., Attrep Jr., M. and Kung, K.S. (2002b). Uptake and translocation of plutonium in two plant species using hydroponics. Environmental Pollution, 61

Lee,S.Y., Elless, M., & Hoffman, F. (1993). Solubility Measurement of Uranium in Uranium-Contaminated Soils. *Oak Ridge National Labs*.

Loeppert, R., Inskeep, W., (1996) Methods of Soil Analysis Part 5 – Mineralogical Methods. SSSA Book Ser. 5.5.

Magnum, S., (2009)., Microwave Digestion - EPA Method 3052 on the Multiwave 3000.

Marschner, H, & Romheld , V. (1994). Strategies of plants for aquisition of iron, 261–274.

McKeague, J.A., Day, J.H., 1966., Dithionite- and oxalate-extractable Fe and Al as aids in differentiating various classes of soils. Can J. Soil Sci. 46:13 – 22.

Megumi, K., (1979)., Radioactive disequilibrium of uranium and actinium series nuclides in soil., Journal of Geophysics., Res., 84.3677-82.

Mehra, O.P., Jackson, M.L., 1960., Iron oxide removal from soils and clays by dithionite-citrate system buffered with sodium bicarbonate., Clays and clay minerals., Proc. 7th Natl. Congr. Pergamon, London.

Mertie J.B. Jr. (1953). *Monazite Deposits of the Southeastern Atlantic States* (No. 237). USGS. Retrieved from https://pubs.usgs.gov/circ/1953/0237/report.pdf

Mertie Jr., J. B. (1975). *Monazite placers in the southeastern Atlantic States* (USGS Numbered Series No. 1390). U.S. Govt. Print. Off.,. Retrieved from http://pubs.er.usgs.gov/publication/b1390

Missouri. University., 2015., Weed ID Guide., Division of Plant Sciences., Web: http://weedid.missouri.edu//weedinfo.cfm?weed_id=196

Murad, E., Fischer,W.R., 1988., The geobiochemical cycle of iron., Iron in soils and clay minerals (J.W. Stucki et al. (ed.)) Dordreecht, the Netherlands.

Nelson, D.W., Sommers, L.E., 2008., Methods of Soil Analysis Part 5 – Mineralogical Methods. SSSA Book Ser. 5.5.

Morrissey, J., Guerinot, M.L., 2009., Iron uptake and transport in plants: the good, the bad, and the ionome., Chem. Rev., 109., 4553-4567.

Overstreet, W.C., 1967., The geologic occurrence of monazite: U.S. Geological Survey Professional Paper 530, 327 p., 2 plates.

Powell, B. A., Hughes, L. D., Soreefan, A. M., Falta, D., Wall, M., & DeVol, T. A. (2007). Elevated concentrations of primordial radionuclides in sediments from the

Reedy River and surrounding creeks in Simpsonville, South Carolina. *Journal of Environmental Radioactivity*, *94*(3), 121–128. https://doi.org/10.1016/j.jenvrad.2006.12.013

Railsback, L.B., 2012., An Earth Scientist's Periodic Table of Elements and Their Ions., 4.8e., Web: gly.uga.edu/railsback/PT.html.

Schwertmann, U., 1964., The differentiation of iron oxide in soils by a photochemical extraction with acid ammonium oxalate. Z. Pflanzenernaehr. Dueng. Bodenkund., 105:194 – 201.

Sheppard, M. I. (1980). *The environmental behaviour of uranium and thorium* (No. AECL--6795). Atomic Energy of Canada Ltd. Retrieved from http://inis.iaea.org/Search/search.aspx?orig_q=RN:12588072

Sheppard, S. C., & Evenden, W. G. (1988). Critical compilation and review of plant/soil concentration ratios for uranium, thorium and lead. *Journal of Environmental Radioactivity*, *8*(3), 255–285. https://doi.org/10.1016/0265-931X(88)90051-3

Snow, A., Ghaly, A.E., Cote, R., Snow, A.M., (2008)., Uptake and translocation of iron by native tree species in a constructed wetland treating landfill leachates., J. Applied Science., 5(9), 1091-1106

Taylor, S.R., 1964., The abundance of chemical elements in the continental crust – a new table. Geochimica et Cosmochimica Acta 28, 1273 – 1285.

Thomas, G.W., 2008., Methods of Soil Analysis Part 5 – Mineralogical Methods. SSSA Book Ser. 5.5.

USDA., 2016., *Dichanthelium commutatum* (Schult.) Gould - variable panicgrass., Web: http://plants.usda.gov/core/profile?symbol=DICO2

USDA., 2016., *Dichanthelium clandestinum* (L.) Gould - deertongue., Web: http://plants.usda.gov/core/profile?symbol=DICL

USGS., 2016., Science in Your Watershed., Web: http://water.usgs.gov/wsc/acc/030601.html

Van Gosen, B.S., Gillerman, V.S., and Armbrustmacher, T.J., 2009, Thorium deposits of the United States—Energy resources for the future?: U.S. Geological Survey Circular 1336, 21 p. [Only available at URL https://pubs.usgs.gov/circ/1336]

Vaughn, M., (2015)., Ten most common trees., Web: https://swain.ces.ncsu.edu/2009/08/ten-most-common-trees/

William, D. N. (2011). *Introduction to Mineralogy* (2nd ed.). Oxford University Press.

Zhang, F., Römheld, V., & Marschner, H. (1991). Role of the Root Apoplasm for Iron Acquisition by Wheat Plants 1. *Plant Physiology*, *97*(4), 1302–1305.

Zhao. F.J., Mao, J.F., Meharg, A.A., McGrath, S.P., (2008)., New Phytologist., 181: 777–794 doi: 10.1111/j.1469-8137.2008.02716.x